ROLE OF PEPTIDYLARGININE DEIMINASE 2 (PAD2) IN EPITHELIAL CARCINOGENESIS AND TUMOR-ASSOCIATED INFLAMMATION

A Dissertation

Presented to the Faculty of the Graduate School

of Cornell University

In Partial Fulfillment of the Requirements for the Degree of

Doctor of Philosophy

by

Sunish Mohanan Nair Padmini

January 2014

ROLE OF PEPTIDYLARGININE DEIMINASE 2 (PAD2) IN EPITHELIAL CARCINOGENESIS AND TUMOR-ASSOCIATED INFLAMMATION

Sunish Mohanan Nair Padmini

Cornell University 2014

Numerous recent studies have shown that epigenetic modifications play a significant role in cancer pathogenesis. The PADs are a family of epigenetic enzymes that catalyze citrullination, a reaction by which PADs convert peptidyl-arginine to neutral citrulline, leading to the disruption of protein-protein interactions. Our lab has found that PAD2 has a critical role in breast cancer progression. The goal of this thesis research was to further elucidate the role of PAD2 in epithelial carcinogenesis using PAD2 overexpression tumor cell lines and a MMTV-FLAG-hPAD2 transgenic mouse model. We also aimed to evaluate how PAD2 may play a direct role in regulating chronic inflammation via macrophage extracellular chromatin trap release (“ETosis”).

Interestingly, we found that 40% of the MMTV-FLAG-hPAD2 overexpressing transgenic mice developed proliferative skin lesions after five months of age. The tumors expressed the transgenic form of FLAG-hPAD2 and showed increased expression for inflammatory cytokines such as IL6 and IL8. As the next step we conducted a two-stage chemical carcinogenesis study to further

evaluate the predilection of MMTV-FLAG-hPAD2 mice to develop more invasive skin tumors and compare the histopathology of these tumors with the WT tumors. We found that a higher percentage of MMTV-FLAG-hPAD2 mice developed skin papillomas and the transgenic tumors were more invasive. Furthermore, hPAD2 expression levels were highly positively correlated with chemokine levels and negatively correlated with the cell adhesion markers suggesting the role of PAD2 in assisting epithelial-mesenchymal transition.

We had previously shown that PAD4 isozyme in neutrophils is involved in chromatin decondensation and extracellular chromatin trap release. In this thesis research we provide evidence on how PAD2 is involved in macrophage extracellular trap (MET) release. Using *in vitro* macrophage culture models, we found that PAD2 is critical in functional MET release and that METs contain high levels of histone H4 citrulline 3 (H4Cit3) modification. Using human tongue SCC tissue, we show that CD68+ macrophage associated ETs exist in tumor tissue and are highly positive for citrullinated histones. Additionally, we show that PAD2-rich macrophages associated with chronic subclinical inflammation in adipose tissue also release METs suggesting the significant role of PAD2 in chronic inflammation via MET release. Collectively, these studies provide strong experimental evidence establishing PAD2 as a potential oncogene, a therapeutic target for immunomodulation and a regulator of obesity and tumor associated inflammation.

BIOGRAPHICAL SKETCH

Sunish Mohanan was born on May 04, 1981, in the city of Trivandrum in Kerala, a beautiful southern state of India. He received his early academic training from the local public school and completed the pre-veterinary training from Kerala University. Based on the excellent merit record in the state entrance exam, he was admitted to College of Veterinary and Animal Sciences in Kerala Agricultural University in 1998. After completing his veterinary medical degree in 2004 and practicing for a short while as a veterinary surgeon, Sunish decided to come to USA to continue his training in animal health research and joined University of Wisconsin-Madison as a Masters student. Here he worked on muscle physiology and pathology projects and attended pathology rounds in the School of Veterinary Medicine. At the completion of the Masters program in 2006, he made the decision join University of Pennsylvania to work on urinary bladder smooth muscle cell biology and pathology projects as a Post-DVM Research Fellow. Realizing the importance of pathology interpretations in advancing basic science research, he then completed a Veterinary Anatomic Pathology residency from Wake Forest School of Medicine from 2007-2010 during which he gained extensive training in lab animal pathology and nonhuman primate pathology. In 2010, he passed the American College of Veterinary Pathologists (ACVP) board exam and received the Diplomate of ACVP status. In order to get more hands-on

experience in hypothesis-driven research, Sunish joined Cornell University Comparative Biomedical Sciences PhD program in 2010 as a Post-DVM graduate student under the mentorship of Dr. Scott Coonrod. Sunish's thesis research focused on the role of Peptidylarginine Deiminase enzymes on cancer epigenetics and cancer-associated inflammation. After completing his PhD program, Sunish plans to pursue a career in comparative pathology and translational biomedical research.

Dedicated to my family and mentors for their incredible support during my academic pursuit

ACKNOWLEDGEMENTS

When I was beginning my PhD training, Dr. Jyotsana Menon who was a young brilliant cancer biology scientist and a wonderful person, used to tell me that PhD training is all about persistence in finding answers. Even though she is not in this world now to see me graduate, my training helped me realize her words are very true and she remains as a source of inspiration in my life.

It will take up a whole thesis to acknowledge everyone who helped me to succeed in my life. So I will choose to mention only a few names. I have enormous respect for my mentor Dr. Scott Coonrod who trained me as a better scientist and also valued my input to research projects as a pathologist. It was a pleasure to work with everyone in Coonrod lab, especially Sachi Horibata, John McElwee, Brian Cherrington, Boram Kim, Xuesen Zhang, Dalton McLean, Angela Yan, Emma, David Olshan, Lynne Anguish, and Kelly Sams, who helped me to succeed in my research projects. I am also grateful for Baker Institute faculty and staff for their support and for creating a conducive environment to do research. My PhD committee members Drs. Avery August, Claudia Fischbach, and Robert Weiss were amazingly helpful and supportive in guiding me through various aspects of cancer biology research, teaching me the importance of critical thinking, and in helping me

understand the big picture of research approaches. The funding and support from CBS program has been critical for my success and I thank Dr. David Lin, Dr.Colin Parrish, Janna Lamey, Arla Hourigan and Dr. Joel Baines who are tremendously helpful in guiding graduate students through the process. I also want to acknowledge the productive collaborations in pathology with laboratories of various research faculty members such as Drs. Claudia Fischbach (David Infanger, Bo Ri Seo , Siddharth Pathi, Maureen Lynch), Avery August (Arun Kannan), Andrew Dannenberg (Neil Iyengar), Brian Cherrington, Mark Hoenerhoff (NIEHS), Joseph Wakshlag, Watt Webb and Judy Appleton (Lu Huang). I express my special thanks to Dr. Wakshlag for helping me with statistical modelling and data analysis.

Without the support of my parents' and my younger brother, I will not be where I am in my life today and I thank them for teaching me the fundamentals of life which always served me well. Also I was fortunate to have grown up in a place rich of spirituality, meditation and prayer and I bow my head in respect to my spiritual master, *Swamiji* who taught me through his humble life that "hardwork is satisfaction". Also, I want to express my gratitude to my parents-in-law, my brother-in-law Dr. Krishnakumar Kurup and sister-in-law Dr. Poornima Sukumar for their support and for understanding the struggles of a graduate student life. Lastly, I want to thank my wife Dr. Neelima Sukumar and my two and a half year old son Arjun Mohanan for their limitless support during my graduate school life and cheering me up during grey skies.

TABLE OF CONTENTS

BIOGRAPHICAL SKETCH **v**

ACKNOWLEDGEMENTS **viii**

TABLE OF CONTENTS **x**

LIST OF FIGURES **xvii**

LIST OF TABLES **xxii**

LIST OF ABBREVIATIONS **xxiii**

CHAPTER ONE

INTRODUCTION: POTENTIAL ROLE OF PEPTIDYLARGININE DEIMINASE ENZYMES (PADS) AND PROTEIN CITRULLINATION IN CANCER PATHOGENESIS **1**

1.1 Abstract 2

1.2 Introduction 3

1.3 Tissue expression patterns and substrate specificity of PAD family members 3

1.4 Hormonal regulation of PADs 9

Pituitary gland and uterus 10
Mammary gland 11
1.5 PAD4 mediated histone tail citrullination: An emerging role for PADs in gene regulation and cancer 12
1.6 PAD2 and cancer pathogenesis 15
1.7 PAD inhibitors block cancer progression 19
1.8 PAD-mediated citrullination: Linking inflammation with cancer progression? 22
Role of inflammation in cancer progression 22
Role of PADs in inflammation 22
Role of PADs in chemokine signaling 24
1.9 Conclusions 26
1.10 Acknowledgements 28
1.12 References 1
CHAPTER TWO
HUMAN PAD2 TRANSGENE OVEREXPRESSION LEADS TO SPONTANEOUS SKIN NEOPLASIA AND PROMOTES MALIGNANCY AND TUMOR-ASSOCIATED INFLAMMATION IN CHEMICALLY INITIATED SKIN TUMORS IN MICE 12

2.2 Introduction 16

2.3 Materials and Methods 19

Generation of MMTV-FLAG-PADI2 mice 19
Lentivirus and plasmids for stable FLAG-PADI2 expression in A431 cells 20
Mouse skin two-stage carcinogenesis assay 21
Immunohistochemistry (IHC) and immunofluorescence (IF) 22
Western blotting 22
RNA isolation, semi-quantitative, and quantitative Real-Time PCR (qRT-PCR) 23
Assays for cellular malignancy and invasion 23
Histopathology scoring 24
Statistical analysis 25

2.4 Results 25

Generation of MMTV-FLAG-PADI2 transgenic mice 25
Transgenic skin lesions have decreased levels of endogenous mouse Padis and increased markers of inflammation and EMT 40
Overexpression of PADI2 in human squamous cell carcinoma A431 cells increases invasiveness and malignancy 47
MMTV-FLAG-hPAD2 mice form larger skin tumors 60
MMTV-FLAG-hPAD2 mice skin tumors show increased CCL7 expression and activation of STAT3 pathway 76

2.5 Discussion 79

2.6 Conclusions 82

2.7 References 91

CHAPTER THREE

ROLE OF HISTONE CITRULLINATION BY PEPTIDYLARGININE DEIMINASE 2 (PAD2) IN MACROPHAGE EXTRACELLULAR TRAP (MET) FORMATION AND CHARACTERIZATION OF METS IN HUMAN TONGUE SQUAMOUS CELL CARCINOMA **101**

3.1 Abstract 102

3.2 Introduction 103

Macrophage extracellular traps in diseases 104
Role of PADs and histone modifications in ETosis 105
Role of ETosis in Cancer Pathogenesis 107
Tumor associated macrophages 108

3.3 Materials and Methods 109

Cell culture and MET induction 109
MET isolation and Quantitation 110
Immunohistochemistry (IHC) and Immunofluorescence (IF) 111

3.4 Results and Discussion 113

PAD2 is highly expressed in RAW 264.7 and peritoneal primary macrophages and is a potential candidate for MET release regulation 113
PAD2KO macrophages show an impaired ability to release METs 116

METs contain high levels of citrullinated histones which is reduced upon PAD2 deletion 116
PAD2 deletion and drug-mediated PAD inhibition reduce chromatin decondensation 117
PAD2 expression and H4Cit3 levels in TAMs in human tSCC 122
3.5 Conclusions 136
3.6 References 140
CHAPTER FOUR
IDENTIFICATION OF MACROPHAGE EXTRACELLULAR TRAP-LIKE STRUCTURES IN MAMMARY GLAND ADIPOSE TISSUE 146
4.1 Abstract 147
4.2 Introduction 148
4.3 Materials and methods 152
RAW 264.7 cell culture and MET induction 152
Mammary gland adipose tissue from obese mice 153
mRNA isolation and RT-PCR 153
Immunohistochemistry (IHC) and Immunofluorescence (IF) 154
4.4 Results and Discussion 156
TNF-α appears to induce MET formation in RAW 264.7 macrophages 156
PAD2 is a likely candidate for catalyzing histone hypercitrullination during ETosis in macrophages 160

Evidence supporting the hypothesis that METs exist in mouse mammary gland CLS lesions 163

4.5 References 171

CHAPTER FIVE 175

DISCUSSION – SUMMARY AND FUTURE ROLE FOR PAD2 IN CARCINOGENESIS AND REGULATION OF TUMOR INFLAMMATORY MICROENVIRONMENT 175

5.1 Summary of findings 176

5.2 PAD2 may function differently in tumor cell regulation Vs immune 181

5.3 Role of PAD2 in breast cancer progression and basement membrane integrity 182

5.4 PAD2 mediated regulation of tumor associated inflammation and EMT 185

5.5 Role of PAD2 mediated extracellular chromatin trap release in DAMP pathway activation in tumors 193

5.6 4-NQ-O oral carcinogenesis model to study the role of PAD2 in head and neck tumor-associated inflammation 199

5.7 Reflections on the role of PAD2 and CLS METs in obesity-associated inflammation and its clinical relevance 200

5.8 Connecting the dots – Current understanding of PAD2's role in epithelial carcinogenesis and tumor-associated inflammation 204

5.8 References 208

LIST OF FIGURES

Figure 1.1: Peptidylarginine deiminase (PAD) enzymes catalyze the conversion of protein arginine residues to citrulline. 6

Figure 1.2: PAD mediated histone tail citrullination leads to chromatin decondensation. 8

Figure 1.3: H4cit3 (green) immunostaining of DCIS xenograft sections. 14

Figure 1.4: PAD2 IHC staining of the normal human mammary gland, a DCIS lesion, and invasive carcinomas. 17

Figure 1.5: PAD2 (green) is expressed in luminal epithelial cells of preinvasive, invasive, and metastatic human mammary tumors. 18

Figure 1.6: PAD inhibitors and their selectivity (TDFA - Threonine-aspartate-F-amidine; TDCA - Threonine-aspartate-Cl-amidine) 21

Figure 1.7: Potential role of PAD enzymes in cancer pathogenesis. 27

Figure 2.1: MMTV-FLAG-PADI2 transgenic construct 27

Figure 2.2: Generation of MMTV-FLAG-PADI2 transgenic mice 28

Figure 2.3: MMTV-FLAG-PADI2 expression in the mammary gland. 32

Figure 2.4: Transgenic FLAG-PADI2 expression in the epidermis of mice leads to the development of skin lesions 36

Figure 2.5: FLAG-PADI2 expression is high in the skin lesions of transgenic mice. 38

Figure 2.6: Confocal immunofluorescence analysis of PADI2, FLAG, and

Ki67 expression in neoplastic skin lesions of the FLAG-PADI2 transgenic mouse 42

Figure 2.7: Normal skin section from wild-type mice as a negative control for FLAG staining. 44

Figure 2.8: Transgene expression in the skin lesions of MMTV-FLAG-PAD2 mice 45

Figure 2.9: Lesions from MMTV-FLAG-PADI2 transgenic mice that express the highest levels of human PADI2, have decreased mouse Padi1, Padi3, and Padi4 48

Figure 2.10: Skin lesions from MMTV-FLAG-PADI2 transgenic mice express markers of inflammation and EMT 50

Figure 2.11: Transient overexpression of FLAG-PADI2 increases markers of inflammation and EMT in the human squamous cell carcinoma A431 cell line. 53

Figure 2.12: A431 cells stably overexpressing PADI2 have increased invasion through a collagen matrix 55

Figure 2.13: Co-localization of FLAG and GFP in A431 cells stably overexpressing FLAG-PADI2 57

Figure 2.14: A431 skin cancer cells overexpressing FLAG-PADI2 show increased malignancy and EMT morphology. 59

Figure 2.15: The incidence and growth of skin papillomas in DMBA-TPA treated mice. 61

Figure 2.16: Anti-FLAG immunostaining and confocal imaging to detect

transgenic expression of hPAD2 in skin tumors 63

Figure 2.17: Histopathological evaluation of DMBA-TPA induced skin tumors in WT and MMTV-FLAG-hPAD2 mice 66

Figure 2.18: Histopathological scoring of DMBA-TPA induced tumors for inflammation and invasiveness 68

Figure 2.19: Lymph node metastasis of SCC in a MMTV-FLAG-hPAD2 mice. 71

Figure 2.20: Inflammatory cytokine expression and EMT markers in DMBA-TPA induced skin tumors in WT and MMTV-FLAG-hPAD2 mice. 74

Figure 2.21: phosho-STAT3 levels in DMBA-TPA induced skin tumors in WT and MMTV-FLAG-hPAD2 mice 77

Figure 2.22: The role of PAD2 overexpression in regulation of tumor invasion and inflammation 84

Figure 3.1: PAD2 expression in cultured RAW 264.7 macrophage cells and in mouse primary peritoneal macrophages. 114

Figure 3.2: Peritoneal macrophages release extracellular traps (ETs) in response to PMA stimulation. 118

Figure 3.3: METs are highly positive for citrullinated histones and MET web interact with other macrophages in their vicinity. 120

Figure 3.4. PAD2 deletion and drug-mediated inhibition affect nuclear chromatin decondensation in macrophages during MET induction 124

Figure 3.5: Quantitation of MET release by WT, PAD2 KO PMΦ, and PAD inhibitor treated macrophages 126

Figure 3.6: Immunohistochemical staining for H4Cit3 levels in human tongue squamous cell carcinomas 128

Figure 3.7: H4Cit3 immunofluorescence staining in extracellular traps associated with tSCC inflammation 130

Figure 3.8: Costaining for macrophage marker F4/80 and DAPI to evaluate METs in tSCC sections 132

Figure 3.9: Costaining for TAM marker CD68, H4Cit3 and DAPI in METs associated with tSCC inflammation 134

Figure 3.10: Proposed functional roles of METs in regulation of tumor microenvironment 138

Figure 4.1: (A) H4Cit3 immunofluorescence staining in RAW 264.7 macrophages following 0 and 2 hour TNF-α treatment. 158

Figure 4.2: PAD2 expression in cultured RAW 264.7 macrophage cells. 161

Figure 4.3: PAD2 expression in cells within CLS lesions of the murine mammary gland. 164

Figure 4.4: Extracellular trap-like structures within CLS lesions of the murine mammary gland stain positive for the histone H4Cit3 166

Figure 4.5: Immunohistochemical localization of the histone H4Cit3 modification within CLS lesions of the mammary gland. 167

Figure 4.6: Schematic illustration of the role of PAD2 mediated histone citrullination during MET formation in CLS lesions 169

Figure 5.1: Cl-amidine (PAD inhibitor) decreases the growth of

MCF10DCIS tumors in a xenograft model of comedo-DCIS and enhances the basement membrane integrity 184

Figure 5.2: Tumor promoting inflammation as an emerging hallmark of cancer 187

Figure 5.3: Overview of epithelial to mesenchymal transition (EMT). 190

Figure 5.4: The potential role of ETosis inflammatory microenvironment regulation and DAMP pathway activation 194

Figure 5.5: Ewing's sarcoma as a model to study the role of PAD2 mediated ETosis in regulating tumor associated inflammation 197

Figure 5.6: 4-NQO chemical carcinogenesis model to study oral tumor progression and inflammation 198

Figure 5.7: The potential role of ETosis obesity-associated inflammatory microenvironment regulation. 201

Figure 5.8: Overview of the potential role of PAD2 in cancer progression and regulation of inflammatory microenvironment 206

LIST OF TABLES

Table 2.1	Primers for semi-quantitative RT-PCR	86
Table 2.2	Occurrence of skin lesions in MMTV-FLAG-hPAD2 mice	34
Table 2.3	Primers for mouse quantitative RT-PCR (SYBR)	87
Table 2.4	Primers for human quantitative RT-PCR (SYBR)	89
Table 2.5	Chi-Square analysis of histopathology scores	70

LIST OF ABBREVIATIONS

AD	Alzheimer's disease
AI	Aromatase inhibitor
AIB1	Amplified in breast cancer
AKT	Murine thyme viral (v-AKT) oncogene homolog-1
ALEXA-seq	Alternative expression analysis by sequencing
AMD	Age-related macular degeneration
AP-1	Activator protein-1
BB-Cl-amidine	Biphenyl-benzimidazole-Cl-amidine
BRCA1/2	Breast cancer gene 1 and 2
CAM	Cl-amidine
CBP	CREB binding protein
CDK	Cyclin-dependent Kinase
cDNA	Complementary DNA
ChIP	Chromatin immunoprecipitation
CK	Cytokeratin
Cl-amidine	N-α-benzoyl-N5-(2-chloro-1-iminoethyl)-L-orn amide

CLS	Crown-like structure
CMV	Cytomegalovirus promoter
COPD	Chronic obstructive pulmonary disease
COX2	Cyclooxygenase-2
CSC	Cancer stem cell
DAPI	4',6-diamidino-2-phenylindole
DAMP	Damage associated molecular pattern
DCIS	Ductal carcinoma in situ
DMBA	Di-methyl-benzanthracene
DNA	Deoxyribonucleic acid
E2	17ß-estradiol
ECM	Extracellular matrix
EGF	Epidermal growth factor
EGFR	Epidermal growth factor receptor (HER1)
EMT	Epithelial-to-mesenchymal transition
ER	Estrogen receptor alpha
ERBB2	Erythroblastic leukemia viral oncogene homolog-2
ERE	Estrogen response element
ERK	Extracellular regulated kinase
ERKO	Estrogen receptor knockout
ET	Extracellular trap
FACS	Fluorescence activated cell sorting

FOXA1	Forkhead box A1
GAPDH	Glyceraldehyde 3-Phosphate Dehydrogenase
GSK3ß	Glycogen synthase kinase 3 beta
H&E	Hematoxylin and eosin
H3Cit2,8,17	Histone H3 citrulline 2,8,17
H3Cit26	Histone H3 citrulline 26
H3R2,8,17	Histone H3 arginine 2,8,17
H3R26	Histone H3 arginine 26
H3K27	Histone H3 lysine 27
H3K27ac	Histone H3 acetyl lysine 27
H4Cit3	Histone H4 citrulline 3
H4R3	Histone H4 arginine 3
HDAC	Histone deacetylase
HER2	Human epidermal growth factor receptor-2
HER3	Human epidermal growth factor receptor-3
HER4	Human epidermal growth factor receptor-4
IF	Immunofluorescence
IGF	Insulin-like growth factor
IGF1R	Insulin-like growth factor type 1 receptor
IHC	Immunohistochemistry
IL6	Interleukin 6
IL8	Interleukin 8

KD	Knock-down (genetic)
KO	Knock-out (genetic)
LAP	Lapatinib
MAPK	Mitogen activated protein kinase
MBP	Myelin basic protein
MEK	MAPK/ERK Kinase
MET	Macrophage extracellular trap
MMTV	Mouse mammary tumor virus
MMTV-LTR	Mouse mammary tumor virus long terminal repeat
mRNA	Messenger RNA
MS	Multiple sclerosis
MYC	Myelocytomatosis viral oncogene
NCoR	Nuclear receptor co-repressor
NET	Neutrophil extracellular trap
Neu	Neuro/glioblastoma derived oncogene homolog (avian)
NFkB	Nuclear factor kappa B
NRG	Neuregulin/heregulin
p300	E1A binding protein p300
PAD1	Peptidylarginine deiminase-1
PAD2	Peptidylarginine deiminase-2
PAD3	Peptidylarginine deiminase-3

PAD4	Peptidylarginine deiminase-4
PAD6	Peptidylarginine deiminase-6
PARP	Poly (ADP-ribose) Polymerase
PAS	Periodic acid-Schiff
PCNA	Proliferating cell nuclear antigen
PCR	Polymerase chain reaction
PEA3	Polyomavirus enhancer activator-3 (ETV4)
PGK	Phosphoglycerate kinase promoter
PI3K	Phosphatidylinositol 3-kinase
PMφ	Peritoneal macrophage
PR	Progesterone receptor
pRb	Retinoblastoma protein (RB1)
PyMT	Polyoma middle T antigen
qRT-PCR	Quantitative real-time PCR
RA	Rheumatoid arthritis
RAS	Rat sarcoma viral oncogene
RNA	Ribonucleic acid
RNA-seq	RNA sequencing
RTK	Receptor tyrosine kinase
SCC	Squamous cell carcinoma
SERD	Selective estrogen receptor down-regulator
SERM	Selective estrogen receptor modulator
shRNA	Short hairpin RNA

siRNA	Small interfering RNA
SMAD	SMA- and –MAD related
SP-1	Specificity protein 1
S-phase	Synthesis phase of the cell cycle
SRC	Steroid receptor co-activator
SV40	Simian virus 40
TCGA	The cancer genome atlas
TF	Transcription factor
TFF1	Trefoil factor-1
Tg (TG)	Transgenic
TGFß	Transforming growth factor beta
TGFα	Transforming growth factor alpha
TNBC	Triple negative breast cancer
TPA	12-O-tetradecanoylphorbol-13-acetate
tSCC	Tongue Squamous Cell Carcinoma
UV	Ultraviolet
VEGF	Vascular endothelial growth factor

CHAPTER ONE

INTRODUCTION: POTENTIAL ROLE OF PEPTIDYLARGININE DEIMINASE ENZYMES (PADS) AND PROTEIN CITRULLINATION IN CANCER PATHOGENESIS

Chapter reprinted from: Sunish Mohanan; Brian D. Cherrington; Sachi Horibata; John L. McElwee; Paul R. Thompson; Scott A. Coonrod. Potential role of peptidylarginine deiminase Enzymes (PADs) and protein citrullination in cancer pathogenesis. Biochemistry Research International. 2012;2012:895343. Epub 2012 Sep 16. PMID: 23019525; PMCID: PMC3457611.

Author contributions: conceived the topic and prepared the manuscript –SM and SAC; performed immunostaining and imaging experiments – SM, SH, BDC; conducted DCIS xenograft studies and Cl-amidine treatment – JLM, SM and PRT; contributed reagents and PAD inhibitor discussion section – PRT.

1.1 Abstract

The peptidylarginine deiminases (PADs) are a family of post-translational modification enzymes that catalyze the conversion of positively charged protein-bound arginine and methylarginine residues to the uncharged, non-standard amino acid citrulline. This enzymatic activity is referred to as citrullination or, alternatively, deimination. Citrullination can significantly affect biochemical pathways by altering the structure and function of the target proteins. Five mammalian PAD family members (PADs 1-4 and 6) have been described and show tissue-specific distribution patterns and function. Recent reviews on PADs have focused on their role in autoimmune diseases such as rheumatoid arthritis, psoriasis, and multiple sclerosis. Here, we will discuss the potential role of PADs in tumor progression and tumor-associated inflammation. In the context of cancer, increasing clinical evidence suggests that PAD4, and possibly PAD2, have important roles in tumor progression. The link between PADs and cancer is strengthened by recent findings showing that treatment of cell lines and mice with PAD inhibitors significantly suppresses tumor growth and, interestingly, inflammatory symptoms. At the molecular level, transcription factors, co-regulators, and histones, are functional targets for citrullination by PADs, and citrullination of these targets can affect gene expression in multiple tumor cell lines. As the novel relationship between PADs, inflammation, and cancer unfolds, next generation isozyme-specific PAD inhibitors may have therapeutic potential to regulate

both the inflammatory tumor microenvironment and tumor cell growth.

1.2 Introduction

PAD-mediated citrullination can alter the tertiary structure of target substrates and/or alter protein-protein interactions; thus affecting various cellular processes[1, 2] (**Figure 1.1**).

Recently, protein citrullination has garnered increased attention due to its role in the pathogenesis of various inflammatory conditions such as rheumatoid arthritis (RA), multiple sclerosis, psoriasis, chronic obstructive pulmonary disease (COPD), neurodegenerative diseases and, also, due to its emerging role in various human and animal cancers [3-7]. In this essay, we will first briefly discuss the tissue-specificity and hormonal regulation of the five PAD isoforms and then focus on the potential role of this enzyme family in carcinogenesis, tumor progression and inflammation.

1.3 Tissue expression patterns and substrate specificity of PAD family members

PADs are Ca^{2+}-dependent enzymes and there are five different isozymes in mammals; namely PAD1, 2, 3, 4, and 6 [8, 9]. The *PAD* genes likely arose by duplication of the ancestral homologue, *PAD2*, and are localized to a well-organized gene cluster at 1p36.13 in humans. Interestingly, this locus is also predicted to contain a novel, yet to be defined, tumor suppressor protein [10].

PAD enzymes are highly homologous, with ~50-60 percent sequence identity at the amino acid level. Although there is some overlap with respect to target proteins, each family member also appears to target a unique set of cellular proteins as well [11, 12]. Additionally, as described below, each family member also exhibits a tissue-selective distribution pattern. We note here that, in this review, we will be using the more commonly utilized gene synonym, *PAD*, while the approved HUGO Gene Nomenclature Committee gene names for the family members are actually *PADI1, PADI2, PADI3, PADI4,* and *PADI6*. PAD1 appears to primarily be expressed in the epidermis and uterus. In the epidermis, PAD1 citrullinates cytokeratin and this modification is important for modulating the cornification of the epidermis and maintaining the barrier function of superficial keratinized epidermal cell layers. The loss of charge following citrullination of cytokeratin causes disassembly of the cytokeratin-filaggrin complex and proteolytic degradation of these targets.

PAD2 is expressed in multiple organs, including the brain, female reproductive tissues, skeletal muscle, and cells of the hematopoietic lineage. In the brain, a major target for PAD2 is myelin basic protein (MBP), a constituent of the myelin sheath [13, 14]. Citrullination of MBP by PAD2 likely plays a key role in the pathogenesis of neurodegenerative disease [15]. PAD2 can also citrullinate the intermediate filament vimentin in macrophages [16], leading to cytoskeletal disintegration and eventually apoptosis. In female reproductive tissues, PAD2 levels appear to be regulated by hormones, predominantly estrogen, and also

possibly by epidermal growth factor [17]. PAD2 has also been found to be expressed in human mammary gland epithelial cells, with a fraction of PAD2 in these cells localizing to the nucleus and binding directly to chromatin [18]. In canine mammary tissue, histone citrullination levels closely correlate with the expression of PAD2 across the estrous cycle, suggesting that PAD2 may target histones for citrullination in this tissue [17]. In support of this prediction, a recent study has found that PAD2-catalyzed citrullination of histone H3 arginine 26 can regulate estrogen receptor α target gene activity [19].

PAD3 expression is highly restricted to the hair follicle and epithelium and a major target for PAD3 is trichohyaline. Additionally PAD3 can also citrullinate filaggrin leading to altered epidermal homeostasis and loss of barrier function [20].

PAD4 is expressed in hematopoietic progenitor cells, immune cells such as granulocytes, monocytes and macrophages, natural killer cells, and carcinoma cells originating from lung, esophagus, lung, breast, and ovary [5, 21]. PAD4 is often localized to the nucleus and is the only PAD family member with a canonical nuclear localization sequence [22]. Antithrombin has been found to be an extracellular PAD4 substrate [23] and citrullination of this target suppresses the ability of antithrombin to inhibit thrombin [24]. Increased thrombin activity is considered to be a hallmark of cancer by promoting angiogenesis, increased tumor growth, and distant metastasis.

<u>Figure 1.1:</u> Peptidylarginine deiminase (PAD) enzymes catalyze the conversion of protein arginine residues to citrulline.

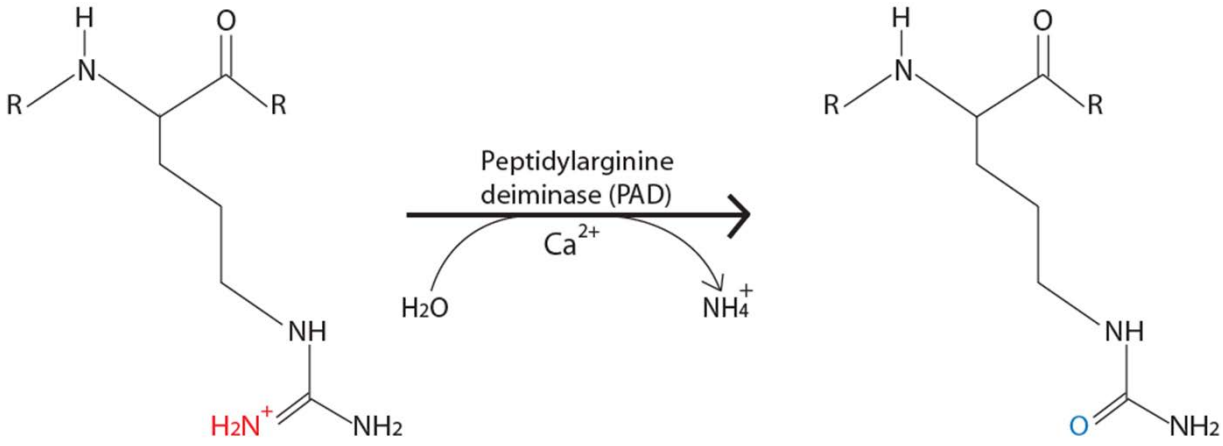

Interestingly, citrullinated anti-thrombin levels are elevated in serum samples from patients with malignant cancers, thus raising the possibility that PADs may affect tumor progression via citrullination of antithrombin [25].

PAD4 also appears to function as a transcriptional coregulator for a range of factors such as p53, ELK1, p300, p21, CIP1, nucleophosmin and ING4 [26-30]. While the mechanism by which PAD4 regulates target gene activity is not entirely clear, Edman degradation and analysis using site-specific anti-citrullinated histone antibodies has found that PAD4 can target the N-terminal tails of histones H2A, H3, and H4 for citrullination. More specifically, PAD4 has been found to directly citrullinate histone H4 and H2A at arginine 3, and histone H3 at arginines 2, 8, 17, and 26. Histone tail citrullination has been found to promote chromatin decondensation *in vitro* and *in vivo* [31, 32]. Thus, it seems likely that the gene regulatory role of PAD4 is mediated by its initial recruitment to target promoters by the relevant transcription factor, followed by subsequent deimination of specific residues in the N-terminal histone tails, leading to local changes in chromatin architecture and modulation of target gene expression (Figure 1.2). PAD4 is both a corepressor and coactivator of gene transcription and also appears to contribute to epigenetic cross-talk [33] during DNA damage by acting in concert with histone deacetylase 2 (HDAC2) to regulate p53 target gene activity [34].

<u>Figure 1.2:</u> PAD mediated histone tail citrullination leads to chromatin decondensation.

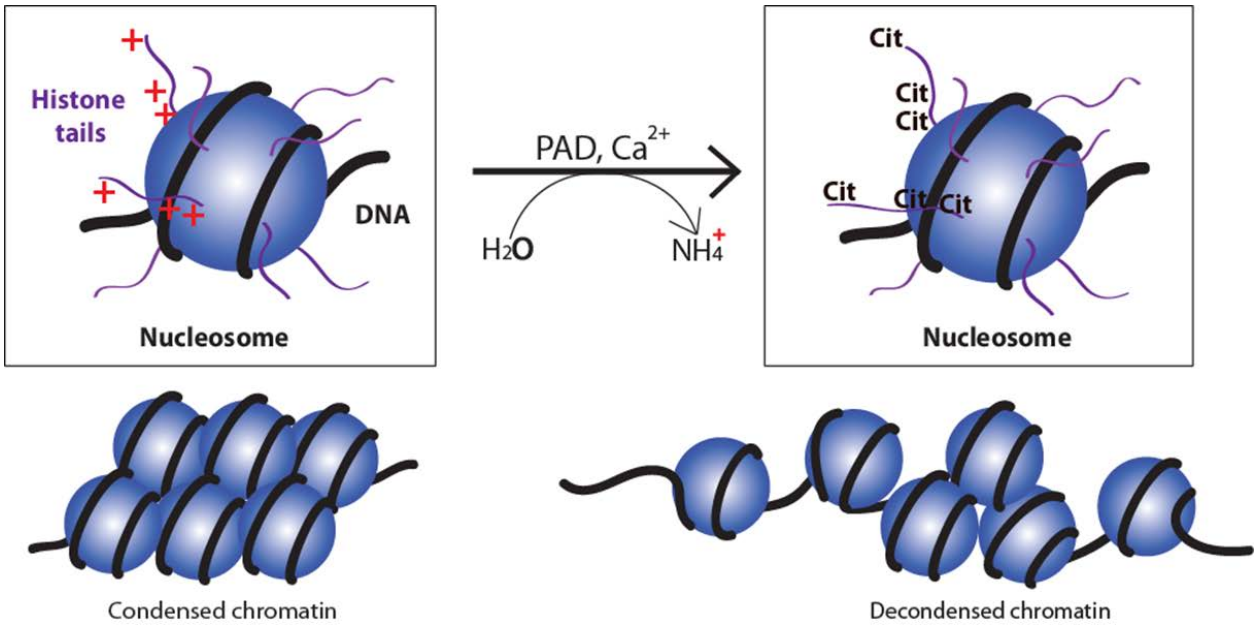

Following DNA damage, PAD4 and HDAC2 separate from the p53-target gene promoters such as p21, GADD45, and PUMA, resulting in an increased incidence of histone Lys acetylation and Arg methylation at these sites.

PAD6 is a maternal effect gene that is specifically expressed in oocytes and pre-implantation embryos and is essential for embryonic development beyond the 2-cell stage [35]. To date, there has been little evidence that this ovarian PAD isozyme is involved in cancer. Interestingly, however, a genome-wide SNP association in Icelanders showed a significant correlation between cutaneous basal cell carcinoma risk and mutations in the PAD4/PAD6 locus at 1p36 [36]. The importance of this PAD family member in developmental biology is reviewed elsewhere [37, 38] and will not be discussed further in this review.

1.4 Hormonal regulation of PADs

Early PAD biological studies focused mainly on the expression patterns of the different family members in reproductive tissues and also on their catalytic activity at these sites. Outcomes from these studies showed that anterior pituitary-localized rat lactotroph cells express PAD2 in a sexually dimorphic fashion, with expression confined to the female. Additional studies showed that PADs 1, 2, and 4 are present in uterine tissue and that protein citrullination is extensive in the uterine epithelium in an estrus cycle-dependent manner [39, 40]. More recently, studies have found that mouse, dog, and human mammary glands express both PAD2 and 4 in luminal epithelial cells [17].

Pituitary gland and uterus

In the female rat pituitary, PAD enzymatic activity is highest during proestrus and estrus when serum estrogen levels are at their peak [39, 41]. Ovariectomy of rats suppressed PAD activity in pituitary lysates, but activity could be restored by injection of exogenous estrogen. Furthermore, treatment of the pituitary-derived MtT/S cell line with estrogen results in a dose-dependent increase in PAD expression and activity [42]. Together, these observations suggest that estrogen directly influences PAD expression and activity in the pituitary. Given that estrogen primes lactotrophs for prolactin biosynthesis, PAD enzymatic activity may play an important role in this normal physiological process, and may also promote pituitary neoplastic growth.

Our examination of Massively Parallel Signature Sequencing (MPSS) transcriptome data (GEO Profiles GDS868) indicates that PADs 1, 2, and 4 expression levels are highest in the mouse uterus as compared to the 50 other tissues examined [43]. Furthermore, analysis of cDNA microarray data from Hewitt et al. shows that PAD1, 2, and 4 mRNA appear to be estrogen regulated [44]. In the uterus, the distribution of these isozymes appears to be primarily limited to glandular and luminal epithelial cells and also displays an estrous cycle-dependent regulation pattern, with the highest expression of these family members occurring during estrus [45, 46]. Similar to the pituitary,

PAD2 and PAD4 expression and activity in the uterus is lost following ovariectomy, but can be restored by injection of exogenous estrogen, indicative of estrogen regulation [45, 46]. Given the known mitogenic properties of estrogen in female cancers, it is possible that estrogen-induced upregulation of PAD expression and activity in the uterus may promote neoplastic growth in this tissue. However, a potential role for PADs in pituitary and uterine tumor progression has yet to be investigated.

Mammary gland

Protein and mRNA expression studies in canine mammary glands collected at various stages of the estrous cycle show that PAD2 expression initiates during estrus, with mRNA and protein levels peaking during diestrus. In the mouse mammary gland PAD2 and 4 expression is highest in luminal epithelial cell populations during the estrus [17, 46]. This species-specific difference in expression levels may reflect differences in estrous cycle stage lengths and hormone levels between species. Ovariectomy in mice also results in loss of PAD2 and 4 expression in the mammary gland, thus further corroborating the role of estrogen in PAD expression in female reproductive tissues. Molecular studies show that treatment of MCF-7 cells with estrogen rapidly induced the upregulation of PAD4 and the involvement of estrogen in PAD4 expression in mammary epithelial cells appears to be mediated by two upstream estrogen response elements (designated ERE -125 and -126) which are bound by ERα

following estrogen treatment. Furthermore, this study showed that the ERα-dependent increase in PAD4 expression can also be mediated by estrogen signaling to the PAD4 proximal promoter via cross talk with the AP-1, Sp-1, and NF-Y transcription factors [47].

1.5 PAD4 mediated histone tail citrullination: An emerging role for PADs in gene regulation and cancer

PAD4 has also been found to regulate estrogen receptor target gene activity following estrogen stimulation via histone tail citrullination [48]. Given the role of estrogen as a mitogen in cancer cells, this observation provides a clear potential link between PAD activity and cancer growth. In addition to estrogen, another mitogen, EGF, has been shown to utilize PAD4 as a cofactor to activate target gene activity. Zhang *e.t al.* documented that treatment of MCF-7 cells with EGF leads to PAD4-mediated citrullination of the ELK1 oncogene. This citrullination event then facilitated subsequent phosphorylation of ELK1 by ERK1/2, which, in turn, promoted histone acetylation and subsequent activation of a range of targets including the immediate early gene, c-fos [30]. PAD4 has also been found to interact with the major tumor suppressor, p53, and affect the expression of p53 target genes such as *p21*, *OKL38*, *CIP1* and *WAF1* [26-30]. Interestingly, a recent study also found that citrullination levels at histone H4 arginine 3 (H4R3) are inversely correlated with p53 protein expression and with tumor size in non-small cell lung cancer tissues [32]. The authors also demonstrated that the p53–PAD4 pathway leads to citrullination

of H4R3 and Lamin C in response to DNA damage and nuclear fragmentation. They also found that PAD4-mediated H4R3 citrullination appears to lead to localized chromatin decondensation around sites of DNA damage, thus facilitating p53-mediated cell death. *In vivo* studies then demonstrated that even though PAD4-null mice were grossly normal with regard to organ morphologies, they appeared resistant to apoptotic stimuli and also showed a consistent reduction in cleaved caspase-3 expression. The authors conclude that the histone H4 citrulline 3 (H4Cit3) modification may form a novel "apoptotic code" which could potentially be used to detect a range of damaged cells, including tumor cells, following treatment of patients with cancer therapies. It is interesting to note, however, that the PAD inhibitor Cl-amidine increases p53 levels both in cell culture and in inflammatory cells isolated from mice treated with this compound [29, 49]. Reconciling these two disparate observations requires further study. In support of a role for the H4Cit3 modification in marking apoptotic tumor cells, recent immunofluorescence studies in our lab found that citrullination at H4R3 was very robust within the nucleus of epithelial cells undergoing morphological changes associated with various stages of apoptosis in comedo-DCIS xenograft sections (**Figure 1.3**). These xenografts were generated from MCF10DCIS cell line which belongs to the group of MCF10AT tumor progression series of cell lines [50, 51].

<u>Figure 1.3</u>: H4cit3 (green) immunostaining of DCIS xenograft sections.

Nuclei are stained with DAPI (blue). Dotted line demarcates the area adjacent to the central necrotic core of the comedo-DCIS lesion. (Magnification 400X)

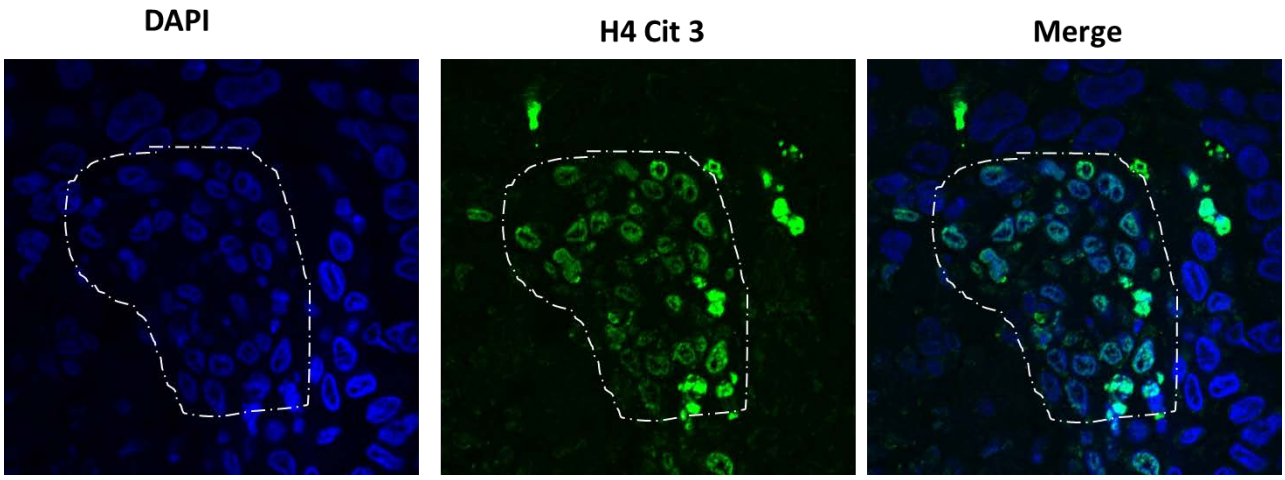

From a more clinical perspective, recent immunohistochemical and western blot studies have found that PAD4 appears to be overexpressed in several types of invasive carcinomas [5, 52, 53]. Outcomes from these studies found that PAD4 expression and, frequently activity, was elevated in neoplastic cells from breast carcinomas, lung adenocarcinomas, hepatocellular carcinomas, esophageal carcinomas with squamous differentiation, colorectal adenocarcinomas, renal carcinomas, ovarian adenocarcinomas, uterine carcinomas, uterine adenocarcinomas and bladder carcinomas [52]. However, PAD4 expression was absent or minimal in the following tumors: benign gastric and uterine leiomyomas, hyperplastic conditions of endometrium, cervical polyps, teratomas, hydatidiform moles, hemangiomas, lymphatic proliferative conditions, schwannomas and neurofibromas [5]. Consistent with the PAD4 protein expression pattern in carcinomas, the same patients also had elevated serum PAD4 activity and citrullinated anti-thrombin levels. Taken together these observations support the potential use of this enzyme as a clinical prognostic biomarker.

1.6 PAD2 and cancer pathogenesis

Given the volume of recent literature linking PAD4 with gene regulation in cancer cells, a role for this family member in tumor progression seems likely. Comparative studies evaluating PAD2 expression in mammary carcinomas from humans, dogs, and cats shows that the nuclear localization of PAD2 may also prove to be associated with tumor progression. Normal human, canine,

and feline mammary tissue shows strong nuclear and cytoplasmic PAD2 staining, but as tumors progress there is a general reduction in the nuclear localization of PAD2 (**Figure 1.4 and 1.5**) [54]. In the mammary gland, PAD2 expression is specific to cytokeratin positive luminal type epithelial cells (**Figure 1.5**). Thus, the loss of nuclear PAD2 may result in alterations in gene expression that lead to neoplastic transformation. It is interesting to note that a subset of invasive breast carcinomas tend to retain strong cytoplasmic and nuclear expression of PAD2. Further characterization of this subclass of tumors with regard to function of PAD2 is warranted as isozyme specific PAD inhibitors may be of use in combinatorial therapies to treat such tumor types. Given these new findings, and PAD4's documented role in cancer biology, it will be interesting to determine whether PAD2 and PAD4 may function in a synergistic manner to promote tumor progression. The observation that both PAD2 and PAD4 expression appears to be regulated at some level by estrogen, suggests that these two PADs may work together to mediate the estrogen response. The observations that PAD2 expression in mammary epithelial cells is induced by EGF [17], and that PAD4 regulates EGF-induced ELK1 target gene activation, suggests that PAD2 and PAD4 may also cooperate to mediate EGFR signaling [30].

Figure 1.4: PAD2 IHC staining of the normal human mammary gland, a DCIS lesion, and invasive carcinomas. Nuclear staining intensity is reduced in most invasive tumors while a subset of these tumors retains strong PAD2 staining. The sections are counterstained with hematoxylin (Magnification 200X)

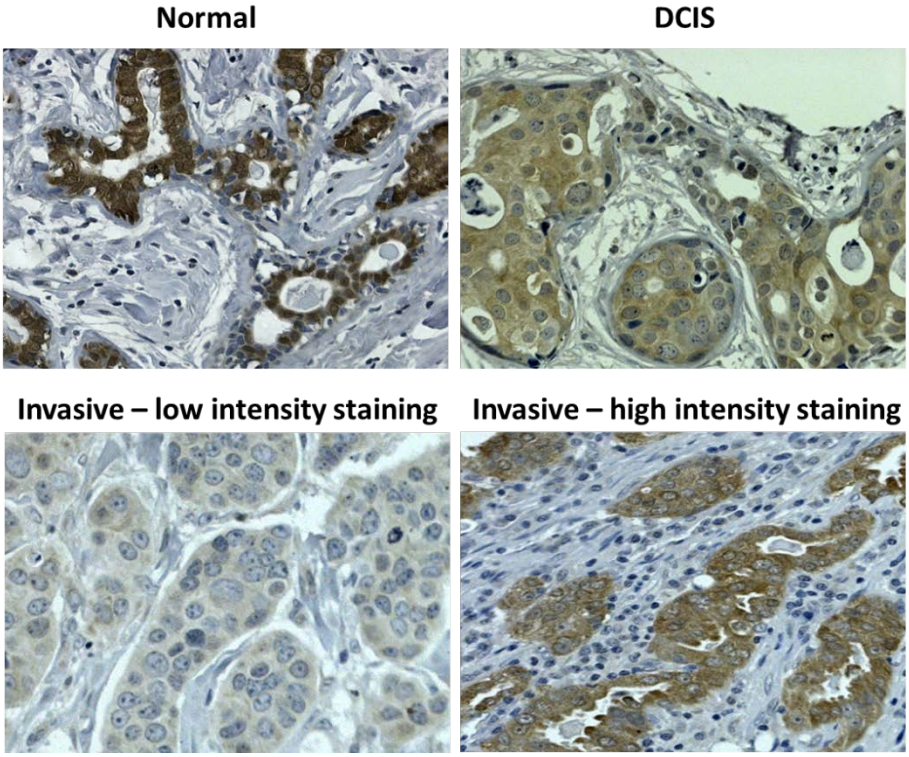

<u>Figure 1.5</u>: PAD2 (green) is expressed in luminal epithelial cells of preinvasive, invasive, and metastatic human mammary tumors. Cytokeratin (red) staining differentiates luminal epithelial type from myoepithelial cells. (Magnification 400X)

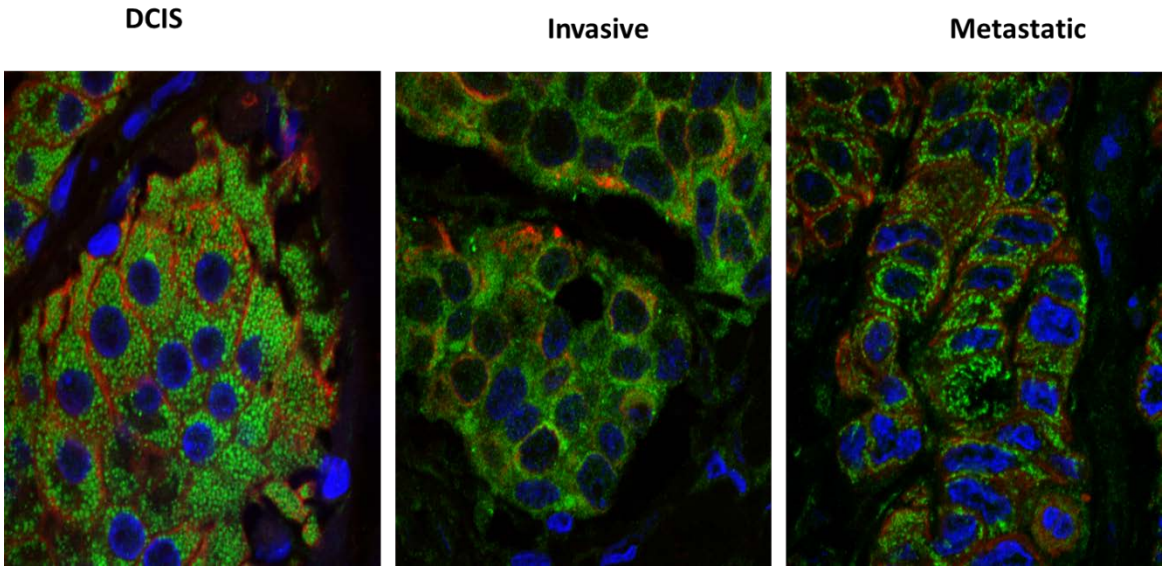

1.7 PAD inhibitors block cancer progression

In further support of a role for PADs in tumor growth, several recent reports have also shown that treatment of cancer cell lines with PAD inhibitors decreases cancer cell viability without affecting the growth of normal cells [55]. Cl-amidine [56], and the related PAD4 inhibitor, F-amidine [57], display low micromolar cytotoxicity towards various tumor cell lines such as U2OS cells, HL-60, HT-29, and MCF-7 [29, 55, 58]. These compounds also can induce the differentiation of HL-60 cells, a leukemic cell line, making these cells more susceptible to drug treatments [55]. Cl-amidine can also act synergistically with the anticancer drug doxorubicin, thus enhancing the efficiency of cell death following a simultaneous treatment with these two compounds. In tumor cell lines such as MCF-7 cells, Cl-amidine also regulates the expression of the tumor suppressor protein OKL38 in a p53-dependent manner by decreasing histone citrullination at the OKL38 promoter [28, 29].

A recent study, using a Cl-amidine derivative with increased cell permeability, YW3-56 (**Figure 1.6**), found that this drug significantly suppressed cancer cell growth and also reduced tumor size in mouse xenograft models of sarcoma [59]. Furthermore, this compound affected the expression of genes related to cell proliferation and cell death and was also found to regulate macro-autophagy in cancer cells. Mechanistically, the authors discovered that the drug likely targeted factors within the mTORC1 pathway for inhibition. These studies, as

well as the demonstration that PAD inhibitors are well tolerated in multiple different mouse disease models [49, 60], underscores the potential of PAD inhibitors as novel epigenetic anticancer drugs. Given that Cl-amidine, F-amidine, and YW3-56 display limited selectivity (**Figure 1.6**), it is unclear whether the inhibition of one or more PADs is required for the *in vivo* effects of these compounds. The development of new, more selective compounds, such as the PAD4 selective inhibitor TDFA and the PAD1 selective inhibitor o-F-amidine (**Figure 1.6**), will undoubtedly prove to be useful for sorting this issue out.

Figure 1.6: PAD inhibitors and their selectivity (TDFA - Threonine-aspartate-F-amidine; TDCA - Threonine-aspartate-Cl-amidine)

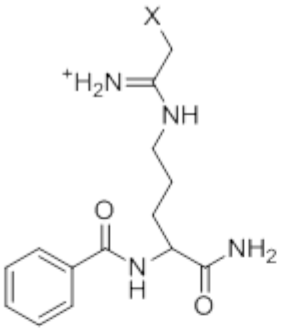

X = F F-amidine X = Cl Cl-amidine

	k_{inact}/K_I ($M^{-1}min^{-1}$)	selectivity	k_{inact}/K_I ($M^{-1}min^{-1}$)	selectivity
PAD1	2,800	1.1	37,000	0.4
PAD2	380	8	1,200	11
PAD3	170	18	2,000	7
PAD4	3,000	1	13,000	1

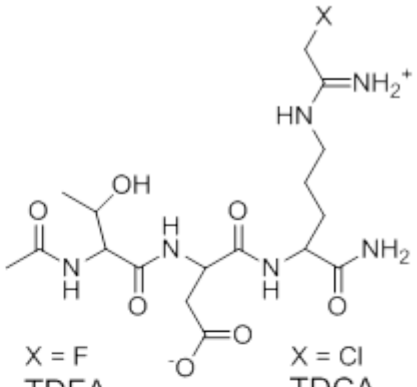

X = F TDFA X = Cl TDCA

	k_{inact}/K_I ($M^{-1}min^{-1}$)	selectivity	k_{inact}/K_I ($M^{-1}min^{-1}$)	selectivity
PAD1	1,700	15	21,000	1.1
PAD2	500	52	300	80
PAD3	400	65	920	26
PAD4	26,000	1	24,000	1

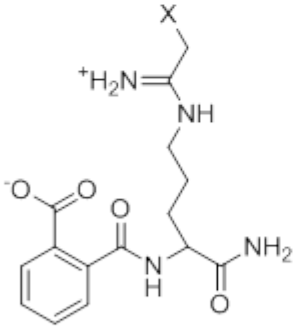

X = F *o*-F-amidine X = Cl *o*-Cl-amidine

	k_{inact}/K_I ($M^{-1}min^{-1}$)	selectivity	k_{inact}/K_I ($M^{-1}min^{-1}$)	selectivity
PAD1	181,000	1	106,000	1
PAD2	7,500	24	14,100	7.5
PAD3	6,700	27	10,400	10
PAD4	32,500	5.6	38,000	2.8

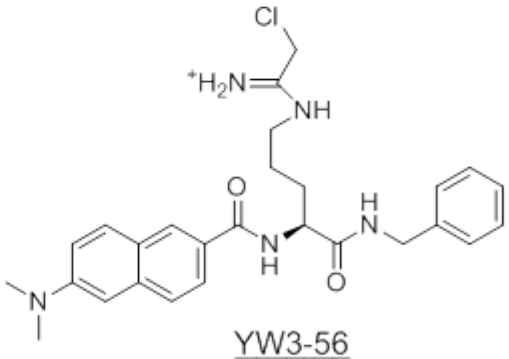

YW3-56

IC_{50} (μM)	selectivity
ND	ND
1-5	~1
ND	ND
1-5	~1

1.8 PAD-mediated citrullination: Linking inflammation with cancer progression?

Role of inflammation in cancer progression

Chronic inflammation is involved in the progression and recurrence of many types of cancer, including breast cancer. Epidemiological studies have documented that high levels of circulating acute phase inflammation-associated proteins at 3 years post-treatment are associated with an elevated risk for subsequent tumor recurrence and mortality in women [61]. Several studies have also demonstrated direct links between circulating inflammatory markers and progression to metastatic breast cancer [62-66]. Additionally, pro-inflammatory cytokines are well known for promoting tumor growth and facilitating metastasis by altering the tumor cell phenotype and by regulating stromal cells (endothelial cells, tumor-associated macrophages, and fibroblasts) within the tumor microenvironment. Furthermore, infiltrating immune cells within the tumor itself can promote tumorigenesis [67]. These findings suggest that the mechanisms by which inflammation in the tumor microenvironment drives metastasis is both intimately linked and fundamentally different to the primary mechanisms driving carcinogenesis [68].

Role of PADs in inflammation

As noted earlier, numerous studies have documented increased protein

citrullination within inflamed tissues from patients with autoimmune diseases such as rheumatoid arthritis and colitis [3, 4, 69]. More recently, these inflammatory symptoms have been shown to be suppressed by the PAD inhibitor, Cl-amidine, in mouse models of colitis and RA [49]. Another emerging link between PADs and inflammation is the newly defined role for PAD4 in catalyzing histone hypercitrullination during Neutrophil Extracellular Trap (NET) formation in inflamed tissues. A number of recent reports have shown that, following activation, peripheral blood neutrophils form a highly decondensed chromatin structure that both captures and kills invading pathogens [70-72] . Mechanistically, PAD4 was found to catalyze this dramatic chromatin decondensation event via histone tail hypercitrullination [73]. Analysis of this process at the ultrastructural level by electron microscopy showed that, following PAD4 activation in HL60 granulocytes, these cells show a dramatic and rapid conversion of multi-lobular heterochromatic nuclei to a more round euchromatic nuclear architecture, suggesting a direct role for PADs in heterochromatic-euchromatic interchange [31]. These new findings indicate that PAD4 can mediate chromatin structure change both at the local and genome-wide level.

Citrullination of vimentin is correlated with the proliferation of fibroblast-like synoviocytes (following isolation from patients with rheumatoid arthritis) and also stimulates TNF-α and IL-1 production in these cells [74]. Given the links between vimentin citrullination, inflammation, and cell proliferation, and given

how important cytoskeletal integrity is for cell motility, we hypothesize that citrullination of vimentin by PAD enzymes may also affect tumor cell migration and promote an inflammatory microenvironment. Additionally, given that PAD2 can regulate cytokine signaling in macrophages via citrullination of IKKγ (thus suppressing NF-kB activity) [75], we predict that PAD-mediated regulation of macrophage activity could also potentially affect cross-talk between tumor-associated macrophages and cancer cells.

While PAD activity has primarily been found to regulate autoimmune-mediated inflammatory events, recent studies suggest that PAD-mediated citrullination is also elevated in a variety of inflammatory states which lack a strong autoimmune component, such as COPD and myositis [76-78]. Perhaps the best demonstration that PAD-mediated citrullination can facilitate non-autoimmune or microbial-induced inflammatory events is the recent finding that PAD activity is strongly upregulated in inflamed tissue following a sterile skin punch biopsy procedure in mice [79]. Thus, it can be inferred that PAD-mediated citrullination plays a critical and fundamental role in inflammatory events induced by a range of pathologies, both infectious and non-infectious.

Role of PADs in chemokine signaling

PAD2 and PAD4 are highly expressed in peripheral blood mononuclear cells such as NK cells, T cells, B cells and monocytes [16] and, thus, are likely to be

the main PAD “players” in chemokine signaling. Chemokines are important for the proper recruitment of leukocytes to the site of inflammation. The chemokine-receptor system can be dramatically modified in neoplasms, especially at the invasive edges, and can act as a pro-angiogenic and a pro-desmoplastic mediator. Several chemokines, including CXCL1, 2 and 8 have been found to exert effects on tumor cell growth. The CXC group of chemokines, with the tripeptide (Glu-Leu-Arg/ELR) at the amino-terminus of the CXC motif (ELR+), is pro-angiogenic and stimulates cell migration and proliferation. The capacity of chemokines to activate or repress biological pathways depends, in part, upon post-translational modifications such as glycosylation and on proteolytic processing of the chemokine’s N- or C-terminus [80]. Importantly, PADs have recently been found to citrullinate CXCL5, CXCL8, CCL17, and CCL26 [81], thus directly modulating the inflammatory milieu. Furthermore, chemokine citrullination does not appear to be a rare event *in vivo,* as, for example, CXCL8 was found to be citrullinated at arginine 5 in 14 % of all blood leukocyte derived CXCL8 [81]. While the role of citrullinated chemokines in the inflammatory process is currently coming to light, their effect in cancer progression has yet to be investigated. However, given the strong links between inflammation and cancer progression, these observations support the hypothesis that PAD activity may play an important role in regulating the inflammatory milieu of the cancer microenvironment.

1.9 Conclusions

Protein citrullination is emerging as a critical post-translational modification in developmental biology, inflammation, and cancer pathogenesis. With respect to cancer, PAD enzymes are now being identified as important potential players in tumor progression that both regulate transcriptional activity and modulate the inflammatory microenvironment via cytokine citrullination. The major likely roles of PADs in cancer pathogenesis are summarized in **Figure 1.7**. Given these emerging links between PADs and cancer biology, a better understanding of the upstream mechanisms that induce PAD expression, and the downstream mechanisms by which PADs regulate gene expression and inflammatory events will likely advance our understanding of tumor biology. Furthermore, the upregulation of specific PAD isozymes and activity at critical points of tumor progression raises the possibility that these enzymes, and their resulting posttranslational modifications, can function as novel cancer biomarkers. Lastly, the observations that (1) PAD inhibitors reduce inflammatory symptoms in mouse models of disease, (2) the link between PADs, inflammation, and cancer is currently unfolding, and (3) next generation isozyme-specific PAD inhibitors are currently being developed, raise the possibility that the use of PAD inhibitors in preclinical and clinical cancer therapies may soon be realized.

Figure 1.7: **Potential role of PAD enzymes in cancer pathogenesis.**

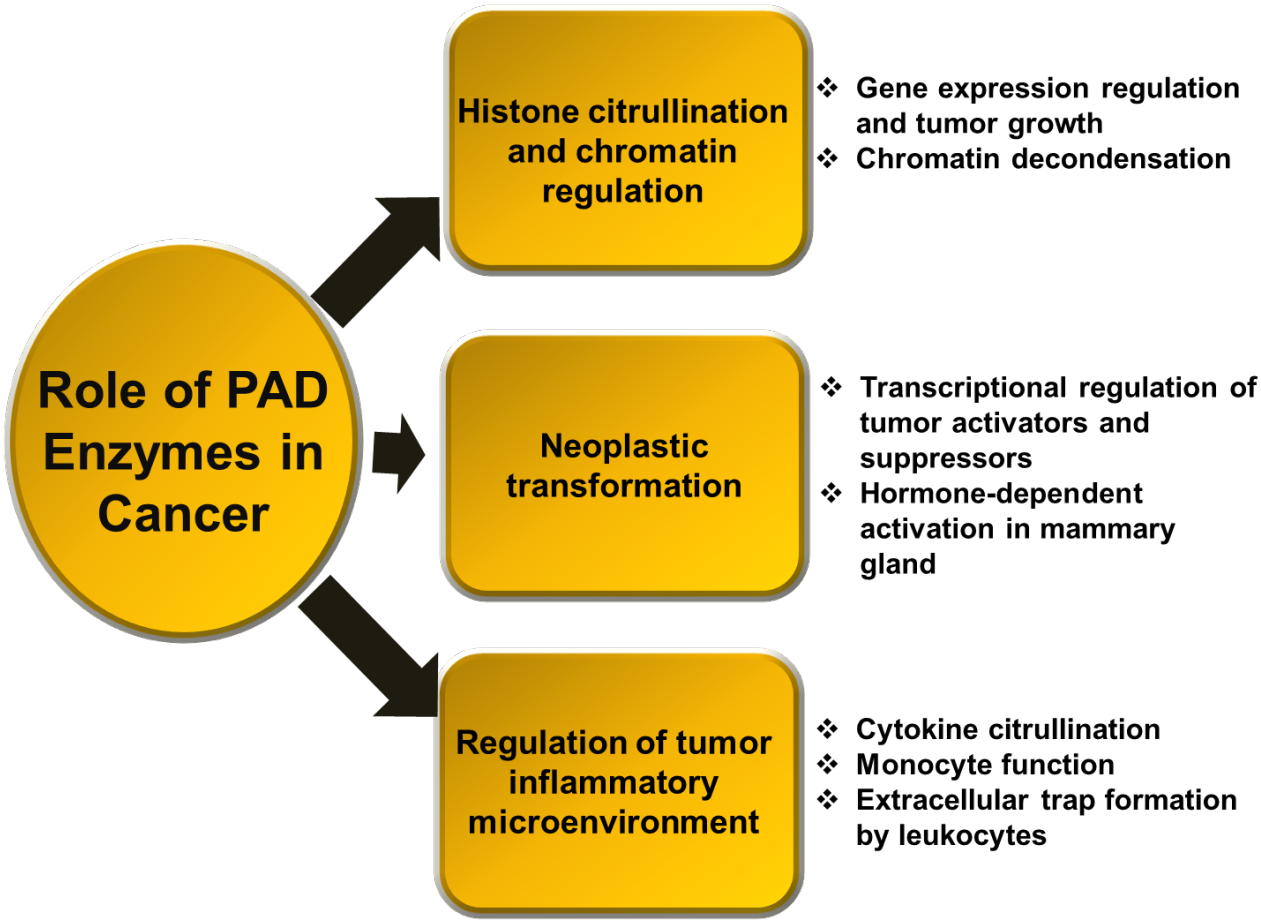

1.10 Acknowledgements

This work was supported by:

1) DOD Era of Hope Scholar Award (grant W871XWH-07-1-0372) to S.A.C.

2) NIGMS grant RO1 GM079357 to P.R.T.

The authors would like to thank Lynne Anguish for providing technical assistance in microscopic imaging and Kelly Emmott for helping with the xenograft studies.

1.12 References

1. Vossenaar, E.R., Zendman, A.J., van Venrooij, W.J. & Pruijn, G.J. PAD, a growing family of citrullinating enzymes: genes, features and involvement in disease. *Bioessays* **25**, 1106-18 (2003).

2. Denman, R.B. PAD: the smoking gun behind arginine methylation signaling? *Bioessays* **27**, 242-6 (2005).

3. Anzilotti, C., Pratesi, F., Tommasi, C. & Migliorini, P. Peptidylarginine deiminase 4 and citrullination in health and disease. *Autoimmun Rev* **9**, 158-60 (2010).

4. Chang, X. et al. Localization of peptidylarginine deiminase 4 (PADI4) and citrullinated protein in synovial tissue of rheumatoid arthritis. *Rheumatology (Oxford)* **44**, 40-50 (2005).

5. Chang, X. & Han, J. Expression of peptidylarginine deiminase type 4 (PAD4) in various tumors. *Mol Carcinog* **45**, 183-96 (2006).

6. Jones, J.E., Causey, C.P., Knuckley, B., Slack-Noyes, J.L. & Thompson, P.R. Protein arginine deiminase 4 (PAD4): Current understanding and future therapeutic potential. *Curr Opin Drug Discov Devel* **12**, 616-27 (2009).

7. De Ceuleneer, M., Van Steendam, K., Dhaenens, M. & Deforce, D. In vivo relevance of citrullinated proteins and the challenges in their detection. *Proteomics* **12**, 752-60 (2012).

8. Chavanas, S. et al. Comparative analysis of the mouse and human peptidylarginine deiminase gene clusters reveals highly conserved non-coding segments and a new human gene, PADI6. *Gene* **330**, 19-27 (2004).

9. Vossenaar, E.R. et al. Citrullination of synovial proteins in murine models of rheumatoid arthritis. *Arthritis Rheum* **48**, 2489-500 (2003).

10. Ellsworth, R.E. et al. Chromosomal alterations associated with the transition from in situ to invasive breast cancer. *Ann Surg Oncol* **15**, 2519-25 (2008).

11. Darrah, E., Rosen, A., Giles, J.T. & Andrade, F. Peptidylarginine deiminase 2, 3 and 4 have distinct specificities against cellular substrates: novel insights into autoantigen selection in rheumatoid arthritis. *Ann Rheum Dis* **71**, 92-8 (2012).

12. Knuckley, B. et al. Substrate specificity and kinetic studies of PADs 1, 3, and 4 identify potent and selective inhibitors of protein arginine deiminase 3. *Biochemistry* **49**, 4852-4863 (2010).

13. Pritzker, L.B., Joshi, S., Harauz, G. & Moscarello, M.A. Deimination of myelin basic protein. 2. Effect of methylation of MBP on its deimination by peptidylarginine deiminase. *Biochemistry* **39**, 5382-8 (2000).

14. Pritzker, L.B., Joshi, S., Gowan, J.J., Harauz, G. & Moscarello, M.A. Deimination of myelin basic protein. 1. Effect of deimination of arginyl residues of myelin basic protein on its structure and susceptibility to digestion by cathepsin D. *Biochemistry* **39**, 5374-81 (2000).

15. Musse, A.A. et al. Peptidylarginine deiminase 2 (PAD2) overexpression in transgenic mice leads to myelin loss in the central nervous system. *Dis Model Mech* **1**, 229-40 (2008).

16. Vossenaar, E.R. et al. Expression and activity of citrullinating peptidylarginine deiminase enzymes in monocytes and macrophages. *Ann Rheum Dis* **63**, 373-81 (2004).

17. Cherrington, B.D., Morency, E., Struble, A.M., Coonrod, S.A. & Wakshlag, J.J. Potential role for peptidylarginine deiminase 2 (PAD2) in citrullination of canine mammary epithelial cell histones. *PLoS One* **5**, e11768 (2010).

18. Cherrington, B.D. et al. Potential Role for PAD2 in Gene Regulation in Breast Cancer Cells. *PLoS One* **7**, e41242 (2012).

19. Zhang, X. et al. Peptidylarginine deiminase 2-catalyzed histone H3 arginine 26 citrullination facilitates estrogen receptor alpha target gene activation. *Proc Natl Acad Sci U S A* **(In Press)** (2012).

20. Nachat, R. et al. Peptidylarginine deiminase isoforms 1-3 are expressed in the epidermis and involved in the deimination of K1 and filaggrin. *J Invest Dermatol* **124**, 384-93 (2005).

21. Chang, X. & Fang, K. PADI4 and tumourigenesis. *Cancer Cell Int* **10**, 7 (2010).

22. Nakashima, K., Hagiwara, T. & Yamada, M. Nuclear localization of peptidylarginine deiminase V and histone deimination in granulocytes. *J*

Biol Chem **277**, 49562-8 (2002).

23. Chang, X. et al. The inhibition of antithrombin by peptidylarginine deiminase 4 may contribute to pathogenesis of rheumatoid arthritis. *Rheumatology (Oxford)* **44**, 293-8 (2005).

24. Ordonez, A. et al. Effect of citrullination on the function and conformation of antithrombin. *FEBS J* **276**, 6763-72 (2009).

25. Ordonez, A. et al. Increased levels of citrullinated antithrombin in plasma of patients with rheumatoid arthritis and colorectal adenocarcinoma determined by a newly developed ELISA using a specific monoclonal antibody. *Thromb Haemost* **104**, 1143-9 (2010).

26. Tanikawa, C. et al. Regulation of protein Citrullination through p53/PADI4 network in DNA damage response. *Cancer Res* **69**, 8761-9 (2009).

27. Guo, Q. & Fast, W. Citrullination of inhibitor of growth 4 (ING4) by peptidylarginine deminase 4 (PAD4) disrupts the interaction between ING4 and p53. *J Biol Chem* **286**, 17069-78 (2011).

28. Yao, H. et al. Histone Arg modifications and p53 regulate the expression of OKL38, a mediator of apoptosis. *J Biol Chem* **283**, 20060-8 (2008).

29. Li, P. et al. Regulation of p53 target gene expression by peptidylarginine deiminase 4. *Mol Cell Biol* **28**, 4745-58 (2008).

30. Zhang, X. et al. Genome-wide analysis reveals PADI4 cooperates with Elk-1 to activate c-Fos expression in breast cancer cells. *PLoS Genet* **7**, e1002112 (2011).

31. Wang, Y. et al. Histone hypercitrullination mediates chromatin decondensation and neutrophil extracellular trap formation. *J Cell Biol* **184**, 205-13 (2009).

32. Tanikawa, C. et al. Regulation of histone modification and chromatin structure by the p53–PADI4 pathway. *Nature Communications* **3**, 676 (2012).

33. Rust, H.L. & Thompson, P.R. Kinase Consensus Sequences: A Breeding Ground for Crosstalk. *ACS Chem Biol* **6**, 881-892 (2011).

34. Li, P. et al. Coordination of PAD4 and HDAC2 in the regulation of p53-target gene expression. *Oncogene* **29**, 3153-62 (2010).

35. Yurttas, P. et al. Role for PADI6 and the cytoplasmic lattices in ribosomal storage in oocytes and translational control in the early mouse embryo. *Development* **135**, 2627-36 (2008).

36. Stacey, S.N. et al. Common variants on 1p36 and 1q42 are associated with cutaneous basal cell carcinoma but not with melanoma or pigmentation traits. *Nat Genet* **40**, 1313-8 (2008).

37. Yurttas, P., Morency, E. & Coonrod, S.A. Use of proteomics to identify highly abundant maternal factors that drive the egg-to-embryo transition. *Reproduction* **139**, 809-23 (2010).

38. Li, L., Zheng, P. & Dean, J. Maternal control of early mouse development. *Development* **137**, 859-70 (2010).

39. Senshu, T., Akiyama, K., Nagata, S., Watanabe, K. & Hikichi, K. Peptidylarginine deiminase in rat pituitary: sex difference, estrous cycle-related changes, and estrogen dependence. *Endocrinology* **124**, 2666-70 (1989).

40. Takahara, H. et al. Peptidylarginine deiminase of the mouse. Distribution, properties, and immunocytochemical localization. *J Biol Chem* **264**, 13361-8 (1989).

41. Watanabe, K. et al. The rat peptidylarginine deiminase-encoding gene: structural analysis and the 5'-flanking sequence. *Gene* **114**, 261-5 (1992).

42. Nagata, S., Uehara, T., Inoue, K. & Senshu, T. Increased peptidylarginine deiminase expression during induction of prolactin biosynthesis in a growth-hormone-producing rat pituitary cell line, MtT/S. *J Cell Physiol* **150**, 426-32 (1992).

43. Barrett, T. et al. NCBI GEO: archive for high-throughput functional genomic data. *Nucleic Acids Res* **37**, D885-90 (2009).

44. Hewitt, S.C. et al. Estrogen receptor-dependent genomic responses in the uterus mirror the biphasic physiological response to estrogen. *Mol Endocrinol* **17**, 2070-83 (2003).

45. Takahara, H. et al. Expression of peptidylarginine deiminase in the

uterine epithelial cells of mouse is dependent on estrogen. *J Biol Chem* **267**, 520-5 (1992).

46. Horibata, S., Coonrod, S.A. & Cherrington, B.D. Role for peptidylarginine deiminase enzymes in disease and female reproduction. *J Reprod Dev* **58**, 274-82 (2012).

47. Dong, S., Zhang, Z. & Takahara, H. Estrogen-enhanced peptidylarginine deiminase type IV gene (PADI4) expression in MCF-7 cells is mediated by estrogen receptor-alpha-promoted transfactors activator protein-1, nuclear factor-Y, and Sp1. *Mol Endocrinol* **21**, 1617-29 (2007).

48. Wang, Y. et al. Human PAD4 regulates histone arginine methylation levels via demethylimination. *Science* **306**, 279-83 (2004).

49. Chumanevich, A.A. et al. Suppression of colitis in mice by Cl-amidine: a novel peptidylarginine deiminase inhibitor. *Am J Physiol Gastrointest Liver Physiol* **300**, G929-38 (2011).

50. Tait, L.R. et al. Dynamic stromal-epithelial interactions during progression of MCF10DCIS.com xenografts. *Int J Cancer* **120**, 2127-34 (2007).

51. Miller, F.R., Santner, S.J., Tait, L. & Dawson, P.J. MCF10DCIS.com xenograft model of human comedo ductal carcinoma in situ. *J Natl Cancer Inst* **92**, 1185-6 (2000).

52. Wang, L., Chang, X., Yuan, G., Zhao, Y. & Wang, P. Expression of

peptidylarginine deiminase type 4 in ovarian tumors. *Int J Biol Sci* **6**, 454-64 (2010).

53. Chang, X. et al. Increased PADI4 expression in blood and tissues of patients with malignant tumors. *BMC Cancer* **9**, 40 (2009).

54. Cherrington, B.D. et al. Comparative analysis of peptidylarginine deiminase-2 expression in canine, feline and human mammary tumours. *J Comp Pathol* **147**, 139-46 (2012).

55. Slack, J.L., Causey, C.P. & Thompson, P.R. Protein arginine deiminase 4: a target for an epigenetic cancer therapy. *Cell Mol Life Sci* **68**, 709-20 (2011).

56. Luo, Y. et al. Inhibitors and inactivators of protein arginine deiminase 4: functional and structural characterization. *Biochemistry* **45**, 11727-36 (2006).

57. Luo, Y., Knuckley, B., Lee, Y.H., Stallcup, M.R. & Thompson, P.R. A Fluoro-Acetamidine Based Inactivator of Protein Arginine Deiminase 4 (PAD4): Design, Synthesis, and in vitro and in vivo Evaluation. *J Am Chem Soc* **128**, 1092-1093 (2006).

58. Knuckley, B., Luo, Y. & Thompson, P.R. Profiling Protein Arginine Deiminase 4 (PAD4): a novel screen to identify PAD4 inhibitors. *Bioorg Med Chem* **16**, 739-45 (2008).

59. Wang, Y. et al. Anticancer Peptidylarginine Deiminase (PAD) Inhibitors Regulate the Autophagy Flux and the Mammalian Target of Rapamycin

Complex 1 Activity. *J Biol Chem* **287**, 25941-53 (2012).

60. Willis, V.C. et al. N-α-Benzoyl-N5-(2-Chloro-1-Iminoethyl)-L-Ornithine Amide, a Protein Arginine Deiminase Inhibitor, Reduces the Severity of Murine Collagen-Induced Arthritis. *J Immunol* **186**, 4396-4404 (2011).

61. Pierce, B.L. et al. Correlates of circulating C-reactive protein and serum amyloid A concentrations in breast cancer survivors. *Breast Cancer Res Treat* **114**, 155-67 (2009).

62. Ahmed, O.I., Adel, A.M., Diab, D.R. & Gobran, N.S. Prognostic value of serum level of interleukin-6 and interleukin-8 in metastatic breast cancer patients. *Egypt J Immunol* **13**, 61-8 (2006).

63. Bachelot, T. et al. Prognostic value of serum levels of interleukin 6 and of serum and plasma levels of vascular endothelial growth factor in hormone-refractory metastatic breast cancer patients. *Br J Cancer* **88**, 1721-6 (2003).

64. Cole, S.W. Chronic inflammation and breast cancer recurrence. *J Clin Oncol* **27**, 3418-9 (2009).

65. Salgado, R. et al. Circulating interleukin-6 predicts survival in patients with metastatic breast cancer. *Int J Cancer* **103**, 642-6 (2003).

66. Zhang, G.J. & Adachi, I. Serum interleukin-6 levels correlate to tumor progression and prognosis in metastatic breast carcinoma. *Anticancer Res* **19**, 1427-32 (1999).

67. Coussens, L.M. & Werb, Z. Inflammation and cancer. *Nature* **420**, 860-7 (2002).

68. Fidler, I.J. The pathogenesis of cancer metastasis: the 'seed and soil' hypothesis revisited. *Nat Rev Cancer* **3**, 453-8 (2003).

69. Auger, I., Charpin, C., Balandraud, N., Martin, M. & Roudier, J. Autoantibodies to PAD4 and BRAF in rheumatoid arthritis. *Autoimmun Rev* (2012).

70. Saffarzadeh, M. et al. Neutrophil extracellular traps directly induce epithelial and endothelial cell death: a predominant role of histones. *PLoS One* **7**, e32366 (2012).

71. Liu, C.L. et al. Specific post-translational histone modifications of neutrophil extracellular traps as immunogens and potential targets of lupus autoantibodies. *Arthritis Res Ther* **14**, R25 (2012).

72. Amulic, B. & Hayes, G. Neutrophil extracellular traps. *Curr Biol* **21**, R297-8 (2011).

73. Li, P. et al. PAD4 is essential for antibacterial innate immunity mediated by neutrophil extracellular traps. *J Exp Med* **207**, 1853-62 (2010).

74. Fan, L. et al. Citrullinated vimentin stimulates proliferation, pro-inflammatory cytokine secretion, and PADI4 and RANKL expression of fibroblast-like synoviocytes in rheumatoid arthritis. *Scand J Rheumatol*, [Epub ahead of print] (2012).

75. Lee, H.J. et al. Peptidylarginine deiminase 2 suppresses inhibitory {kappa}B kinase activity in lipopolysaccharide-stimulated RAW 264.7 macrophages. *J Biol Chem* **285**, 39655-62 (2010).

76. Ruiz-Esquide, V. et al. Anti-citrullinated peptide antibodies in the serum of heavy smokers without rheumatoid arthritis. A differential effect of chronic obstructive pulmonary disease? *Clin Rheumatol* **31**, 1047-50 (2012).

77. Kilsgard, O. et al. Peptidylarginine deiminases present in the airways during tobacco smoking and inflammation can citrullinate the host defense peptide LL-37, resulting in altered activities. *Am J Respir Cell Mol Biol* **46**, 240-8 (2012).

78. Makrygiannakis, D. Citrullination is an inflammation-dependent process. *Annals of the rheumatic diseases* **65**, 1219 (2006).

79. Coudane, F. et al. Deimination and expression of peptidylarginine deiminases during cutaneous wound healing in mice. *Eur J Dermatol* **21**, 376-84 (2011).

80. Mortier, A., Gouwy, M., Van Damme, J. & Proost, P. Effect of posttranslational processing on the in vitro and in vivo activity of chemokines. *Exp Cell Res* **317**, 642-54 (2011).

81. Proost, P. et al. Citrullination of CXCL8 by peptidylarginine deiminase alters receptor usage, prevents proteolysis, and dampens tissue inflammation. *J Exp Med* **205**, 2085-97 (2008).

CHAPTER TWO

HUMAN PAD2 TRANSGENE OVEREXPRESSION LEADS TO SPONTANEOUS SKIN NEOPLASIA AND PROMOTES MALIGNANCY AND TUMOR-ASSOCIATED INFLAMMATION IN CHEMICALLY INITIATED SKIN TUMORS IN MICE

Printed from the manuscript: Sunish Mohanan[†]; John L. McElwee[†]; Sachi Horibata; Kelly Sams; Dalton McLean; Lynne Anguish; Angela Yan; Iva Cvitaš; and Scott A. Coonrod. PAD2 overexpression in transgenic mice leads to premalignant skin lesions and progression to squamous cell carcinoma. In preparation (**[†]** Equal contribution).

Author contributions: Conceived and designed experiments – SM, JLM, SAC; Performed chemical carcinogenesis treatment – LA, KS; Performed qPCR analysis and western blots – JLM, SH IC, DM, AY; Performed histopathological analysis and scoring – SM; Performed IHC and IF experiments – SM and AY; Manuscript preparation and editing – SM and JLM.

2.1 Abstract

Introduction:

Peptidylarginine deiminases (PADIs) are a family of posttranslational modification enzymes that convert positively charged arginine residues on substrate proteins to neutrally charged citrulline. This activity, called citrullination or deimination, has been shown to have wide-ranging effects on target protein structure, function, and protein-protein interactions. PADI2 has been implicated in various diseases, including multiple sclerosis, inflammatory diseases such as RA and COPD, and more recently, cancer. We have recently reported that PADI2 and HER2 expression is correlated in breast cancer cell lines, and that PADI2 plays a role in the proliferation of mammary tumors *in vitro* and *in vivo*. The goal of this study was to analyze whether the transgenic over-expression of PADI2 driven by the MMTV-LTR promoter can induce oncogenesis in hormone-responsive epithelium.

Methods:

To examine whether the overexpression of PADI2 is sufficient to drive tumorigenesis in epithelial tissue, we cloned human FLAG-tagged PADI2 cDNA downstream of the hormone-responsive MMTV-LTR promoter. We generated four founder lines in FVB mice expressing the MMTV-FLAG-PADI2 transgene, and performed phenotypic and genetic analysis of these mice. We have created stable cell lines overexpressing FLAG-PADI2 in the human skin cancer cell line A431 to validate our findings in the transgenic mice. Lastly, In

order to further characterize the rate of tumor formation and histopathological properties of skin tumors, in this study we initiated skin tumors in wild type (WT) and MMTV-FLAG-hPAD2 mice using a 9,10-dimethyl-1,2-benzanthracene followed by *O*-tetradecanoylphorbol-13-acetate (DMBA - TPA) chemical carcinogenesis treatment model.

Results:

The ectopic expression of human PADI2 in mouse epithelium is sufficient to promote neoplasia, as we report that ~20% of transgenic mice develop proliferative skin lesions. Interestingly we found that in a subset of these mice, these lesions further progress to more invasive phenotype such as squamous cell carcinomas. In addition, we note that these skin lesions express high levels of transgene, as well as display alteration in markers of EMT (decreased E-cadherin) and inflammation (increased IL6/IL8). We further confirmed these results in the human squamous cell carcinoma cell line A431, where we report that stable over-expression of FLAG-PADI2 increases markers of inflammation (IL6/IL8) and EMT, ultimately resulting in increased tumor cell invasiveness. No untreated mice developed skin lesions during the evaluation period in this study. The MMTV-FLAG-hPAD2 mice developed higher number of papillomas with a faster tumor growth rate. More significantly, histopathologic analysis showed that in MMTV-FLAG-hPAD2 mice, skin tumors developed to invasive SCC more frequently than the WT controls. The MMTV-FLAG-hPAD2 tumors were highly inflamed with dense

inflammatory cell infiltrate and increased markers for tumor-associated inflammation and epithelial-mesenchymal transition (EMT). Specifically, CCL17, IL6 and murine IL8 homologues (LIX, MIP2), and the mesenchymal marker, Vimentin, were elevated in the transgenic tumors while the cell adhesion marker, E-cadherin, expression was decreased compared to the WT tumors suggesting the enhanced invasiveness of the transgenic tumors. Furthermore, the levels of nuclear phospho-STAT3 (signal transducer and activator of transcription 3) were increased in the transgenic tumors which are consistent with the IL8 and IL6 downstream signaling in a cytokine rich microenvironment.

Conclusion:

Collectively, these studies provide functional and mechanistic evidence establishing PADI2 as a potential novel oncogene in the development of skin neoplasia, and might offer a new target for cancer therapy. These data suggest that hPAD2 transgene can dramatically increase the malignant conversion rate of benign tumors and cause elevated tumor-associated inflammation.

Key words: Peptidylarginine deiminase, PAD2/PADI2, MMTV-LTR, MMTV-FLAG-PADI2, Skin Neoplasia, Squamous Cell Carcinoma, A431, Tumor-associated Inflammation, EMT

2.2 Introduction

The peptidylarginine deiminase family of posttranslational modification enzymes converts positively charged arginine residues on substrate proteins to neutrally charged citrulline. This activity, alternatively called citrullination or deimination, has been shown to have wide-ranging effects on target protein structure, function, and protein-protein interactions. The PADI enzyme family is thought to have arisen by gene duplication and localizes within the genome to a highly organized cluster at 1p36.13 in humans. At the protein level, each of the five well-conserved PADI members shows a relatively distinct pattern of substrate specificity and tissue distribution [1, 2]. Increasingly, the dysregulation of PADI activity is associated with a range of diseases, including rheumatoid arthritis (RA), multiple sclerosis, ulcerative colitis, neural degeneration, COPD, and cancer [3-5]. While the presumptive function of PADI activity in most diseases is linked to inflammation, the role that PADIs play in cancer progression is still under investigation. Others have shown that citrullination of the p53 tumor suppressor protein by PADI4 affects the expression of p53-target genes *p21*, *OKL38*, *CIP1* and *WAF1* [6-8]. While PADI2 has historically been defined as a cytoplasmic protein, recent evidence from our lab showed that PADI2 can localize to the nucleus and directly bind chromatin to influence target gene expression [9-12].

Our recent studies suggest a role for PADI2 in the oncogenic progression of breast cancer, more specifically, HER2-positive tumors, as RNA-seq data

reveal that *PADI2* is highly correlated with *HER2/ERBB2* overexpression across 57 breast cancer cell lines. We concluded this study with the first preclinical evidence showing that the PADI inhibitor, Cl-amidine, could be utilized as a therapeutic agent for the treatment of tumors *in vivo*.

To further investigate the involvement of PADI2 in the oncogenesis of epithelial tumors, we generated FVB mice expressing FLAG-PADI2 under the control of the hormone-responsive mammary tumor virus (MMTV) promoter. However, while transgenic expression of human *PADI2* in mammary glands was detected, the MMTV-FLAG-PADI2 mice failed to develop any mammary tumors. While expression from the MMTV-LTR promoter is normally found to be localized to the mammary and salivary gland, other tissues have been implicated, including the skin and ovaries [13, 14]. Our results confirm this pattern of expression, as we see increased transgenic human *PADI2* transcript levels in the all four of those tissues. Surprisingly, we discovered that 20% of the transgenic mice developed skin proliferative lesions after five months. These tumors expressed high levels of transgenic human *PADI2* and display markers of increased invasiveness and epithelial to mesenchymal transition (EMT). Furthermore, some of these tumors display the hallmarks of malignant progression to highly invasive squamous cell carcinomas.

Previous studies have reported that three PADI isozymes, PADI1, PADI2, and PADI3, re expressed in the epidermis, with all three displaying the ability to

target filaggrin for citrullination, a key protein involved in tissue hydration and barrier functions [15]. PADI1 and PADI3 have been the primary isozymes characterized in the epidermis to date; with PADI3 being found to deiminate trichohyalin in hair follicles [16, 17] and PADI1 deiminating keratin (K1 and K10) and filaggrin during epidermal differentiation [18, 19]. Moreover, the overexpression of PADI1 (along with PADI2 and PADI3), has been shown to generate abnormal levels of citrullinated keratin K1 in the epidermis of psoriatic patients [20]. This suggests that aberrant expression of PADIs, including PADI2, might play a role in diseases of the skin, including cancer.

Interestingly, the original cloning of human *PADI2* cDNA was from the human skin cancer cell line, HSC-1, which is derived from a cutaneous squamous carcinoma [21]. We report here a novel model of skin neoplasia in FVB transgenic mice, driven by human PADI2 under the MMTV-LTR promoter; thus, establishing a novel role for PADI2 in cancer progression. We further characterized this novel model of skin neoplasia in MMTV-FLAG-hPAD2 transgenic mice by conducting a two-stage chemical carcinogenesis study.

DMBA-TPA chemical carcinogenesis model is widely used to test the susceptibility of transgenic mice to develop skin neoplasia [22-24]. DMBA has been shown to induce an irreversible mutation in mouse skin (an A-to-T transversion in codon 61 of the oncogene Ha-ras) [25-27]. Two stage chemical carcinogenesis models use phorbol esters or other mitogenic agents to

promote proliferation of an initiated cell. This results in expansion of a clonal population of cells which typically develops into benign non-invasive tumors such as papilloma. After withdrawal of these agents these benign lesions may regress or remain stable [28]. This phenomenon allows this model to study tumor progression into invasiveness in the presence of a transgene. Tumor invasion and metastasis involve evolution of benign tumor cells permitting their expansion and growth within a nonphysiological microenvironment [24, 29]

We were also interested in comparing the histopathological features of tumor invasiveness, tumor associated inflammation and cytokine levels between the transgenic and WT tumors. The significant contribution of inflammation to tumor development, progression, and microenvironment regulation has gained increased acceptance in recent years [30]. we predicted that hPAD2 overexpressing skin tumors in the DMBA-TPA treated mice also will show increased inflammatory cytokine expression and invasiveness compared to the WT tumors.

2.3 Materials and Methods

Generation of MMTV-FLAG-PADI2 mice

To generate the MMTV-FLAG-PADI2 construct, a human PADI2 cDNA fragment was removed from pcDNA3.1-FLAG-PADI2 [11], and cloned into the EcoRI sites of the MMTV-SV40-Bssk plasmid (Addgene plasmid #1824) that

was originally generated in the laboratory of Dr. Philip Leder at Harvard Medical School [31]. The linear MMTV-FLAG-PADI2 construct was purified and microinjected into the pronuclei of fertilized embryos from super-ovulated FVB mice, and 2-cell stage embryos were transferred to pseudopregnant mothers. The microinjection and embryo transfer was performed by the Stem Cell and Transgenics Core at the Cornell University College of Veterinary Medicine. Mice were genotyped for the presence of human PADI2 transgene by PCR with the primers hPADI2-cds-F/R (**see Table 2.1**).

Lentivirus and plasmids for stable FLAG-PADI2 expression in A431 cells

The human squamous cell carcinoma A431 cell line was obtained from ATCC and cultured according to manufacturer's directions. To generate A431 cells overexpressing FLAG-tagged PADI2, two separate plasmids were generated. First, for stably transfected A431, FLAG-PADI2 was subcloned (NheI/XhoI) from pcDNA3.1-FLAG-PADI2 [11] into the pIRES2-EGFP vector (Clontech). This vector has bicistronic expression of both FLAG-PADI2 and EGFP by means of an internal ribosome entry site (IRES). A431 cells were transfected with pIRES2-FLAG-PADI2 using X-tremeGENE 9 (Roche) and stable cells were selected in 800 µg/ml G418 for 2-weeks. To generate lentiviral-transduced cells, the FLAG-PADI2-IRES-EGFP fragment was excised from the pIRES2-FLAG-PADI2 plasmid by digestion with MluI and SspI. The linearized fragment was blunted with T4 DNA polymerase (NEB), and subcloned into the BamHI-SalI digested/ T4 blunted pLenti-PGK-GFP-Puro plasmid (Addgene #19070)

that was originally generated by Campeau et al. at the University of Massachusetts Medical School [32]. This plasmid was verified by restriction digest and sequencing, and transduction of A431 cells was performed as previously described in Campeau et al. using 3rd generation lentiviral packaging/envelope vectors (pLP1-pMDLg/pRRE, Addgene #12251; pLP2-pRSV-Rev, Addgene #12253; and pVSV-G-pMD2.G, Addgene #12259). Stably transduced cells were selected in 1 µg/ml puromycin for 2-weeks.

Mouse skin two-stage carcinogenesis assay

Two sets of 20 mice each from wild type and PAD2OE groups were selected at 6 weeks of age for the carcinogenesis study. We used a well characterized two-stage chemical carcinogenesis protocol [33] which included tumor initiation by an initial topical application of 10 nm of DMBA (9, 10-dimethyl-1,2-benzathracene) in 200 µL of acetone to previously shaved dorsal skin. Tumors were promoted by twice weekly applications of 1.0 µg of 12-O-tetradecanoylphorbol-13-acetate (TPA) in 200 µl of acetone beginning 2 weeks after initiation. The mice were monitored for tumor development, scored for number of visible papillomas at the DMBA-TPA application site, and the size of papillomas was measured. After 20 weeks of treatment, mice were euthanized and the skin lesions were fixed in 4% PFA at 4C for 24 hours, paraffin embedded, and sectioned for histopathological evaluation and immunostaining.

Immunohistochemistry (IHC) and immunofluorescence (IF)

IHC and IF experiments were carried out using a standard protocol as previously described [9]. Primary antibodies are as follows: anti-PADI2 (12110-1-AP, ProteinTech), anti-FLAG-M2 (F1804, Sigma), anti-Ki67 (ab15580, Abcam), anti-phosphoSTAT3 (9131S, Cell signaling) and anti-GFP (ab290, Abcam). Sections prepared for IHC were incubated in DAB chromagen solution (Vector Laboratories) according to the manufacturer's protocol, washed, and then counterstained with hematoxylin. The IF slides were incubated in streptavidin conjugated-488 (Invitrogen), washed, and then mounted using Vectashield containing DAPI (Vector Laboratories). Negative controls for both IHC and IF experiments were either rabbit or mouse IgG antibody at the appropriate concentrations. Formalin fixed, paraffin embedded, H&E stained tumor sections from transgenic mice were examined for histopathological characteristics by a pathologist.

Western blotting

Western blotting was carried out as previously described [9]. Primary antibodies against PADI2 (12110-1-AP, ProteinTech), anti-phosphoSTAT3 (9131S, Cell signaling) and FLAG-M2 (F1804, Sigma) were incubated overnight at 4^{o}C. To confirm equal protein loading, membranes were stripped and re-probed with anti-β-actin (ab8227, Abcam).

RNA isolation, semi-quantitative, and quantitative Real-Time PCR (qRT-PCR)

RNA was purified using the Qiagen RNAeasy kit, including on-column DNase treatment to remove genomic DNA. The resulting RNA was reverse transcribed using the ABI High Capacity RNA-to-cDNA kit according to the manufacturer's protocol (Applied Biosystems). Semi-quantitative PCR was performed using primers (see **Table 2.2**) for human *PADI2* and mouse *Padi1*, *Padi2*, *Padi3*, and *Padi4*, using mouse *Gapdh* as the loading control. TaqMan Gene Expression Assays (ABI) were used to measure relative mRNA levels for the transgenic human *PADI2* (Hs00247108_m1), along with endogenous mouse *Padi1* (Mm00478062_m1), *Padi2* (Mm00447020_m1), *Padi3* (Mm00478075_m1), and *Padi4* (Mm01341658_m1). Mouse *Gapdh* (4352932E) was used as the loading control. In addition, primer sequences for gene expression analysis via SYBR-qPCR can be found in **Table 2.3** for mouse genes, and **Table 2.4** for human genes. Expression levels were analyzed using the $2^{-\Delta\Delta C(t)}$ method [34]. Data are shown as means ± SD from three independent experiments, and were separated using Student's t-test.

Assays for cellular malignancy and invasion

Collagen coated inserts for 24-well plate wells (Falcon BD Fluoroblok; Catalog number: 351152, 8 µm pore size) were used to conduct transwell migration assays. Briefly, cells were trypsinized into an individual cell suspension, washed with DPBS, and added on the coated filters in serum-free DMEM

(10,000 cells per filter). The lower chamber of the companion plate (Falcon BD Labware) was filled with DMEM supplemented with 10% FBS. At different time points (4 and 24 hours) of incubation, the filters were removed for evaluation. Cells that had migrated to the other side of the membrane were fixed in 4% paraformaldehyde (PFA), and stained with DAPI for visualization of the nuclei. The nuclei were counted under fluorescent wide-field microscope. Values for cell invasion are expressed as the mean number of cells/20X microscopic field over five fields per filter for triplicate experiments. Focus formation assays were carried out using stable A431 cells (pIRES2-EGFP-FLAG-PADI2 or empty vector control) that were grown in 6-well plates. After 4d, cells were fixed with 4% PFA, and stained with crystal violet for subsequent analysis of focus formation. After imaging, the crystal violet was removed from the cells with 10% acetic acid and absorbance levels were measured (600 nM).

Histopathology scoring

Hematoxylin and Eosin (H&E) slides were evaluated by a pathologist (SM), who was blinded to the transgenic status of the mice, any clinical history and macroscopic features of the tumors. The tumor sections were scored for overall inflammatory intensity, cellular EMT features, and local invasion on a scale from 0 to 4. The mitotic indexes of the tumors were quantitated as the mean value of the number of mitotic figures in 10 randomly selected 400X field. The sections were also evaluated for progression of tumors from benign papillomas to invasive SCC phenotype as characterized by poorly defined

tumor margins, invasive clusters of carcinoma cells extending deep into the dermis and subcutis away from the primary tumor site, high desmoplastic tissue response, increased degree of anisokaryosis and anisocytosis and presence of poorly differentiated carcinoma cells. The scores were statistically analyzed for significance by Mann-Whitney-U test and Chi-Square analysis. The results were tabulated to show median scores for each histopathologic parameter evaluated in WT and transgenic group and the 25%/75% interquartile range of scores to show the variation within each group.

Statistical analysis

All experiments were independently repeated at least three times unless otherwise indicated. Values were expressed as the mean $\pm$ the SD. Means were separated using Student's t-test.

2.4 Results

Generation of MMTV-FLAG-PADI2 transgenic mice

To assess the potential role of PADI2 in pithelial carcinogenesis, we generated a mouse model in which the human *PADI2* gene is overexpressed under control of the hormone-responsive MMTV-LTR promoter. The transgenic construct consists of a MMTV-LTR promoter placed upstream of the human FLAG-tagged PADI2 cDNA, followed by an SV40 splice/polyadenylation site (**Figure 2.1**). MMTV-FLAG-PADI2 mice were generated, and seven potential

founders were tested for the presence of transgene by PCR. We identified 4 founders (indicated in red, **Figure 2.2a**), 4807, 4853, 4680, and 4863, that carried germline transmission of the FLAG-PADI2 transgene. While founder 4854 initially appeared to be a low-copy founder line, we failed to see transmission of the transgene to subsequent generations at Mendelian ratios, perhaps indicating mosaicism. Using semi-quantitative RT-PCR.

<u>Figure 2.1</u>: MMTV-FLAG-PADI2 transgenic construct. Schematic of the linearized MMTV-FLAG-hPADI2 transgene, containing a FLAG-tagged human *PADI2* cDNA fragment that was cloned between the EcoRI sites of the MMTV-SV40-Bssk plasmid [31]. The construct used for generation of FLAG-hPADI2-transgenic mice (also referred to as FLAG-PADI2) consists of FLAG-PADI2 under the control of the hormone-responsive MMTV-LTR promoter-enhancer with an SV40 splice-polyadenylation signal (SV40pA).

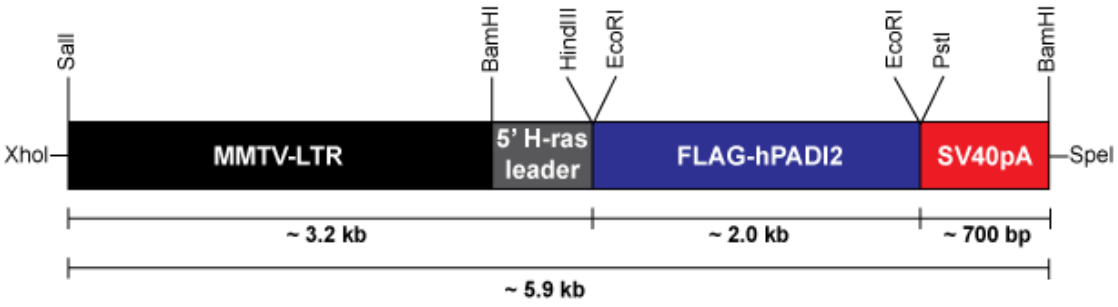

Figure 2.2: Generation of MMTV-FLAG-PADI2 transgenic mice. (a) PCR screening of DNA extracted from mouse tails for the presence of integrated human *PADI2* transgene (TG – hPADI2). Four founders were identified (red); primers for mouse *Padi4* were used as a wild-type (WT – mPADI4) control for amplification. Primer sequences can be found in **Table 2.1**. (b) Semi-quantitative RT-PCR was performed on tissues known to have high expression in MMTV-LTR transgenic mice: skin, salivary gland (SG), mammary gland (MG), and ovary (note: 4807 founder line was not used due to breeding issues and this line was subsequently terminated). Total RNA was isolated from tissues and relative mRNA levels for the transgenic human *PADI2*, along with endogenous mouse *Padi1*, *Padi2*, *Padi3*, and *Padi4* are shown. Mouse *Gapdh* was used as the loading control. (c) Quantitative RT-PCR (qPCR) for the human *PADI2* transgene was performed across the same tissues, using WT skin as the reference, with mouse *Gapdh* normalization. Expression levels were analyzed using the $2^{-\Delta\Delta C(t)}$ method, and data are expressed as the mean ± SD from three independent experiments (* $p < 0.05$).

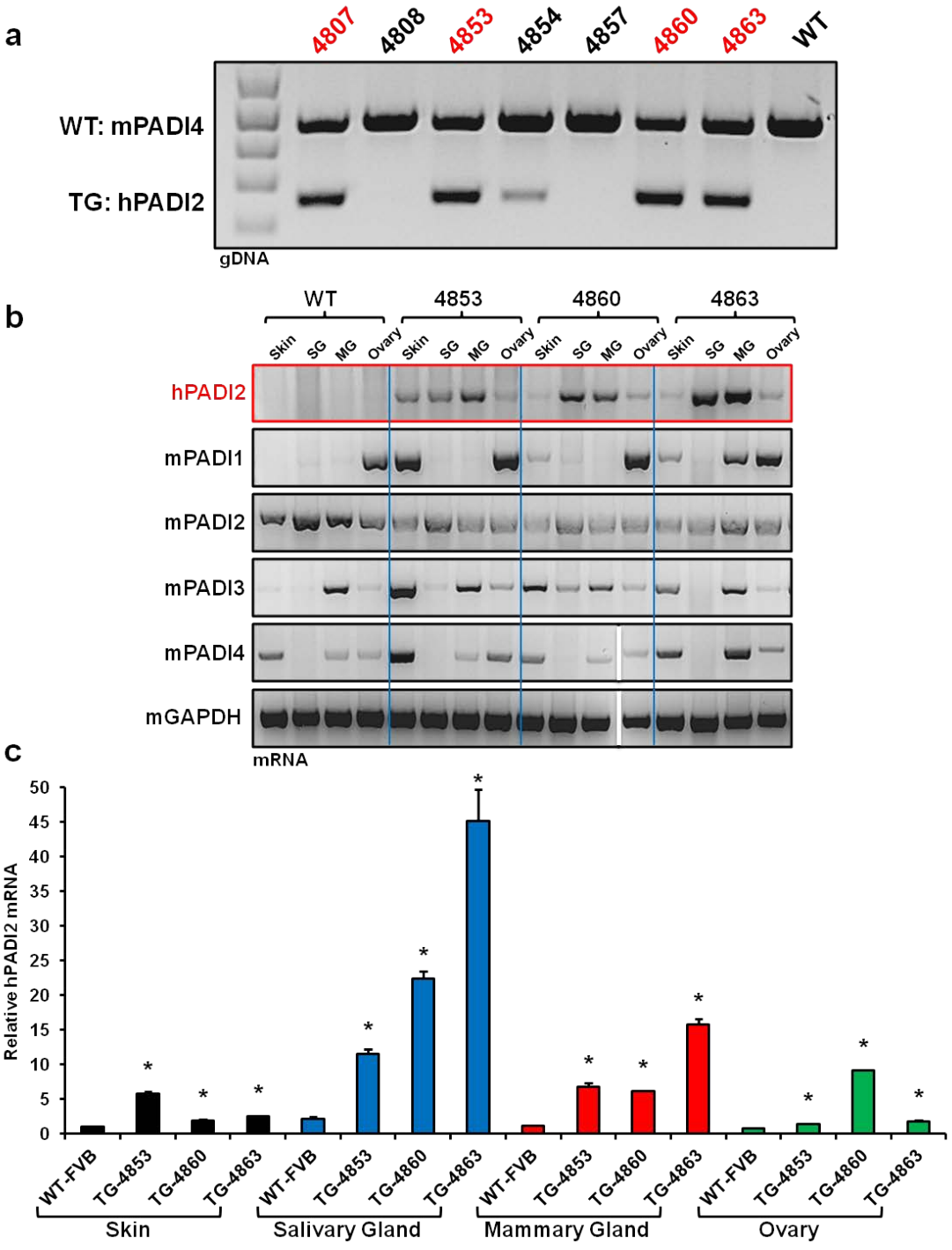
a
4807
4808
4853
4854
4857
4860
4863
WT
WT: mPADI4
TG: hPADI2
gDNA
b
WT
4853
4860
4863
Skin
SG
MG
Ovary
hPADI2
mPADI1
mPADI2
mPADI3
mPADI4
mGAPDH
mRNA
c
Relative hPADI2 mRNA
50
45
40
35
30
25
20
15
10
5
0
WT-FVB
TG-4853
TG-4860
TG-4863
Skin
Salivary Gland
Mammary Gland
Ovary

we confirmed the presence of FLAG-PADI2 transcript in the skin, salivary gland, mammary gland, and ovary of the transgenic mice (**Figure 2.2b**). These four tissues were chosen for analysis as they have previously been shown to have high expression of MMTV-LTR driven transgenes [14]. We note that the subsequent analysis is for only three founders (4853, 4860, 4863), as founder line 4807 had breeding issues and was subsequently terminated. Quantitative real-time PCR analysis (qPCR) of these founders for the four same tissues was performed; in comparison to other founders, founder 4853 showed the highest expression in skin, while founder 4863 had the highest expression in salivary and mammary glands (**Figure 2.2c**).

We first analyzed the mammary glands of the transgenic mice, as we have previously established a link between PADI2 and breast cancer. Our initial goal was to generate MMTV-driven transgenic mice to investigate the effects of ectopic PADI2 overexpression in mammary epithelium *in vivo*. However, while PADI2 transgenic expression in the mammary glands was detected at high levels in both virgin (**Figure 2.3a**) and multiparous mice (**Figure 2.3b**), we failed to detect any gross abnormalities or any observable phenotype in the mammary gland of these mice.

PADI2 transgenic mice develop benign and malignant proliferative skin lesions

While expression from the MMTV-LTR promoter is predominantly localized to the mammary and salivary gland, other tissues have been implicated,

including the skin and ovaries [13, 14]. Surprisingly, we discovered that 20% of the mice developed skin lesions after five months (**Table 2.2**). These lesions are macroscopically characterized by abnormalities, such as alopecia, multifocal epidermal ulceration often covered in sero-cellular crust, hyperkeratosis and thickening of the adjacent epidermis (**Figure 2.4a**). These lesions occur on both the dorsum and ventrum of transgenic mice. We note that we have not observed any of these lesions in the wild-type FVB mice, indicating that the phenotype is most likely a result of the FLAG-PADI2 transgene. Histological evaluation of skin lesions by H&E reveals highly neoplastic tissue, with features consistent with invasive squamous cell carcinoma (SCC). There are nests of neoplastic cells arising from the epidermis invading the dermis and subcutis (**Figure 2.4b, i**). Epidermis overlying the neoplasm is extensively ulcerated and the adjacent epidermal layers are hyperplastic (**Figure 2.4b, i**). Keratin pearls characterized by concentric layers of keratin embedded within tumor islands are noted which are a characteristic feature of SCC (**Figure 2.4b, ii and iii**). The carcinoma cells in the nests and islands of neoplastic cells within the subcutis show high degree of anisokaryosis and anisocytosis, with the nuclei often containing utliple prominent nucleoli (**Figure 2.4b, iv**). Clusters of neoplastic cells are often surrounded by abundant loose collagenous stroma replacing the dermal adnexal structures, consistent with a desmoplastic response (**Figure 2.4b, iii and iv**). Moreover, these skin lesions often contain carcinoma cells that are found budding off from the primary neoplasm (**Figure 2.4b, iv**), indicating the

Figure 2.3: MMTV-FLAG-PADI2 expression in the mammary gland.

(a) Confocal immunofluorescence analysis of FLAG (red) expression in virgin mouse mammary gland of a transgenic mouse. The luminal epithelial cells of mammary acini strongly express FLAG-PADI2 protein. (b) Immunohistochemical staining for PADI2 and FLAG in a multiparous mammary gland. The representative image shows a hyperplastic mammary gland with acinar epithelial cells strongly expressing both PADI2 and FLAG, confirming proper expression of the tagged transgene.

a

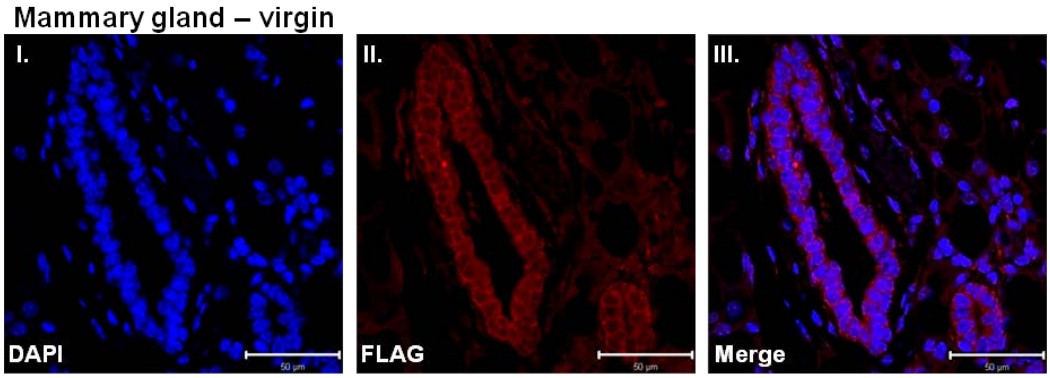
Mammary gland – virgin
I.
DAPI
II.
FLAG
III.
Merge

b

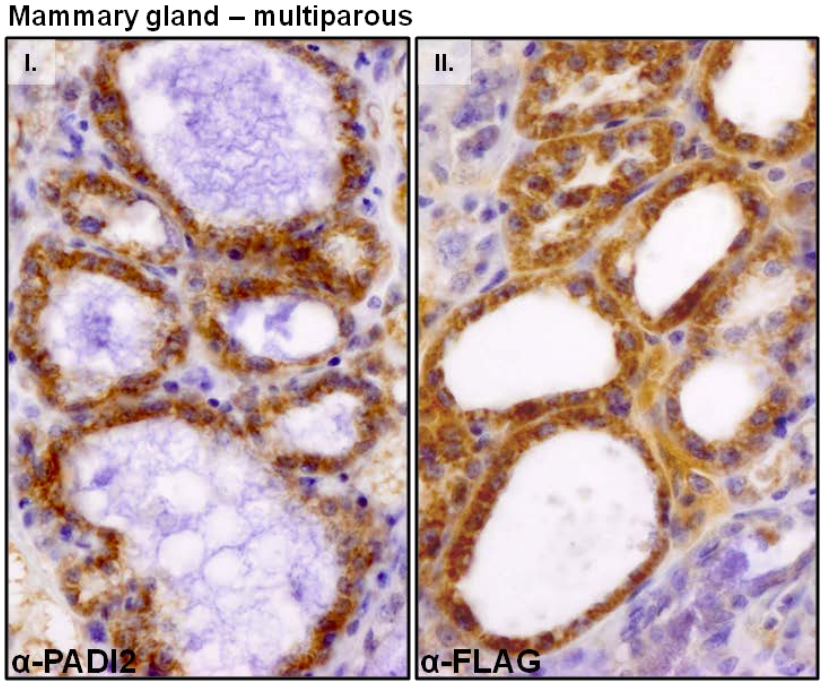
Mammary gland – multiparous
I.
α-PADI2
II.
α-FLAG

Table 2.2: Occurrence of skin lesions in MMTV-FLAG-PAD2 mice

Total n			Mice With Skin Lesions (%)		Sex of PAD2OE Mice Affected (%)	
PAD2OE Founder Line		**Age matched WT mice**	**WT**	**PAD2OE**	**M**	**F**
PAD2OE-1	17	17	0	58.8	80	20
PAD2OE-2	20	20	5	20.0	25	75
PAD2OE-3	47	47	4.4	42.6	55	45
PAD2OE-4	24	24	4.2	37.5	33	67
Total	**n=108**	**n=108**	**3.4**	**39.7**	**48.3**	**51.8**

invasive nature of these tumors. These skin lesions express high levels of transgenic PADI2, as immunohistochemical analysis shows PADI2 protein expression in the hyperplastic epidermis, neoplastic islands, and in hair follicular epithelium (**Figure 2.5a, i**). In addition, we see high expression of PADI2 protein in the neoplastic epithelium surrounding the keratin pearl (**Figure 2.5a, ii and iii**). Furthermore, these tumors are characterized by budding nests of carcinoma cells, which invade the adjacent stroma from the primary neoplasm. We note that PADI2 protein expression is high in these invading clusters of carcinoma cells (**Figure 2.5a, iv**). Because the PADI2 antibody can also detect endogenous mouse Padi2, we also evaluated the lesions for FLAG-tagged PADI2, and found that we see identical expression pattern. FLAG-PADI2 is highly expressed especially within the proliferating basal layers of hyperplastic/neoplastic epidermis; thus, suggesting that the increased PADI2 expression is a result of the transgene.

Figure 2.4: Transgenic FLAG-PADI2 expression in the epidermis of mice leads to the development of skin lesions. (a) Representative gross lesion showing the skin phenotype, which includes alopecia, multifocal epidermal ulceration often covered in a sero-cellular crust, and thickening of the adjacent epidermis. (b) Histological evaluation of the skin sections by H&E reveals features consistent with invasive squamous cell carcinoma. (i) Nests of neoplastic cells arising from the epidermis are shown invading the deep dermis and subcutis, with the epidermis overlying the neoplasm extensively ulcerated. (i) and (ii) Adjacent epidermal layers are hyperplastic with the loss of adnexal structures and increase in desmoplastic response (iii). Carcinoma cells are often found budding off from the primary neoplasm (iv).

a Representative MMTV-FP2+ lesion

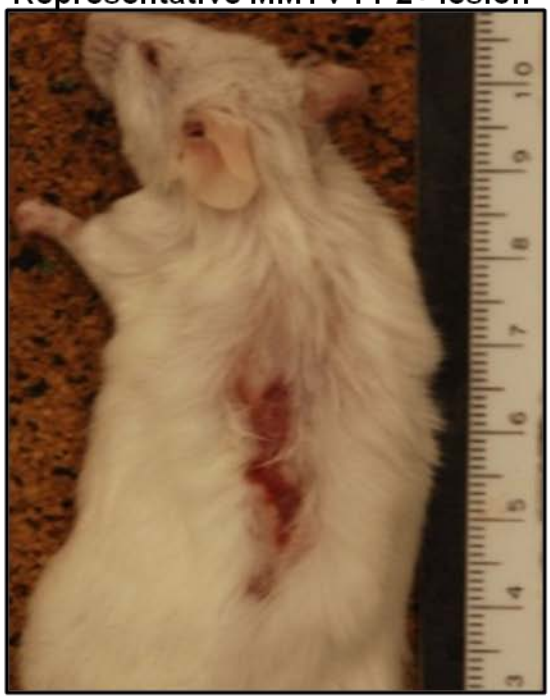

b H&E – MMTV-FP2+ skin lesion

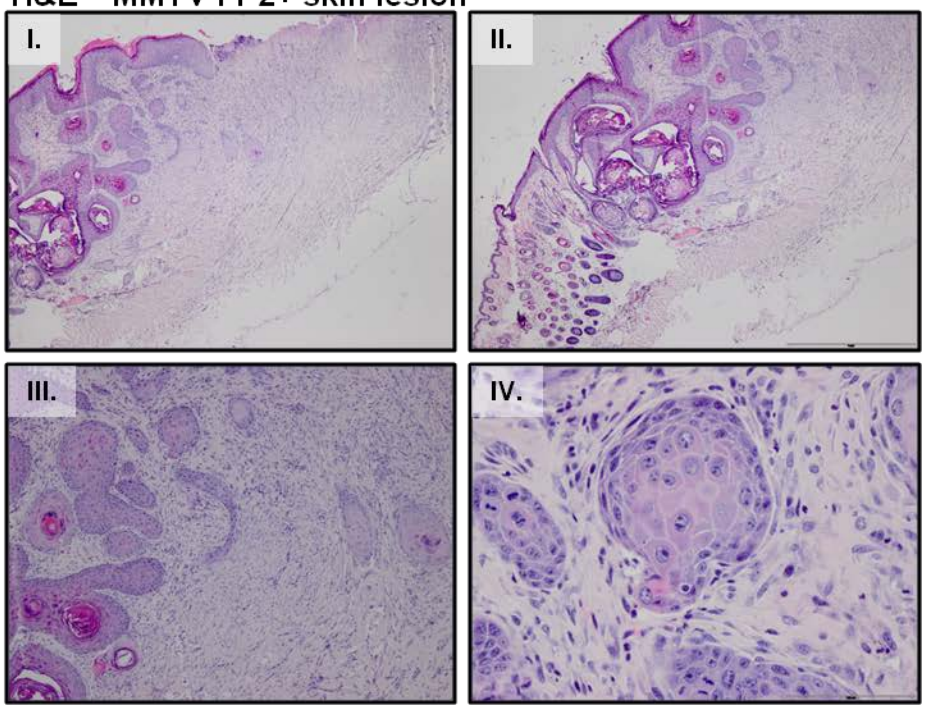

Figure 2.5: FLAG-PADI2 expression is high in the skin lesions of transgenic mice. (a) Immunohistochemical analysis of FLAG-PADI2 protein expression in skin neoplasms from transgenic mice. (i) Lower magnification image showing PADI2 protein expression in the hyperplastic epidermis, neoplastic islands, and in the hair follicular epithelium. (ii) – (iii) PADI2 protein expression in neoplastic cells surrounding concentric layers of keratin (arrow = keratin pearl). (iv) Representative image showing high levels of PADI2 protein expression in budding nest of carcinoma cells (broken arrow). (b) FLAG expression in skin neoplasms from transgenic mice. Scattered clusters of neoplastic cells show strong FLAG-tag expression. This staining is especially evident in the proliferating basal layers of hyperplastic or neoplastic epidermis.

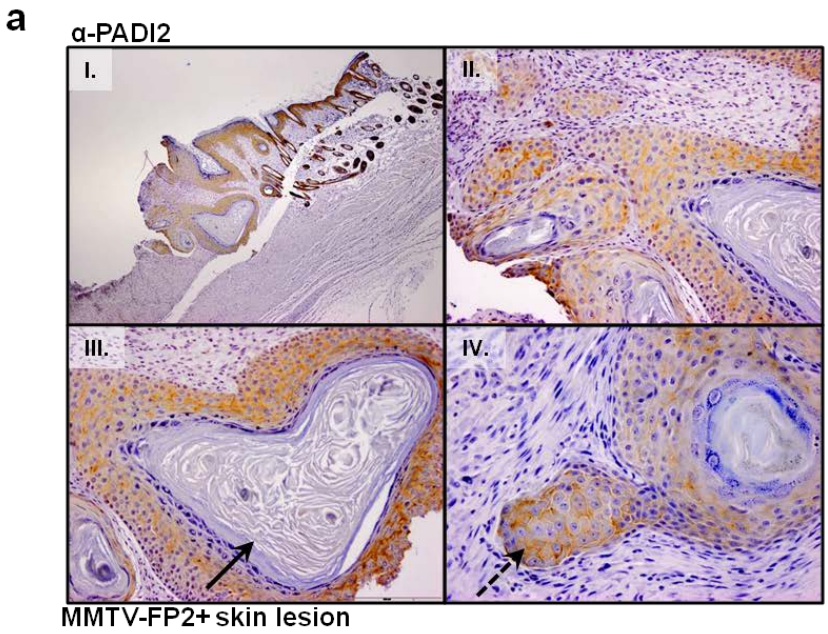
a
α-PADI2
I.
II.
III.
IV.
MMTV-FP2+ skin lesion
b
α-FLAG
I.
α-FLAG
II.
MMTV-FP2+ skin lesion

confirmed this using indirect-immunofluorescence to co-stain for FLAG and PADI2 expression in the skin lesions of transgenic mice. PADI2 and FLAG both co-localize to the neoplastic epithelial cells of a squamous cell carcinoma (**Figure 2.6, i-iv**). While PADI2 shows strong staining in multiple layers of the epidermis, we find that FLAG (i.e. transgene) is slightly more restricted to the basal layer, which is known to be more stem-cell like and highly proliferative [35]. Interestingly, we also see a slight increase in the proliferative marker, Ki67, within the FLAG staining section of the SCC lesion (**Figure 2.6b, ii-iv**). Therefore, this indicates that transgene expression in the skin might lead to an increase in proliferation, which is also supported by the identification of a subset of these lesions as highly proliferative and invasive SCC. We also note that we do not see any expression of the FLAG transgene in normal skin from wild-type mice (**Figure 2.7, i-vi**), as well as very little to any in adjacent normal skin from transgenic mice (data not shown).

Transgenic skin lesions have decreased levels of endogenous mouse Padis and increased markers of inflammation and EMT

Since we know that other PADIs can play a role in diseases of the skin, we were curious to see what the levels of other PADIs might be in the lesions from transgenic mice. Using semi-quantitative RT-PCR, we show human PADI2 transgene levels are present as expected in the lesions, as well as varying degrees of endogenous mouse Padis (**Figure 2.8a**). We show by

qPCR that representative lesions (2) and (4) have the highest transgene expression (**Figure 2.8b**), and that these two lesions have the highest levels of protein expression (lesion 2 = SCC, **Figure 2.8c**). Surprisingly, we noticed what appeared to be a protein-dimer in the western blot that was probed with anti-FLAG. Previous evidence has indicated that PADI4 can associate as a dimer, and that PADI-activity (i.e. citrullination) is highest in dimerized PADI4 [36]. Interestingly, Liu et al. predict that PADI2 also functions as a dimer, as they report a high degree of conservation between the two family members, especially at the residues important for dimerization [36]. We wanted to quantify the levels of endogenous mouse Padis by qPCR, and show that in lesions (2) and (4), which have the highest levels of human *PADI2*, also have the lowest levels of mouse *Padi1*, *Padi3*, and *Padi4* (**Figure 2.9**). There is no observable difference reported for endogenous mouse *Padi2* levels. To gain better perspective as to the potential pathways involved in the progression of MMTV-FLAG-PADI2 skin lesions, we examined genes known to be involved in inflammation and invasion in cancer. We chose these genes based on previous reports indicating a role for PADI2 in inflammatory diseases, coupled with our report here of the invasive nature of these carcinomas. Interestingly, when we examined the two representative lesions with the highest levels of transgenic *PADI2* (lesions 2 and 4), we found that they have sharply elevated levels of *Il6* and *Il8* (*Cxcl15*) gene expression (**Figure 2.10**).

Figure 2.6: Confocal immunofluorescence analysis of PADI2, FLAG, and Ki67 expression in neoplastic skin lesions of the FLAG-PADI2 transgenic mouse.

(a) Representative image showing co-staining (iv) of FLAG (red, ii) and PADI2 (green, iii) in the neoplastic epithelial cells of a squamous cell carcinoma from a transgenic mouse. Nuclei are stained with DAPI (blue, i). Endogenous Padi2 shows strong positive staining in 2-3 layers of epidermal cells, while FLAG-PADI2 is predominantly localized to the basal cell layer. Scattered tumor cell islands underlying the epidermis show high levels of PADI2 expression. (b) Representative image showing co-staining (iv) of the proliferative marker, FLAG (red, ii), and Ki67 (green, iii) in neoplastic epithelial cells of squamous cell carcinoma. Tumor islands that are strongly positive for FLAG-PADI2 expression levels contain an increased number of Ki67 positive cells (iv). Nuclei are stained with DAPI (blue, i)

a

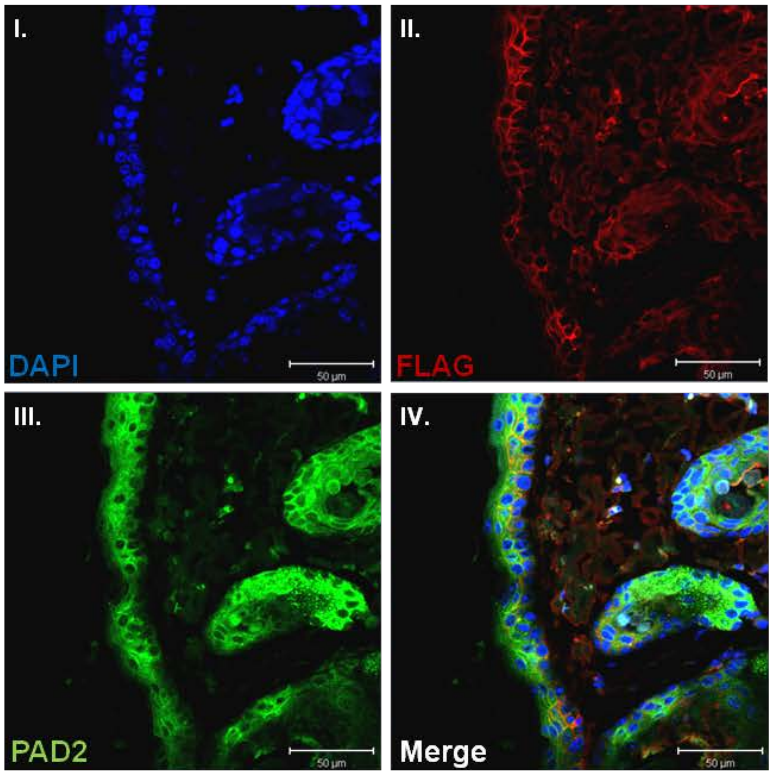

MMTV-FP2+ skin lesion

b

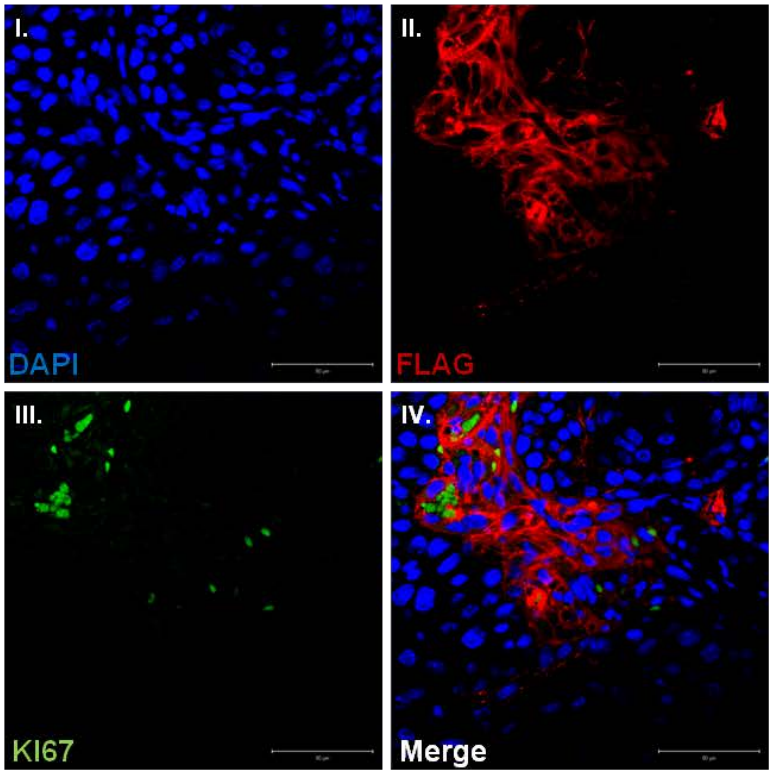

MMTV-FP2+ skin lesion

<u>Figure 2.7</u>: Normal skin section from wild-type mice as a negative control for FLAG staining. (a) Representative image showing co-staining (vi) of FLAG (red, iii) and Ki67 (green, iv) in normal skin sections from a wild-type (WT) mouse. Bright-field image (ii and v). Both FLAG-tag and PADI2 protein expression are absent, concomitant with reduced Ki67 levels. Nuclei are stained with DAPI (blue, i)

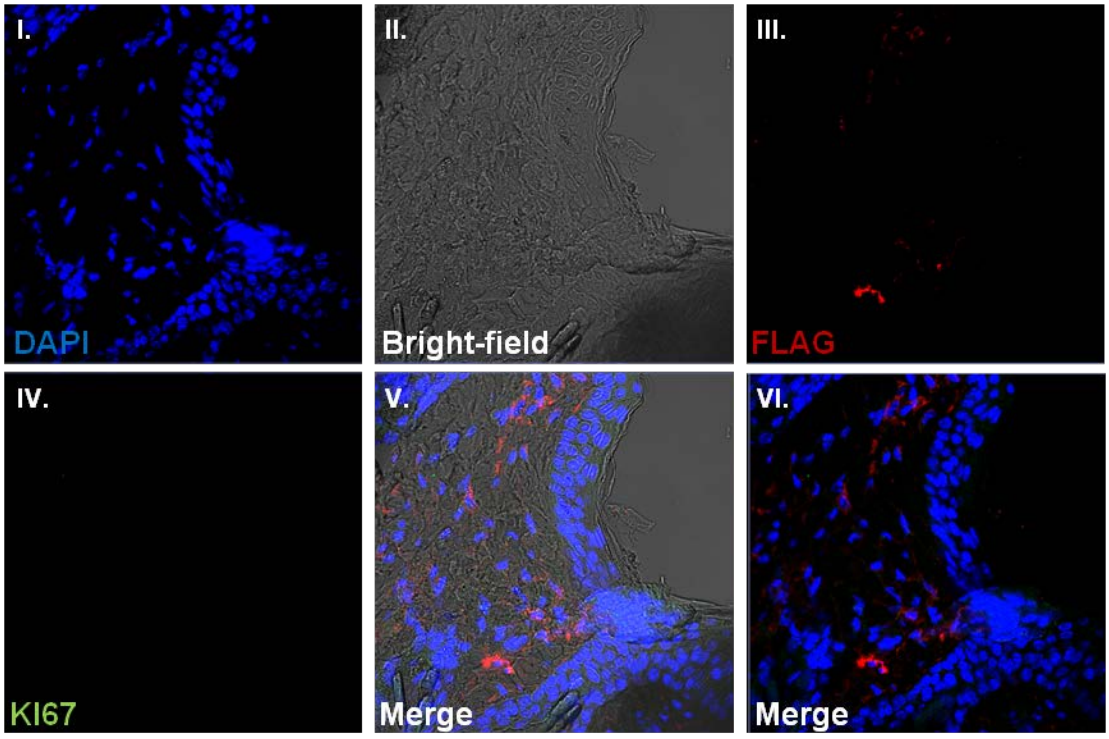

Figure 2.8: Transgene expression in the skin lesions of MMTV-FLAG-PAD2 mice. (a) Semi-quantitative RT-PCR on four representative skin lesions from transgenic mice (Lesions 1-4). Total RNA was isolated from lesions and normal wild-type skin, and relative mRNA levels for the transgenic human *PADI2*, along with endogenous mouse *Padi1*, *Padi2*, *Padi3*, and *Padi4* are shown. Mouse *Gapdh* was used as the loading control. (b) Quantitative RT-PCR (TaqMan) for the human *PADI2* transgene was performed across the same lesions, using normal WT skin as the reference, along with mouse *Gapdh* normalization. Expression levels were analyzed using the $2^{-\Delta\Delta C(t)}$ method, and data are expressed as the mean ± SD from three independent experiments (* $p < 0.05$). (c) Representative western blot for skin from WT and transgenic (TG) mice, along with lesions (3) and (4), as well as (2), which is noted as a SCC skin tumor. Whole-cell lysates were probed for FLAG expression, with a predicted protein size of ~75 kDa (note the presence of a suspected homodimer at 150 kDa). β-actin was used as a loading control.

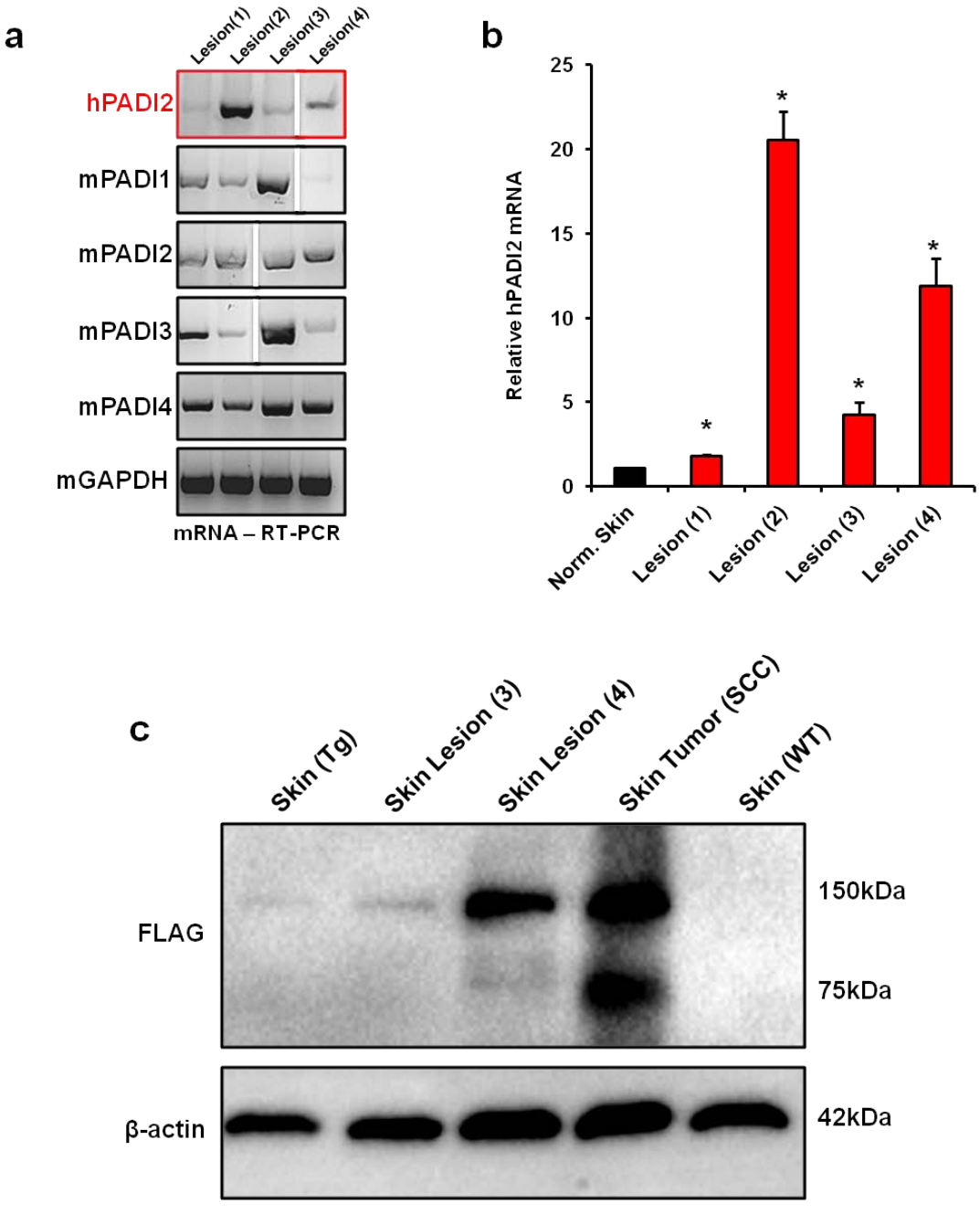
a
Lesion(1)
Lesion(2)
Lesion(3)
Lesion(4)
hPADI2
mPADI1
mPADI2
mPADI3
mPADI4
mGAPDH
mRNA – RT-PCR
b
Relative hPADI2 mRNA
25
20
15
10
5
0
Norm. Skin
Lesion (1)
Lesion (2)
Lesion (3)
Lesion (4)
c
Skin (Tg)
Skin Lesion (3)
Skin Lesion (4)
Skin Tumor (SCC)
Skin (WT)
FLAG
150kDa
75kDa
β-actin
42kDa

Furthermore, these two lesions also display markers of EMT, as E-cadherin is decreased, along with a concomitant increase in vimentin (*Vim*) and the E-cadherin repressor, *Snai1* (**Figure 2.10**).

Overexpression of PADI2 in human squamous cell carcinoma A431 cells increases invasiveness and malignancy

Transgenic MMTV-FLAG-PADI2 mice show that ectopic expression of PADI2 is sufficient to drive tumorigenesis in epithelial cells and that this expression correlates with an increase in markers of invasion and EMT. We wanted to see if could replicate these results in a human skin cancer cell line, A431. The A431 cell line is a human squamous carcinoma cell line that was isolated from a vulva epidermoid carcinoma. To test the oncogenic potential of PADI2 in this cell line, we first transiently expressed FLAG-PADI2 using standard plasmids for mammalian protein expression

Figure 2.9: Lesions from MMTV-FLAG-PADI2 transgenic mice that express the highest levels of human PADI2, have decreased mouse Padi1, Padi3, and Padi4. Total RNA from transgenic skin lesions (1-4) and normal wild-type skin was isolated and reverse transcribed to cDNA. The relative mRNA levels for human transgenic *PADI2*, along with mouse *Padi1*, *Padi2*, *Padi3*, and *Padi4*, were determined by qPCR (TaqMan) using normal WT skin as the reference, along with *Gapdh* normalization. Expression levels were analyzed using the $2^{-\Delta\Delta C(t)}$ method, and data are expressed as the mean ± SD from three independent experiments (* $p < 0.05$).

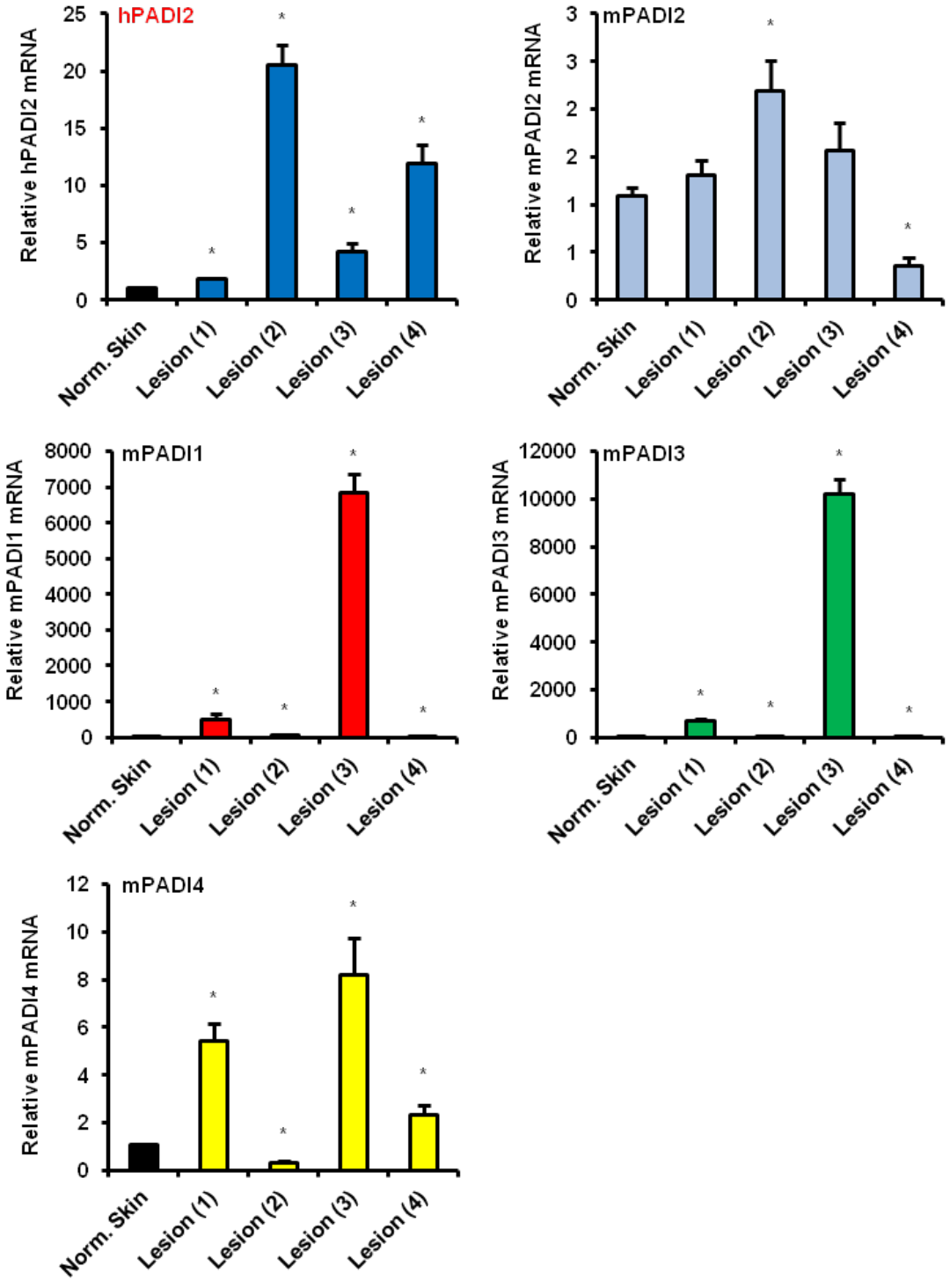
hPADI2
Relative hPADI2 mRNA
25
20
15
10
5
0
Norm. Skin
Lesion (1)
Lesion (2)
Lesion (3)
Lesion (4)
mPADI2
Relative mPADI2 mRNA
3
3
2
2
1
1
0
mPADI1
Relative mPADI1 mRNA
8000
7000
6000
5000
4000
3000
2000
1000
0
mPADI3
Relative mPADI3 mRNA
12000
10000
8000
6000
4000
2000
0
mPADI4
Relative mPADI4 mRNA
12
10
8
6
4
2
0

<u>Figure 2.10</u>: Skin lesions from MMTV-FLAG-PADI2 transgenic mice express markers of inflammation and EMT. Total RNA from transgenic skin lesions (1-4), along with transgenic and wild-type (WT) skin, was isolated and reverse transcribed to cDNA. Relative mRNA levels for the representative genes (see **Table 4.3** for gene list and primer sequences) were determined by qPCR (SYBR) using normal WT skin as the reference, along with β-actin (*Actb*) normalization. Expression levels were analyzed using the $2^{-\Delta\Delta C(t)}$ method, and data are expressed as the mean ± SD from three independent experiments (* $p < 0.05$).

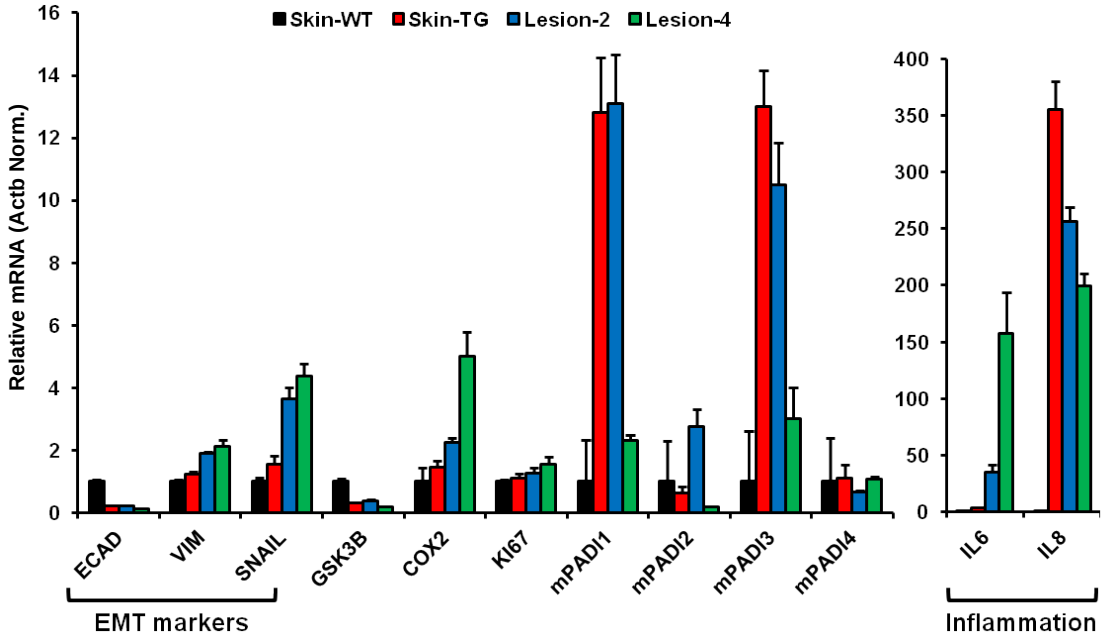

(pcDNA3.1-FLAG-PADI2) and (pIRES2-FLAG-PADI2) and associated empty vectors. We found that in both of the cell lines expressing high levels of FLAG-PADI2 (**Figure 2.11a and b**), E-cadherin protein levels were reduced when compared to the empty vector control cells (**Figure 2.11a**). In addition, we see a concomitant increase in vimentin in these two cell lines. We examined the FLAG-PADI2 overexpressing A431 cells for expression of genes involved in inflammation and EMT, and found the results were similar to those seen in the transgenic mice. Both *IL6* and *IL8* gene levels are increased, while we see a reduction in E-cadherin, along with concomitant increases in *SNAIL* and *SLUG* (**Figure 2.11b**).

Given the data from our transiently transfected A431 cells, along with our data from the transgenic mice, we decided to test whether stable overexpression of FLAG-PADI2 might have an effect on the cellular malignancy and/or invasiveness of A431 cells. Using both lentiviral transduction of FLAG-PADI2, and traditional transfection, we created two stable cell lines overexpressing various levels of PADI2. The lentiviral generated stable cell line (pLenti-FLAG-PADI2) is under the control of the phosphoglycerate kinase (PGK) promoter, which is weaker than the cytomegalovirus promoter used in the pIRES2-FLAG-PADI2 stably transfected cells. After selecting for 2-3 weeks, we assayed for PADI2 levels, showing, as expected, that pLenti-FLAG-PADI2 (pLenti-FP2) had slightly less expression of PADI2 than pIRES2-FLAG-PADI2 (pIRES-FP2) (**Figure 2.12a**). Next, we tested the invasive properties of these cell lines by measuring their ability to

migrate through a collagen matrix. For both cell lines, we see a significant increase in cellular migration after 24h, while the pIRES2-FP2 cell line also has a significant increase after 4h (**Figure 2.12b**). These results suggest that PADI2 dosage might correlate with invasion. Recent evidence from our lab suggests that PADI2 can be expressed in the nucleus, as well as the cytoplasm [10]; therefore, we decided to analyze the localization of PADI2 *in vitro* using indirect- immunofluorescence and confocal microscopy. Interestingly, we show that FLAG-PADI2 expression is predominantly nuclear in the stable A431-pIRES-FP2 cells (**Figure 2.13b**) compared to empty vector control cells (**Figure 2.13a**). Both the pLenti-FP2 and pIRES2-FP2 plasmids express GFP bicistronically via an internal ribosome entry site (IRES); therefore, we show that GFP in the pIRES2-FP2 stable cells is predominantly cytoplasmic (**Figure 2.13a, iii; and b, iii**), indicating different localization of the two overexpressed proteins (FLAG-PADI2 and GFP). Finally, we wanted to test the stable A431-pIRES2-FP2 cells for any increase in cellular malignancy. Assaying for focus formation, we show a significant increase in the FLAG-PADI2 overexpressing A431 cells compared to the empty vector control (**Figure 2.14a**). In addition, we show that the morphology of these cells also displays an elongated, fibroblast-like shape, indicative of cells that have undergone EMT (**Figure 2.14b**).

Figure 2.11: Transient overexpression of FLAG-PADI2 increases markers of inflammation and EMT in the human squamous cell carcinoma A431 cell line.

(a) Human squamous cell carcinoma cells, A431, were transiently transfected with FLAG-PADI2 (pcDNA3.1-FP2 or pIRES2-FP2) or empty vector (pcDNA3.1-emtpy). Western blot analysis of protein expression for EMT markers, E-cadherin and vimentin, along with PADI2, was performed on transfected A431 cells. β-actin was used as a loading control. Total RNA was isolated and relative *PADI2* levels for the FLAG-PADI2 transfected A431 cells, relative to empty vector control (*ACTB* normalized), were analyzed by qPCR (SYBR). Additional genes were also analyzed, see **Table 2.4** for full gene list and primer sequences. Expression levels were analyzed using the $2^{-\Delta\Delta C(t)}$ method, and data are expressed as the mean ± SD from three independent experiments (* $p < 0.05$).

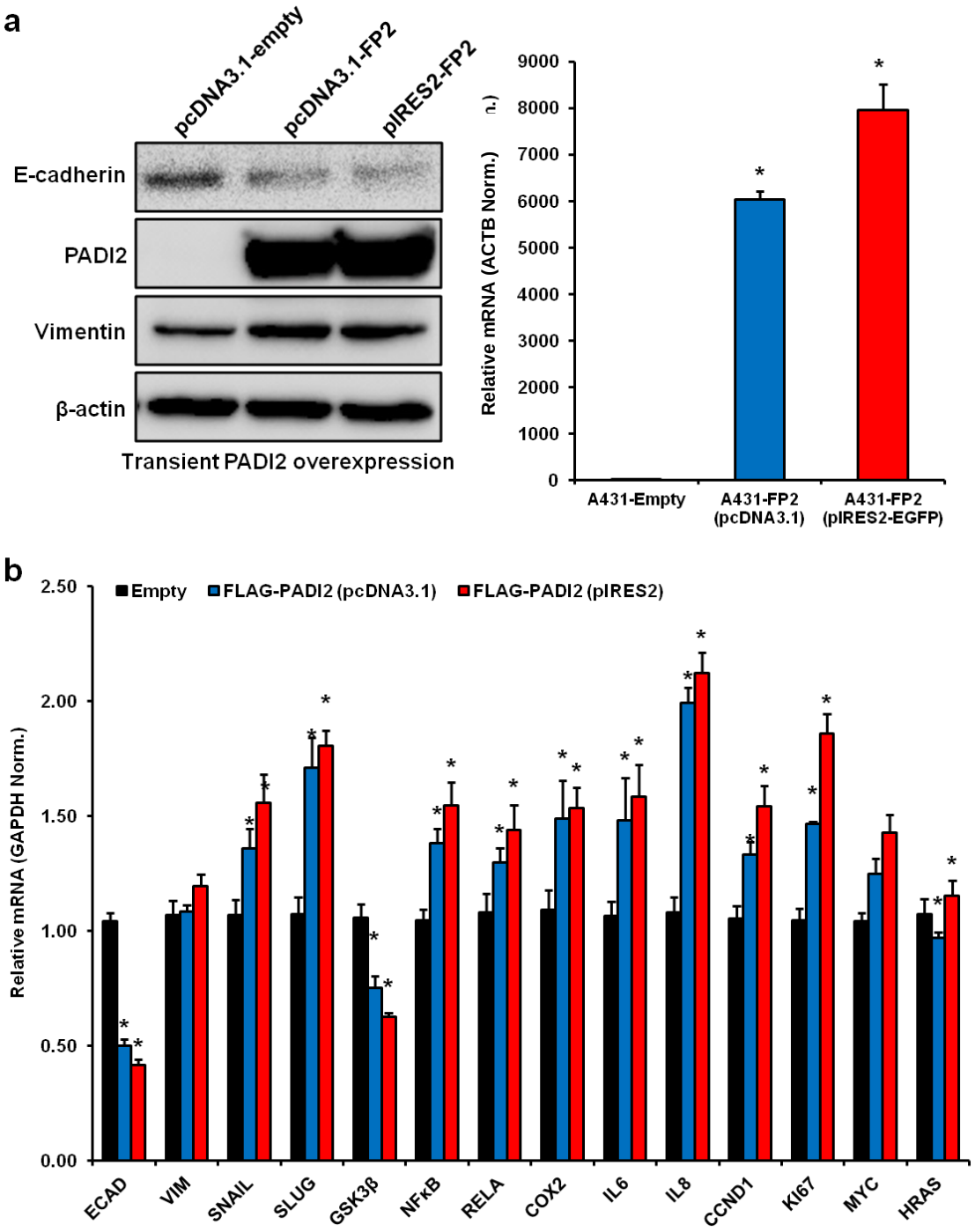
a
pcDNA3.1-empty
pcDNA3.1-FP2
pIRES2-FP2
E-cadherin
PADI2
Vimentin
β-actin
Transient PADI2 overexpression
Relative mRNA (ACTB Norm.)
9000
8000
7000
6000
5000
4000
3000
2000
1000
0
A431-Empty
A431-FP2 (pcDNA3.1)
A431-FP2 (pIRES2-EGFP)
b
Empty
FLAG-PADI2 (pcDNA3.1)
FLAG-PADI2 (pIRES2)
Relative mRNA (GAPDH Norm.)
2.50
2.00
1.50
1.00
0.50
0.00
ECAD
VIM
SNAIL
SLUG
GSK3β
NFκB
RELA
COX2
IL6
IL8
CCND1
KI67
MYC
HRAS

<u>Figure 2.12:</u> A431 cells stably overexpressing PADI2 have increased invasion through a collagen matrix. (a) A431 cells were stably transfected with pIRES2-FLAG-PADI2 (pIRES2-FP2) or infected with lentivirus expressing FLAG-PADI2-EGFP (pLenti-FP2). Control vectors only express the *EGFP* gene (pIRES2-GFP and pLenti-GFP). Western blot analysis for PADI2 protein expression levels, β-actin was used as a loading control. Total RNA was isolated and relative *PADI2* levels for the FLAG-PADI2 transfected A431 cells, relative to GFP vector control (*ACTB* normalized), were analyzed by qPCR (SYBR). Expression levels were analyzed using the $2^{-\Delta\Delta C(t)}$ method, and data are expressed as the mean ± SD from three independent experiments (* $p < 0.05$). (b) Transwell migration assay through a collagen matrix – cells were seeded and allowed to migrate through a collagen matrix. After 4h or 24h, cells that migrated were counted under a microscope at 40X magnification. Data are expressed as the mean ± SD from three independent experiments (* $p < 0.05$).

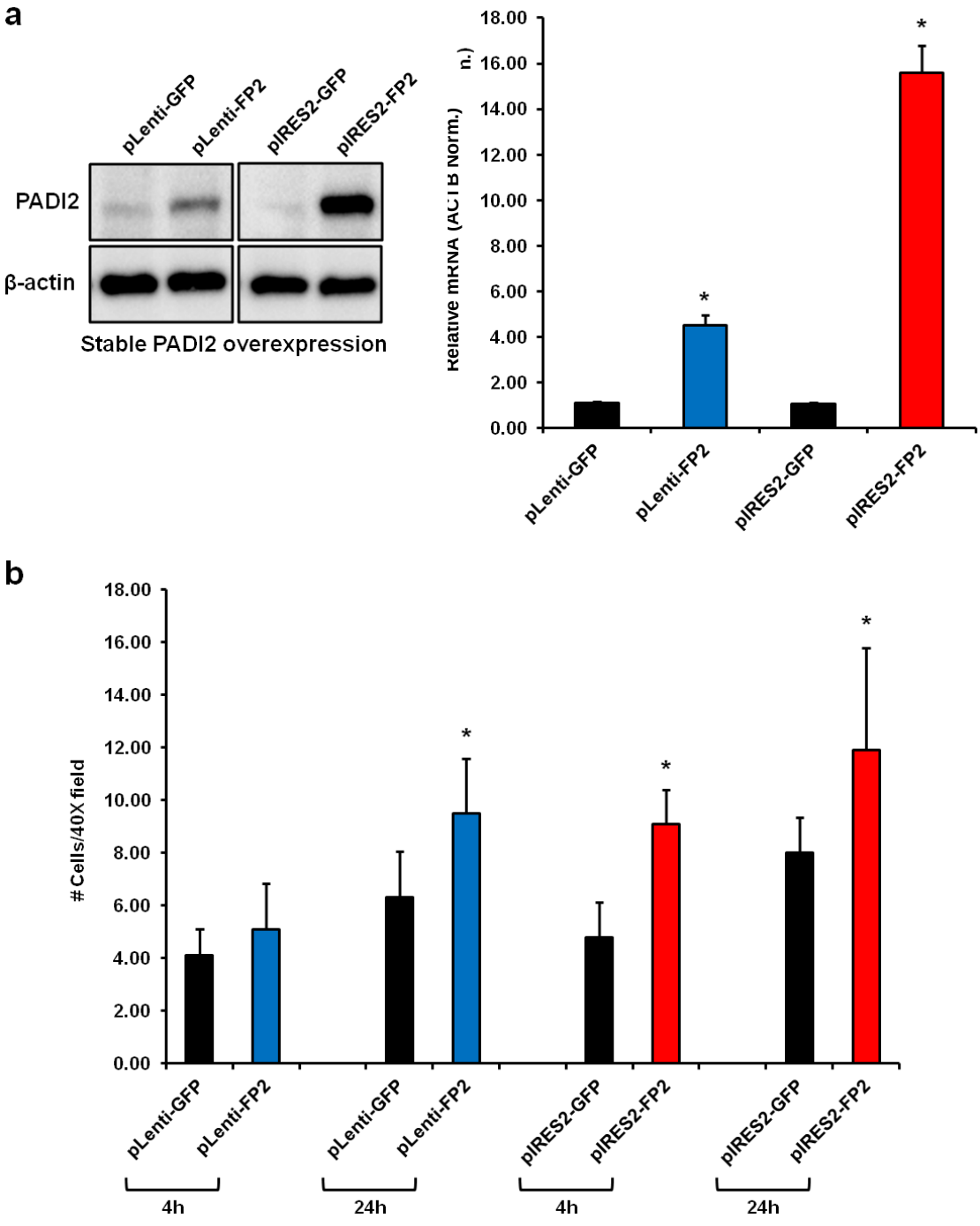
a
pLenti-GFP
pLenti-FP2
pIRES2-GFP
pIRES2-FP2
PADI2
β-actin
Stable PADI2 overexpression
Relative mRNA (ACTB Norm.)
18.00
16.00
14.00
12.00
10.00
8.00
6.00
4.00
2.00
0.00
*
pLenti-GFP
pLenti-FP2
pIRES2-GFP
pIRES2-FP2
b
#Cells/40X field
18.00
16.00
14.00
12.00
10.00
8.00
6.00
4.00
2.00
0.00
*
pLenti-GFP
pLenti-FP2
pLenti-GFP
pLenti-FP2
pIRES2-GFP
pIRES2-FP2
pIRES2-GFP
pIRES2-FP2
4h
24h
4h
24h

Figure 2.13: Co-localization of FLAG and GFP in A431 cells stably overexpressing FLAG-PADI2. (a) Confocal immunofluorescence analysis of the co-localization (iv) of FLAG (red, ii) and GFP (iii) in the nucleus and cytoplasm of A431 cells expressing the empty vector (pIRES2-GFP) or the FLAG-PADI2 expressing vector (b), which has bicistronic expression of both *PADI2* and *EGFP* (pIRES2-GFP-FLAG-PADI2). Note the nuclear expression of FLAG (*PADI2)*. Nuclei are stained with DAPI (blue, i).

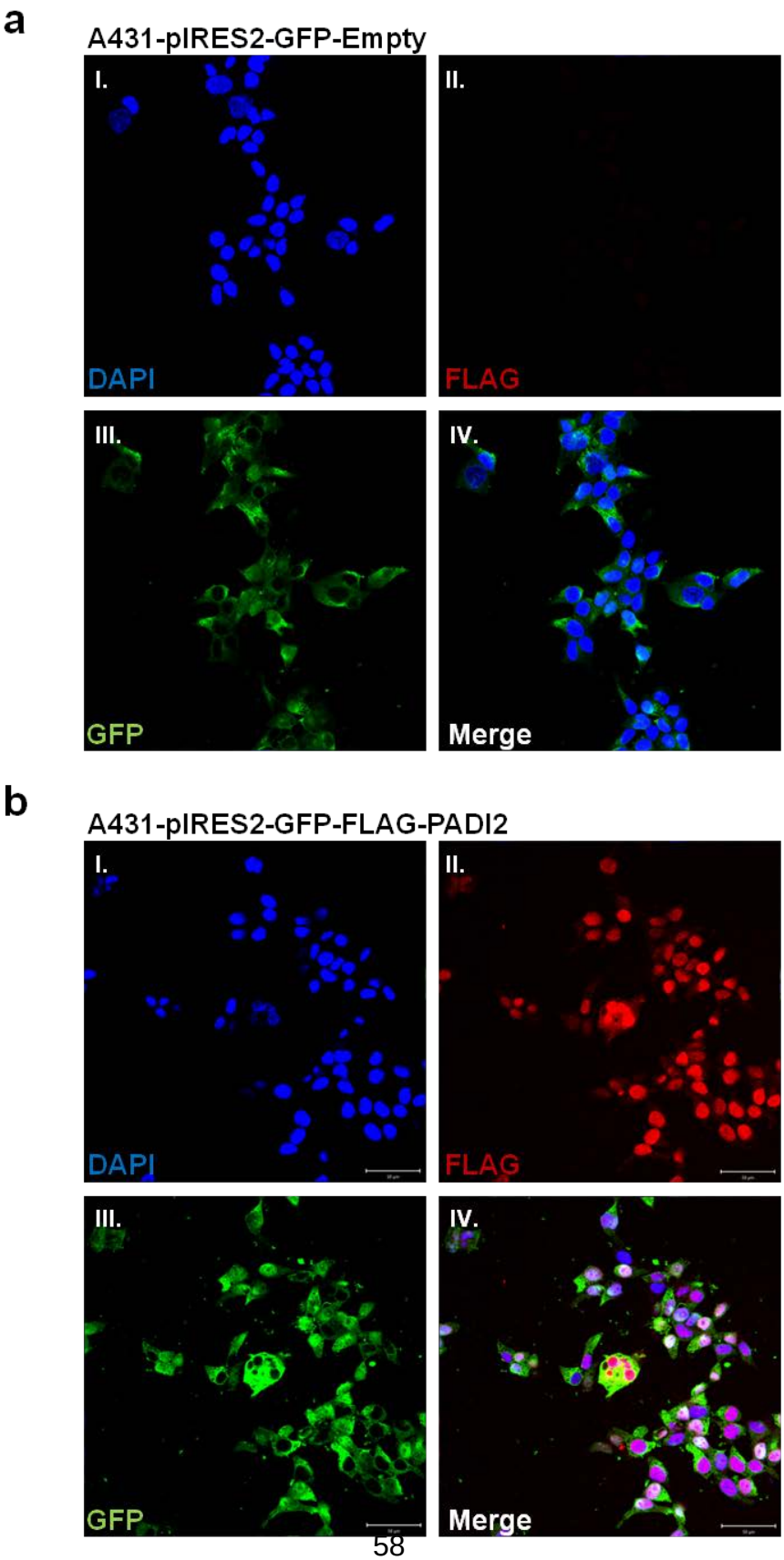
a
A431-pIRES2-GFP-Empty
I.
II.
DAPI
FLAG
III.
IV.
GFP
Merge
b
A431-pIRES2-GFP-FLAG-PADI2
I.
II.
DAPI
FLAG
III.
IV.
GFP
Merge

<u>Figure 2.14</u>: A431 skin cancer cells overexpressing FLAG-PADI2 show increased malignancy and EMT morphology. (a) Cells stably overexpressing FLAG-PADI2 (A431-FP2), or EGFP control (A431-GFP), were grown for 4d in a 6-well plate, fixed with 4% PFA, and stained with crystal violet for subsequent analysis of focus formation. After imaging, the crystal violet was removed from the cells with 10% acetic acid and absorbance levels were measured (600 nM). Data are expressed as the mean ± SD from three independent experiments (* $p < 0.05$). (b) Representative morphology of A431 cells overexpressing FLAG-PADI2, showing elongated cells with fibroblast-like shape, indicative of cells that have undergone EMT.

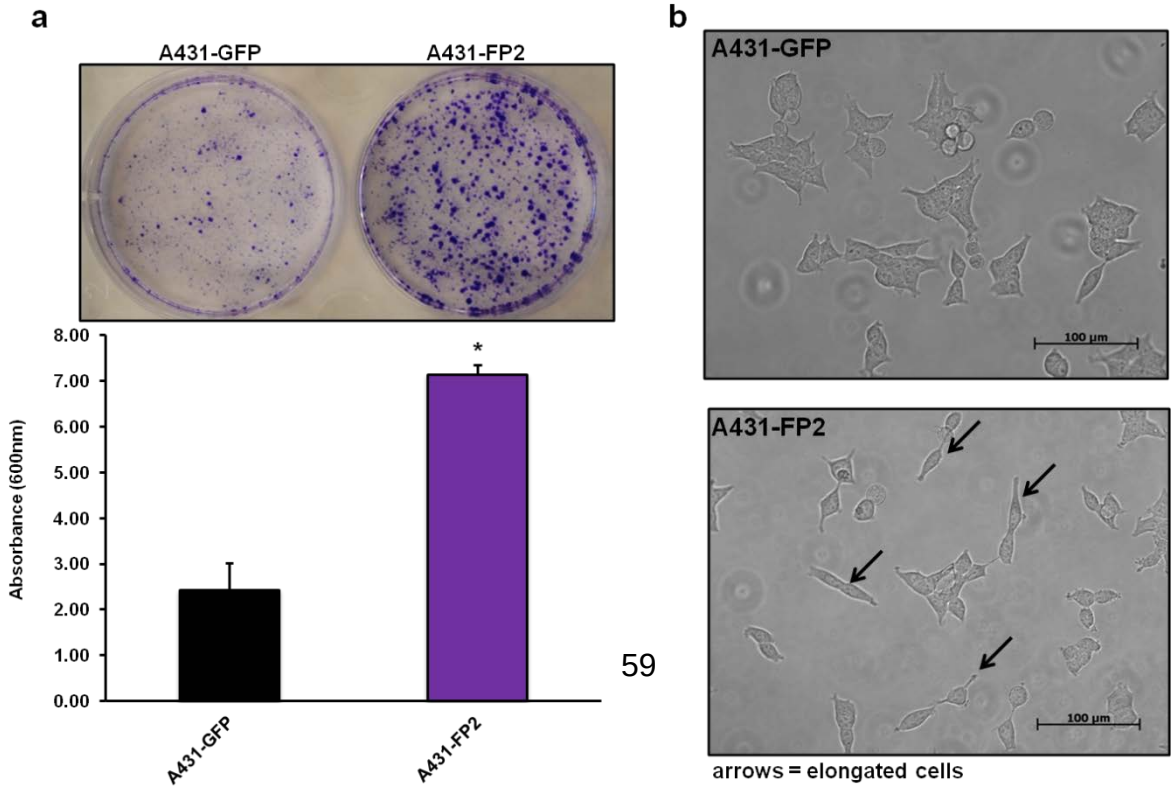

MMTV-FLAG-hPAD2 mice form larger skin tumors

Control and transgenic mice were treated with both DMBA and TPA and monitored for the development of skin tumors such as papillomas and carcinomas. The transgenic mice developed increased number of papillomas and these tumors grew at a faster rate (**Figure 2.15A and 2.15B**). The increased frequency of papilloma formation in the transgenic mice was especially evident in the earlier weeks of the study. The tumor sections were immunostained for the FLAG-hPAD2 expression and the MMTV-FLAG-hPAD2 tumors showed positive staining for FLAG-PAD2, confirming that the transgene is being translated in the DMBA-TPA induced tumor cells (**Figure 2.16**). The WT tumor tissue showed only minimal background staining for FLAG.

Figure 2.15: The incidence and growth of skin papillomas in DMBA-TPA treated mice. DMBA treated mice were further treated with TPA twice weekly and monitored for the number of papillomas developed and the size of each papilloma. The average of number of papillomas in both wild type (WT) and MMTV-FLAG-hPAD2 (TG) group were plotted in Figure 3.2A (mean ± SEM, * p value <0.05). Average size of the largest papilloma plotted against week of TPA treatment is shown in Figure 3.2B (mean ± SEM). MMTV-hPAD2 mice show statistically significant increase in the number of papillomas and these tumors tend to be of larger size.

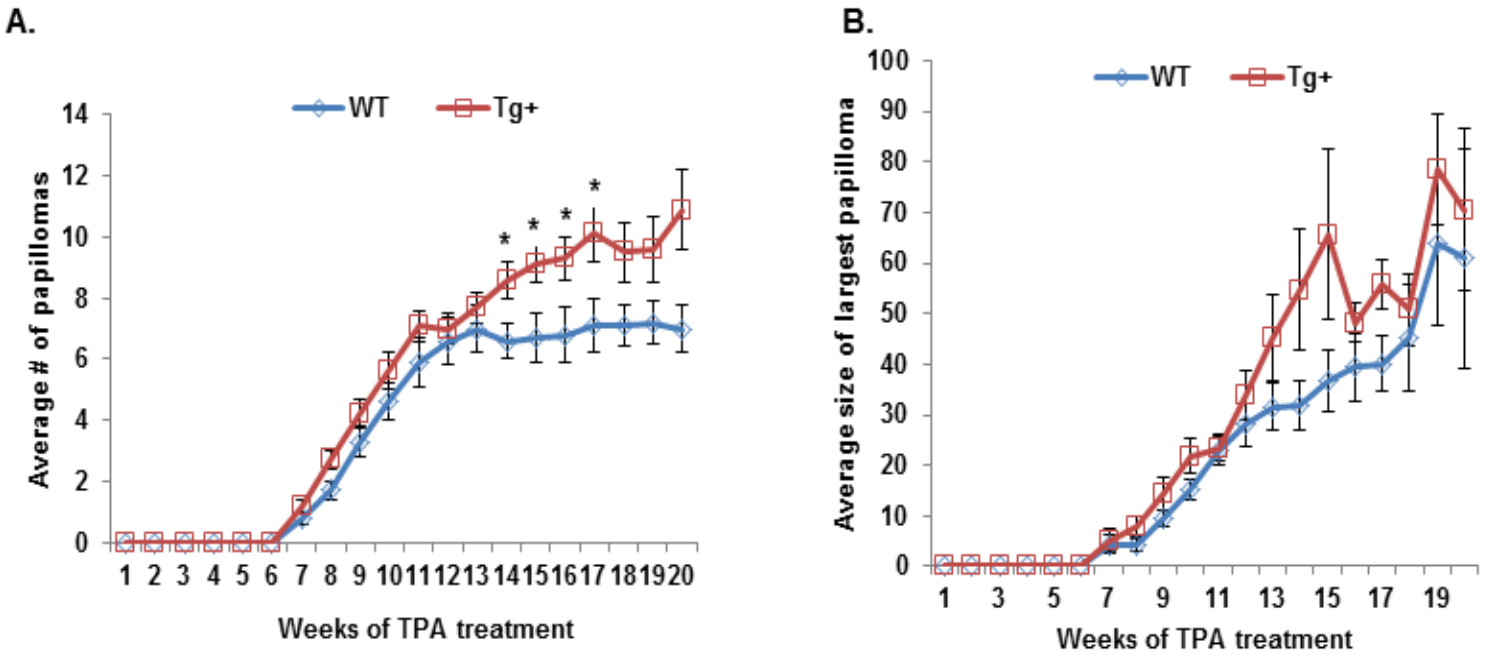
A.
WT
Tg+
Average # of papillomas
0
2
4
6
8
10
12
14
1 2 3 4 5 6 7 8 9 10 11 12 13 14 15 16 17 18 19 20
Weeks of TPA treatment
B.
WT
Tg+
Average size of largest papilloma
0
10
20
30
40
50
60
70
80
90
100
1 3 5 7 9 11 13 15 17 19
Weeks of TPA treatment

Figure 2.16: Anti-FLAG immunostaining and confocal imaging to detect transgenic expression of hPAD2 in skin tumors. Formalin fixed, paraffin embedded tumor sections were stained with anti-FLAG antibody and imaged using a confocal microscope for the expression of FLAG-hPAD2 in tumor cells (Red). There is strong staining for FLAG-hPAD2 in the transgenic tumor sections while the WT tumor tissue show minimal background staining (measurement bar = 200μm).

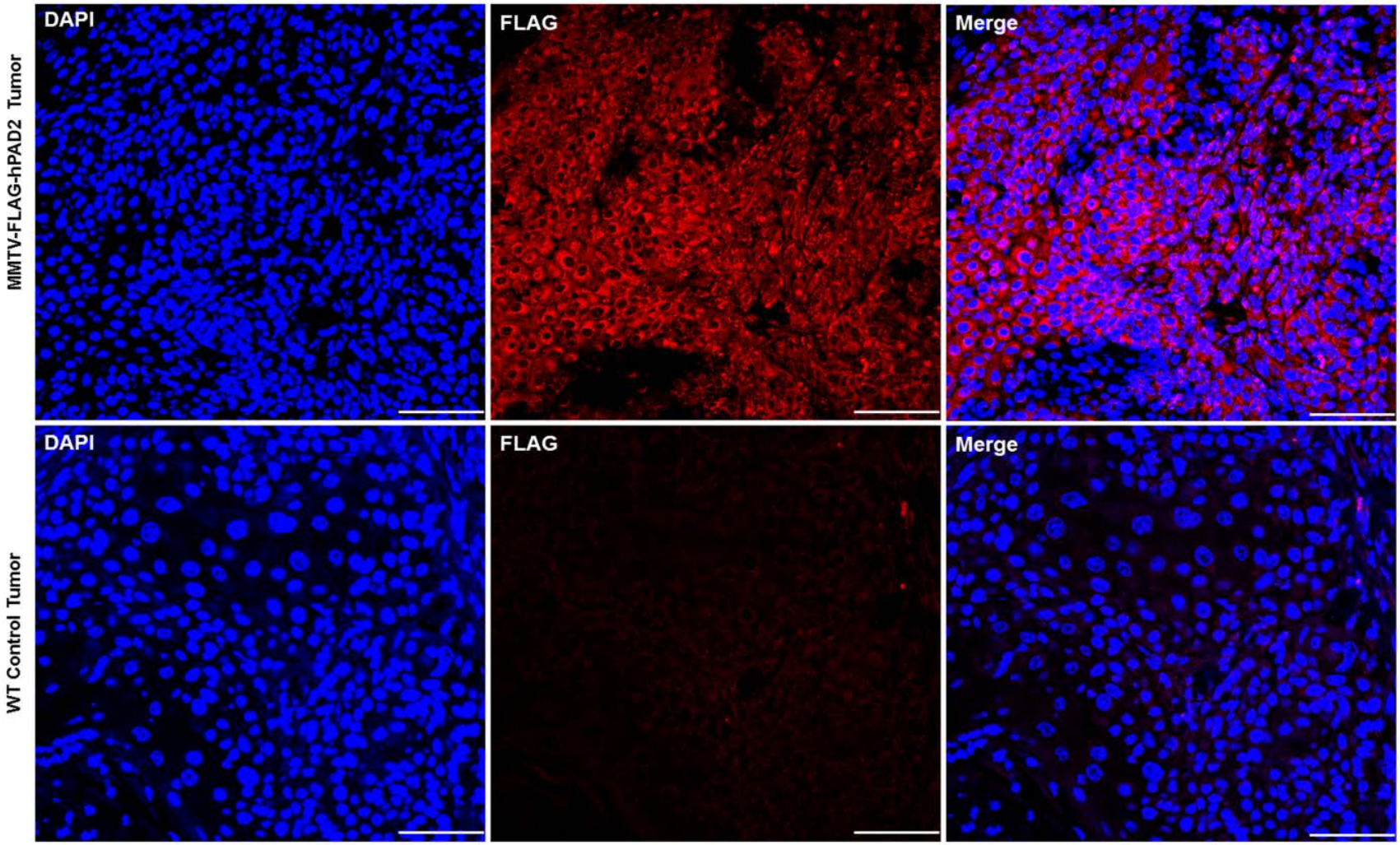
MMTV-FLAG-hPAD2 Tumor
WT Control Tumor
DAPI
FLAG
Merge
DAPI
FLAG
Merge

PAD2OE tumors show increased inflammation and invasiveness

The histopathological examination confirmed that the DMBA-TPA tumors in treated mice ranged from epidermal hyperplasia, benign papillomas to invasive squamous cell carcinomas (**Figure 2.17A**). Histopathological examination of the tumor sections from WT and transgenic mice showed that the tumors carrying hPAD2 transgene contained significantly higher levels of inflammatory cell infiltrate compared to the WT tumors (**Figure 2.17B**). WT tumors mostly were benign papillomas with hyperkeratosis, numerous invaginations, and intact basement membrane limiting the tumor cells. Approximately in 80 percent of the transgenic mice, the tumors developed into squamous cell carcinoma with invasive features such as breaching of the basement membrane, poorly defined tumor borders, high degree of anaplasia and local or regional lymph node metastasis (**Figure 2.18A**). Blinded histopathology scores were analyzed by Mann-Whitney-U test and Chi-sqyare analysis and there were significant differences between transgenic and WT tumors with respect to tissue characteristics such as intensity of inflammation, EMT cellular features, mitotic index, and invasiveness (**Figure 2.18B and Table 2.5**). The median score values are plotted in **Figure 2.18B**, which represent the intense inflammatory component observed within the transgenic tumors. The inflammatory cells are predominantly neutrophils, often forming inflammatory cell islands embedded within clusters of papilloma and carcinoma cells.

Figure 2.17: Histopathological evaluation of DMBA-TPA induced skin tumors in WT and MMTV-FLAG-hPAD2 mice. Figure 3.4A shows that following DMBA-TPA treatment, mice developed skin lesions varying in their histopathologic properties and invasiveness ranging from hyperplasia/dysplasia, benign papillomas to invasive squamous cell carcinomas. In comparison to the WT tumors, the transgenic tumors contained increased areas of tumor associated inflammation consisting of infiltrating immune cells.

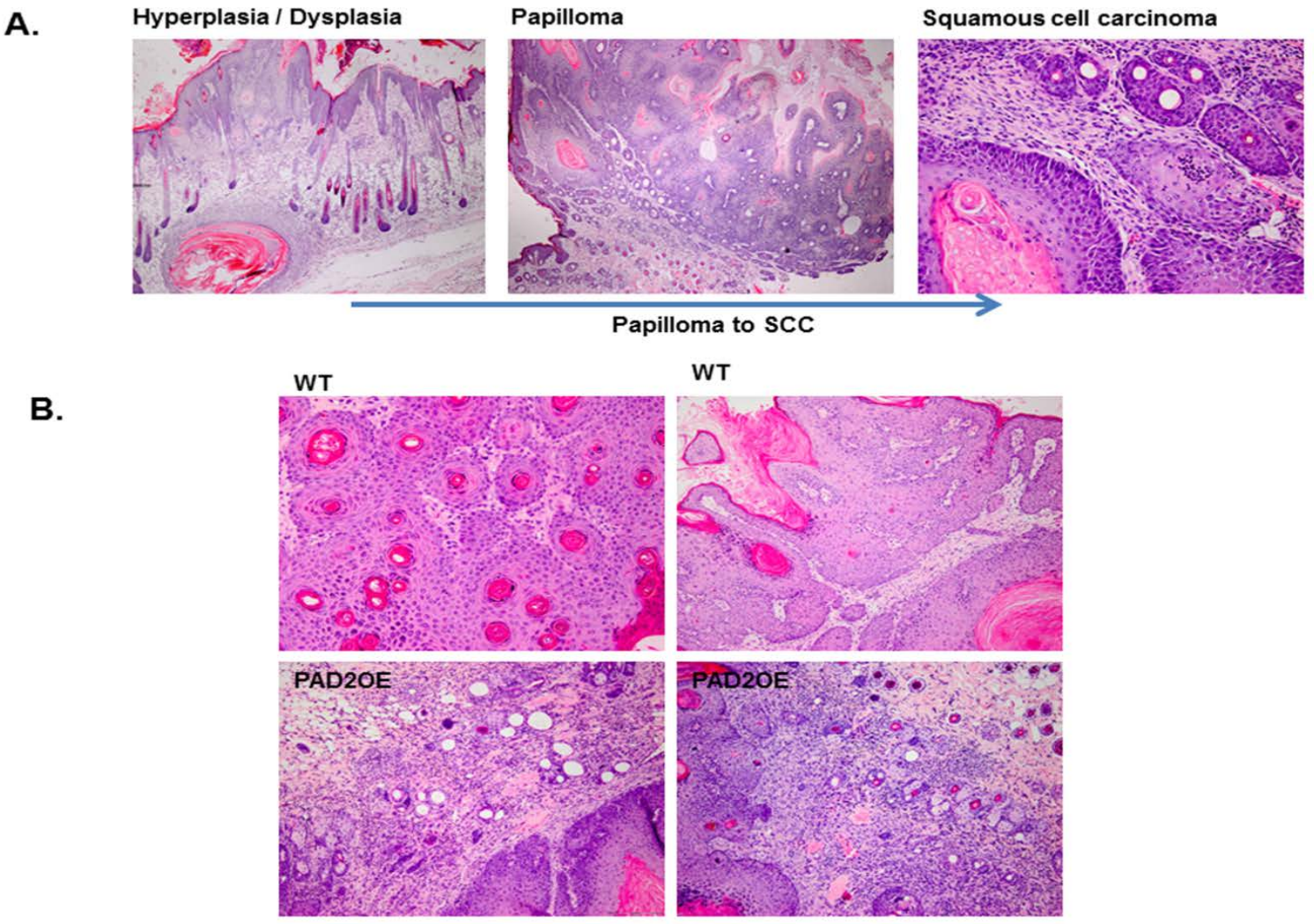
A.
Hyperplasia / Dysplasia
Papilloma
Squamous cell carcinoma
Papilloma to SCC
B.
WT
WT
PAD2OE
PAD2OE

Figure 2.18: Histopathological scoring of DMBA-TPA induced tumors for inflammation and invasiveness. The tumors were classified into benign papillomas and invasive SCC based on histopathological features and the percentage of mice with papillomas and mice with both papillomas and SCC were plotted. A significantly higher percentage of the transgenic mice developed invasive SCC compared to the WT mice which developed predominantly benign papillomas (Figure 3.5A). The median scores for histopathology parameters are plotted in Figure 3.5B and table 3.2 based on the pathologist's blinded evaluation of 17 different cases in each group. Transgenic tumors received a higher score for inflammation, invasion, EMT cellular morphological features and mitotic index compared to the WT tumors.

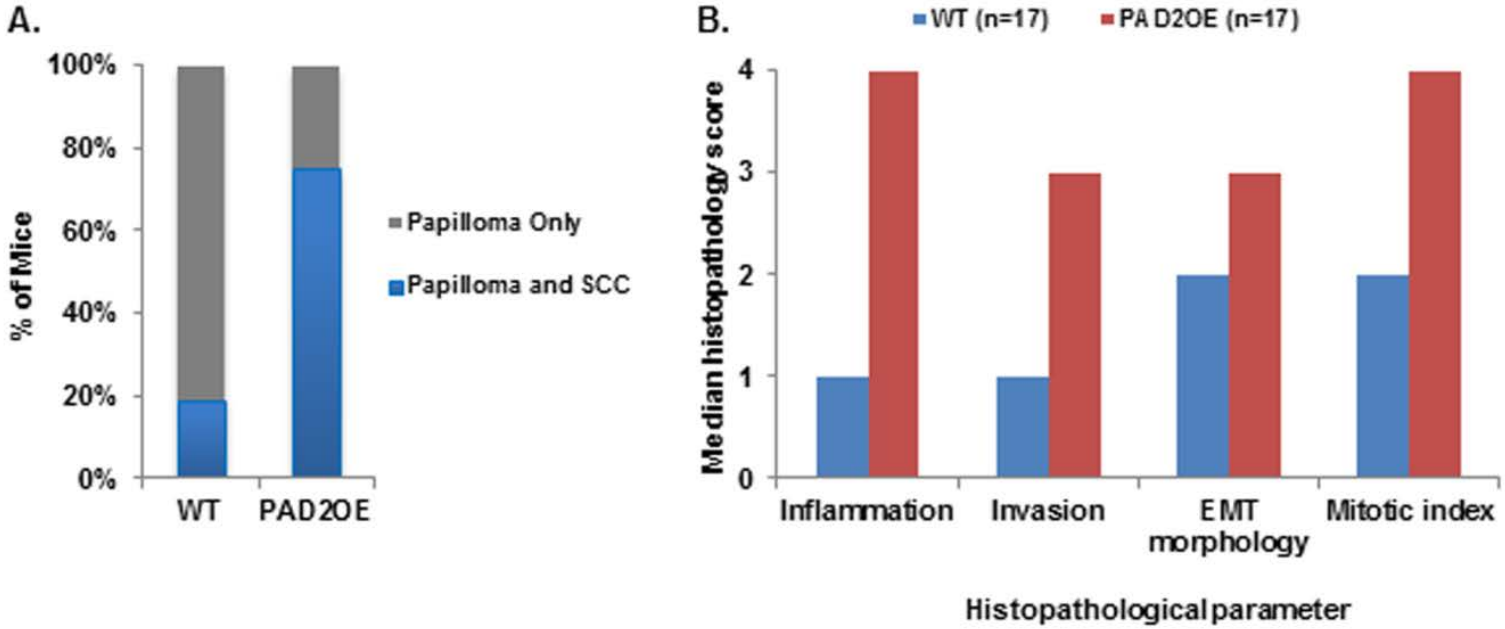
A.
100%
80%
60%
40%
20%
0%
% of Mice
WT
PAD2OE
Papilloma Only
Papilloma and SCC
B.
WT (n=17)
PAD2OE (n=17)
Median histopathology score
4
3
2
1
0
Inflammation
Invasion
EMT morphology
Mitotic index
Histopathological parameter

Table 2.5: Chi-square (X^2) analysis of histopathology scoring of DMBA-TPA induced tumors. H&E sections from WT and transgenic tumors were scored for histopathological features by a pathologist blinded to the genotype of the mice. The tumors scored on a scale of 0 to 4 for inflammation, invasion and EMT morphology. Mitotic index was calculated as the average of total of mitotic figures observed in 10 randomly selected 400X microscopic field. The results were analyzed by Mann-Whitney-U test and Chi-square analysis and the results are given as the median score for each group, 25%/75% interquartile range, X^2 values and the corresponding p-values. The transgenic tumors received significantly higher scores for these four histopathologic parameters of inflammation, invasion and cell proliferation compared to the WT tumors.

Histopathological parameter	Median (25%/75% interquartile range)		X^2
	WT (n=17)	PAD2OE (n=17)	
Inflammation	1 (1-2)	4 (2-4)	33.5 (P <0.001)
Invasion	1 (1-2)	3 (2-4)	31.0 (P <0.001)
EMT morphology	2 (1-2)	3 (2-3)	27.0 (P <0.001)
Mitotic index	2 (2-3)	4 (3-5)	19.0 (P <0.001)

Figure 2.19: Lymph node metastasis of SCC in a MMTV-FLAG-hPAD2 mice.

A H&E stained section of axillary lymph node (LN) from a MMTV-FLAG-hPAD2 mice showing regional LN metastasis of SCC. An unaffected control LN image from the WT mice is shown to the left. The SCC metastatic focus is composed of sheet of carcinoma cells with poorly defined borders, no basement membrane and with a central core of inflammatory cells predominantly neutrophils.

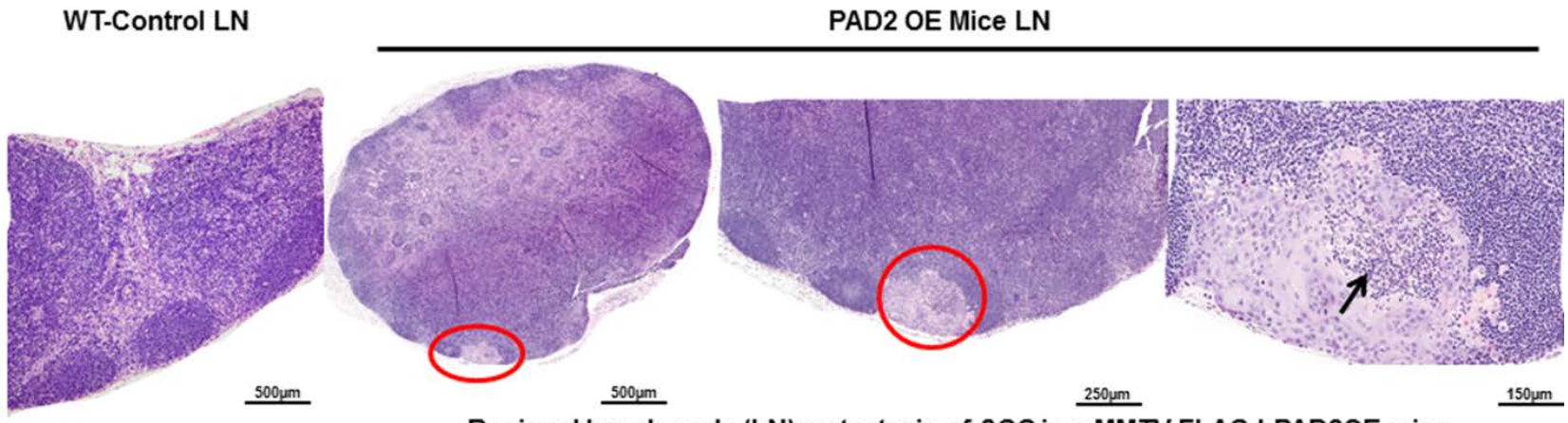

Regional lymph node (LN) metastasis of SCC in a MMTV-FLAG-hPAD2OE mice

Figure 2.19 shows an example of focal regional lymph node metastasis of SCC cells in a MMTV-FLAG-hPAD2 mouse. Interestingly, the core of this microinvasive focus of tumor cells harbors a cluster of immune cells, predominantly neutrophils, suggesting that the tumor cells favor recruitment of immune cells potentially by regulating cytokine secretion. The mRNA expression of inflammatory cytokines such as IL6, mouse IL8 homologues (LIX, MIP2), and Vimentin were elevated in the transgenic tumors while the cell adhesion marker E-cadherin mRNA was reduced. This finding was in consistent with the histopathological pattern of neutrophil rich inflammation in these transgenic tumors which may be regulated by LIX and MIP2 levels. A correlation analysis between transgene mRNA expression and these inflammatory and EMT markers showed that hPAD2 mRNA levels are highly positively correlated with inflammatory cytokine levels (MIP2 and LIX) and vimentin while showing a strong negative correlation with E-cadherin mRNA levels (**Figure 2.20**). This suggested that potentially hPAD2 transgene overexpression may be affecting the transcription of various inflammatory and cell adhesion markers in the tumor cells thus regulating the tumor microenvironment and tumor cell migration.

Figure 2.20: Inflammatory cytokine expression and EMT markers in DMBA-TPA induced skin tumors in WT and MMTV-FLAG-hPAD2 mice.

The DMBA-TPA induced skin tumors were collected in RNA-later at the end of the study, extracted RNA and qRT-PCR was performed. Figure 3.7A shows that IFNγ, CCL17 and IL8 homologues MIP2 and LIX are elevated in transgenic tumors compared to WT tumors. The correlation coefficients of inflammatory markers (MIP2, LIX) and EMT markers (Vimentin, E-cadherin and Snail) to the transgene hPAD2 levels and is given in Figure 3.7B. The inflammatory cytokines and EMT marker vimentin and the E-cadherin repressor, Snail showed strong positive correlation with the hPAD2 levels while the cell adhesion marker E-cadherin showed a strong negative correlation.

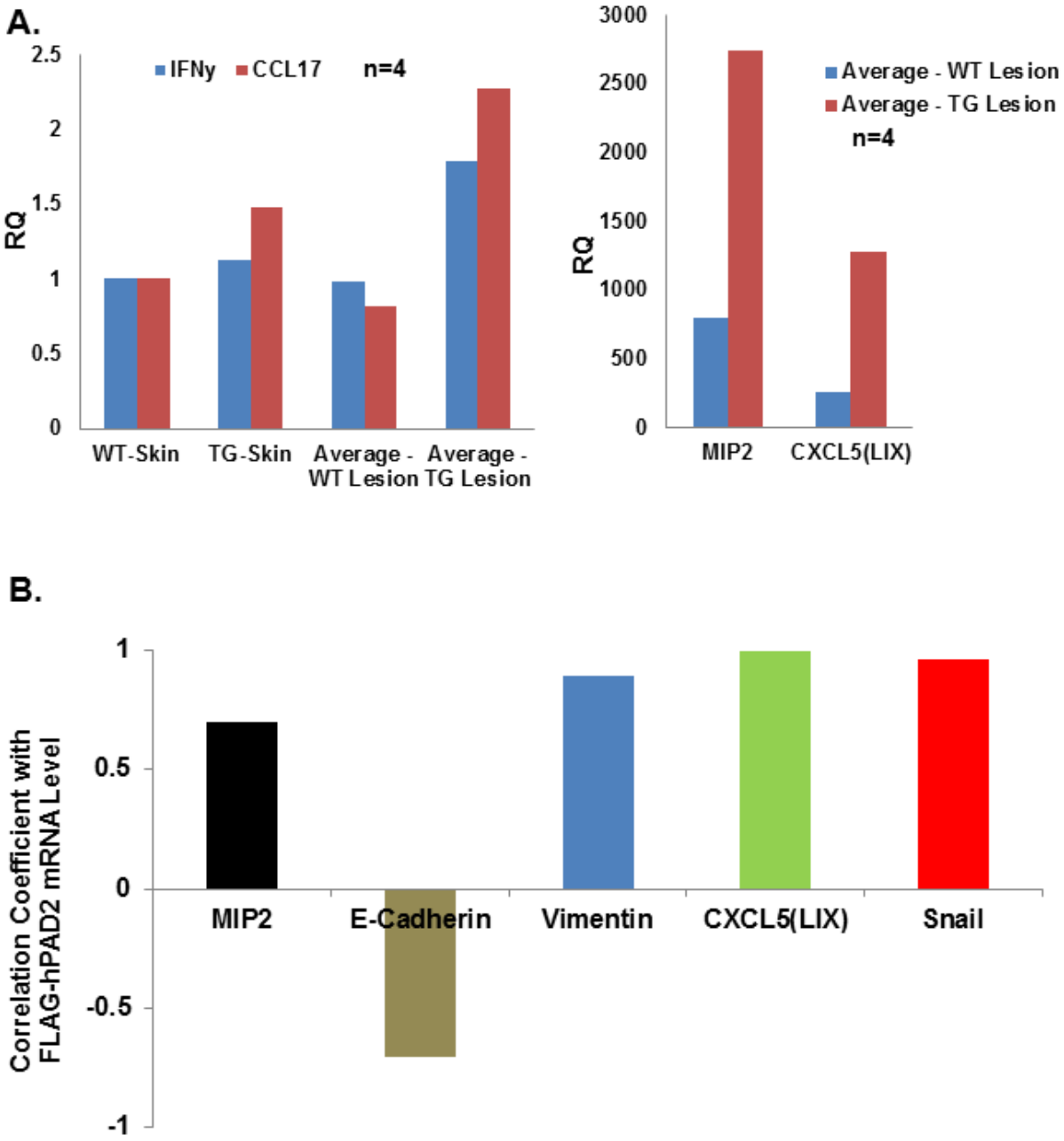
A.
IFNy
CCL17
n=4
RQ
2.5
2
1.5
1
0.5
0
WT-Skin
TG-Skin
Average - WT Lesion
Average - TG Lesion
3000
2500
2000
1500
1000
500
0
MIP2
CXCL5(LIX)
Average - WT Lesion
Average - TG Lesion
n=4
B.
Correlation Coefficient with FLAG-hPAD2 mRNA Level
1
0.5
0
-0.5
-1
MIP2
E-Cadherin
Vimentin
CXCL5(LIX)
Snail

MMTV-FLAG-hPAD2 mice skin tumors show increased CCL7 expression and activation of STAT3 pathway

We observed that the IL8 mouse homologues MIP2, LIX and IL6 mRNA levels were highly elevated in PAD2 overexpressing tumors. This result is consistent with the results we previously observed in the lab using a PAD2 overexpressing human SCC cell line [37] and the pattern observed in the spontaneous skin tumors in these transgenic mice. One of the known downstream pathways activated by IL8 and IL6 receptor activation is the STAT3 pathway. Given the high levels of IL6 present in the transgenic tumor cells, we predicted that these tumor cells will also contain increased levels of nuclear phospho-STAT3 in higher frequency. Immunofluorescence staining using anti-phospho-STAT3 antibody and confocal microscopic imaging showed that nuclear localization of phospho-STAT3 is significantly increased in the transgenic tumors (**Figure 2.21**). Activation of phospho-STAT3 has been shown to assist in tumor progression and can lead to anti-apoptotic effects in tumor cells.

Figure 2.21: phosho-STAT3 levels in DMBA-TPA induced skin tumors in WT and MMTV-FLAG-hPAD2 mice. Formalin fixed, paraffin embedded tumor sections were stained with anti-phospho-STAT3 antibody and imaged using a confocal microscope to detect levels and nuclear localization of phosphor-STAT3 (Red). There was strong nuclear staining for phosphor-STAT3 in the transgenic tumor sections while the WT tumor tissue showed reduced nuclear staining (measurement bar = 200µm).

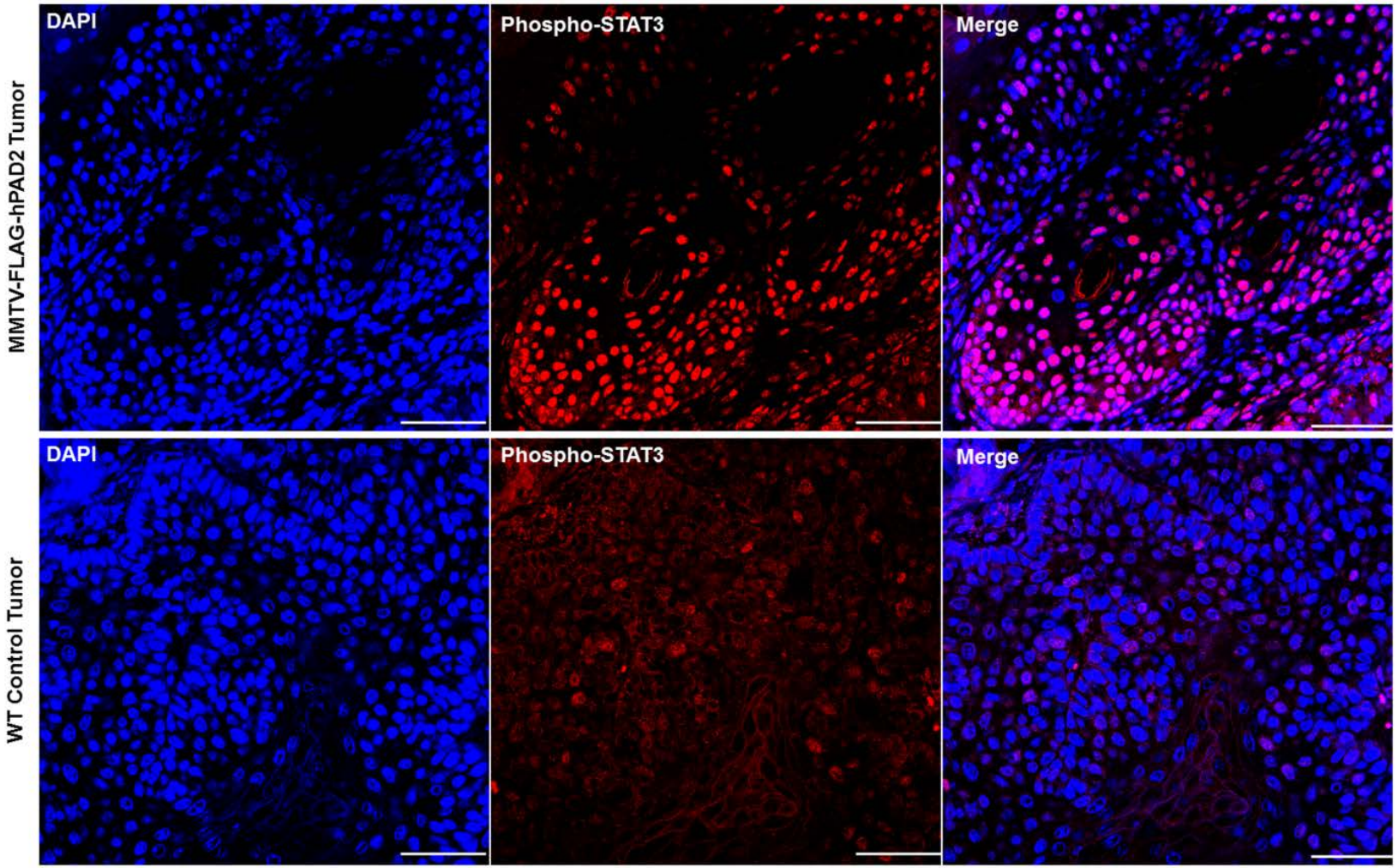
DAPI
Phospho-STAT3
Merge
MMTV-FLAG-hPAD2 Tumor
DAPI
Phospho-STAT3
Merge
WT Control Tumor

2.5 Discussion

In the present study, we have demonstrated that transgenic mice overexpressing PADI2 in the epidermis are sufficient to develop skin lesions that progress to invasive squamous cell carcinomas (SCC). Moreover, we have verified these results using the human squamous cell carcinoma cell line, A431, in which we stably overexpressed PADI2, resulting in the increased invasiveness and malignancy of these cells.

While *PADI2* transgenic expression in the mammary glands was detected, the MMTV-FLAG-PADI2 mice failed to develop any mammary tumors. Transgenic mice under control of the MMTV-LTR promoter can often have low expression in the mammary gland, or only noticeable expression in the mammary glands of lactating or multi-parous mice [38-40]. In addition, the MMTV promoter often becomes hypermethylated, and thus silenced [41]. While we have noted high expression in the mammary glands of our transgenic mice, perhaps further analysis of transgenic PADI2 expression over the life span of the mice might indicate age-related variation in expression. Future studies will examine the effectiveness of challenging our MMTV-FLAG-PADI2 mice, either genetically or chemically, to induce mammary carcinomas.

Recent research has shown that inflammation plays an important role in the development of advanced SCC tumors in mice [42]. As mentioned previously, numerous studies have documented a role for PADI-mediated

citrullination in immune diseases characterized by inflammation. In addition, we recently identified a new role for PADI2 in inflammation, as we found that PADI2-mediated histone tail hypercitrullination is important during macrophage extracellular trap (MET) formation in inflamed tissues [43, 44]. Increasing evidence supports a pro-tumorigenic role for immune cells and inflammatory processes, with tumor-promoting inflammation recently defined as an emerging hallmark of cancer [45, 46]. Many inflammatory mediators, including cytokines and chemokines, are important for the growth and proliferation of pre-malignant cells [47]. These mediators often activate oncogenic transcription factors, such as NFκB and STAT3 [48-50]. PADI2 has been shown to regulate cytokine signaling in macrophages via citrullination of IKKγ, which controls NFκB expression activity [51]. Furthermore, PADI2 has also been shown to citrullinate CXCL8 (IL8) [52], again suggesting a role for regulating the inflammatory microenvironment of the cancer microenvironment.

We show here that *Il6* and *Il8* expression is increased in the skin lesions of MMTV-FLAG-PADI2 transgenic mice. These results were also confirmed using the A431 cell line overexpressing FLAG-PADI2. Both IL6 and IL8 have been shown to be important in the progression of cancer, having a critical role in tumor growth, angiogenesis, and EMT [53-62]. Further work is needed to identify exactly how PADI2 regulates the expression of these two inflammatory mediators.

In addition to increased *Il6* and *Il8* expression, skin lesions in the MMTV-FLAG-PADI2 mice also display increased markers of invasiveness and

EMT. Furthermore, the A431 cells overexpressing FLAG-PADI2 show increased invasion through a collagen matrix when compared to control transfected cells. Cells undergoing EMT are often at the leading edge of invasive tumors that are epithelial in origin. EMT is an important process during normal development by which epithelial cells acquire mesenchymal, fibroblast-like properties, and show reduced intercellular adhesion and increased motility. Several oncogenic pathways have been implicated in EMT, including Src, Ras, Ets, Wnt/β-catenin, as well as signaling downstream from the PI3K-AKT-axis resulting from IGF1, TGFβ, EGFR, and HER2 activation [63, 64]. Recently, studies have suggested a variety of epigenetic mechanisms may also play a role in EMT [65]. Interestingly, we have recently reported on a role for PADI4 in the progression of breast cancer and EMT, via the citrullination of GSK3β, which is known to regulate TGFβ [66]. Stadler et al. establish that PADI4 serves as a tumor suppressor, with dysregulation of PADI4-mediated citrullination of nuclear GSKβ activating TGFβ signaling, thereby inducing EMT in breast cancer cells and the production of more invasive tumors *in vivo*. Interestingly, the two representative skin lesions from MMTV-FLAG-PADI2 mice, which express the highest levels of transgenic *PADI2*, have markedly reduced levels of endogenous *Padi4*. Perhaps this indicates cross-talk between *PADI2* and *Padi4*, working in opposite fashion to promote tumorigenesis and invasiveness in tumors. Nevertheless, the critical molecular feature of EMT is the downregulation of E-cadherin, a cell adhesion molecule present in the plasma membrane of most normal epithelial cells. This is the

earliest event in EMT; however, as the cell progresses from epithelial-like to mesenchymal-like cells, they are often accompanied by the increased expression of Snail1 (*Snai1*) and the intermediate filament vimentin. We show here that *Snail1* is upregulated in the skin lesions of MMTV-FLAG-PADI2 mice, E-cadherin is reduced, and that vimentin levels increase, all indicative of EMT. This molecular evidence matches well with the invasive histology of the lesions, as we report that a subset of lesions advance to highly invasive squamous cell carcinomas. Snail expression is inversely correlated with E-cadherin expression, and has been shown to bind to E-boxes in the promoter of E-cadherin, directly repressing gene expression via various mechanisms [67, 68]. The most established method of repression is via the recruitment of HDAC containing complexes to the E-cadherin promoter, such as the Sin3A/HDAC1/HDAC2 complex [69]. We have already shown that PADI2 can function as an epigenetic regulator of genes in breast cancer cells [11]; however, further work is needed to characterize the mechanism behind PADI2 regulation of genes involved in both inflammation and EMT.

2.6 Conclusions

These tumors express high levels of transgenic human *PADI2* and display markers of increased invasiveness (i.e. EMT). Furthermore, a subset of these tumors shows the hallmarks of malignant progression from skin lesions to highly invasive squamous cell carcinomas. We have also replicated these results in the human squamous cell carcinoma cell line, A431. Using a two

stage chemical carcinogenesis model, in this study we show that MMTV-FLAG-hPAD2 mice are susceptible to skin tumor formation and in the presence of the transgene. These tumors often develop into invasive SCC and tend to increased more tumor associated inflammation. The cytokine profile between WT and transgenic tumors also showed a striking contrast with the transgenic tumors expressing more IL8 homologues (MIP2 and LIX), CCL17 and IL6. Furthermore, we found that STAT3 pathway is activated in the transgenic tumors as evidenced by increased nuclear localization of phosphor-STAT3, which is consistent with the effect of IL8 and IL6 receptor activated downstream signaling. We also showed that PAD2 levels are inversely correlated with cell adhesion marker E-cadherin and favor the EMT transition by increasing Snail expression, which is an E-cadherin repressor. This study provides novel insight into the role of PAD2 in tumor progression, regulation of invasive properties, and tumor associated inflammation and cytokine expression by tumor cells. Collectively, these studies provide functional and mechanistic evidence establishing PADI2 as a potential novel oncogene in the progression of epidermal carcinomas (**Figure 2.22**).

Figure 2.22: The role of PAD2 overexpression in regulation of tumor invasion and inflammation. hPAD2 transgene overexpression in DMBA-TPA induced skin tumors play critical role in regulating tumor associated inflammation and tumor invasiveness. Cytokines such as IL8 homologues MIP2 and LIX and IL6 can activate STAT3 pathway which in turn regulate antiapoptotic marker expression and tumor cell proliferation. Elevated levels of CCL17 in the transgenic tumors contribute to lymphocyte recruitment to the tumor microenvironment. PAD2 overexpressing tumors show EMT characteristics compared to the WT tumors making them more invasive. A positive feedback loop may exist between paracrine signaling of IL8 and IL6 activation of tumor cells and enhanced secretion of cytokines by these tumor cells which further favor immune cell recruitment.

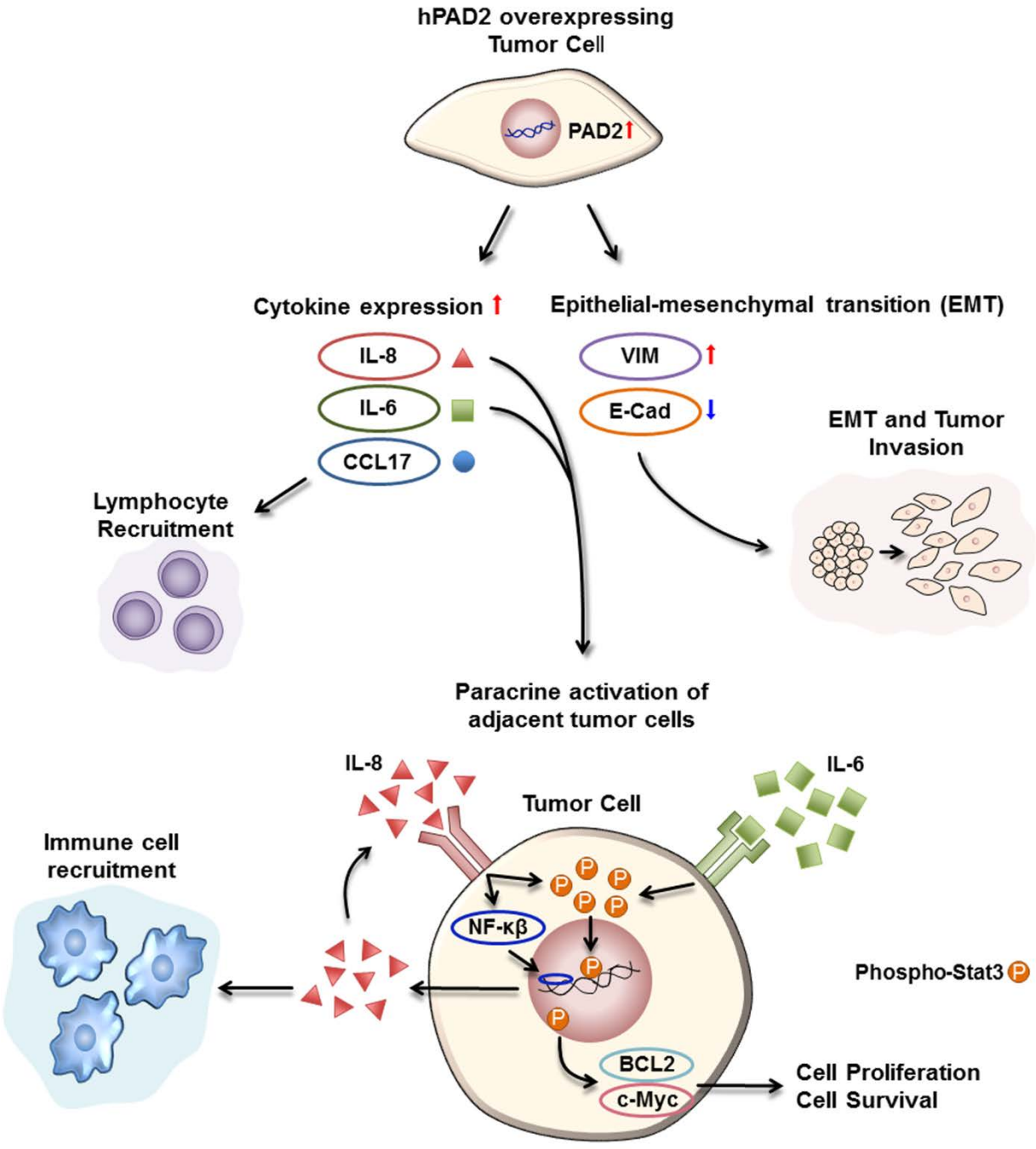
hPAD2 overexpressing
Tumor Cell
PAD2
Cytokine expression
Epithelial-mesenchymal transition (EMT)
IL-8
IL-6
CCL17
VIM
E-Cad
EMT and Tumor
Invasion
Lymphocyte
Recruitment
Paracrine activation of
adjacent tumor cells
IL-8
IL-6
Tumor Cell
Immune cell
recruitment
NF-κβ
Phospho-Stat3
BCL2
c-Myc
Cell Proliferation
Cell Survival

Table 2.1: Primers for Semi-quantitative RT-PCR

Primer Name	Sequence	Amplicon
mPADI4-gDNA-F	CCCACCCTGTGTGAGTTCTT	395bp
mPADI4-gDNA-R	GCCCAGAGCTTCATGTCTTC	
hPADI2-cds-F	ATTGAGATCTCCCTGGATGTG	194bp
hPADI2-cds-R	TCCTTGAGATCTTCCTTGCTG	
mPADI1-cds-F	CGTCTATAGTGATGTGCCCA	219bp
mPADI1-cds-R	CTCCTGTGACTCAAAGTATGAC	
mPADI2-cds-F	CAAGATCCTGTCCAATGAGAG	189bp
mPADI2-cds-R	ATCATGTTCACCATGTTAGGGA	
mPADI3-cds-F	GATTCTTAACAACCAGAGCCT	183bp
mPADI3-cds-R	CAGCATATTCACCAAGTCGG	
mPADI4-cds-F	CTACTCTGACCAAGAAAGCC	193bp
mPADI4-cds-R	ATTTGGACCCATAACTCGCT	
mGAPDH-cds-F	GGGCATCTTGGGCTACAC	209bp
mGAPDH-cds-R	GGTCCAGGGTTTCTTACTCC	

Table 2.3: Primers for mouse quantitative RT-PCR (SYBR)

Primer Name	Sequence
mECAD-F	ATCCTCGCCCTGCTGATT
mECAD-R	ACCACCGTTCTCCTCCGTA
mVIM-F	TGCGCCAGCAGTATGAAA
mVIM-R	GCCTCAGAGAGGTCAGCAAA
mSNAIL-F	CTTGTGTCTGCACGACCTGT
mSNAIL-R	CAGGAGAATGGCTTCTCACC
mCOX2-F	GATGCTCTTCCGAGCTGTG
mCOX2-R	GGATTGGAACAGCAAGGATTT
mGSK3B-F	TCCTTATCCCTCCACATGCT
mGSK3B-R	CCACGGTCTCCAGCATTAGT
mIL6-F	GCTACCAAACTGGATATAATCAGGA
mIL6-R	CCAGGTAGCTATGGTACTCCAGAA
mIL8-F	TGCTCAAGGCTGGTCCAT
mIL8-R	GACATCGTAGCTCTTGAGTGTCA
mKI67-F	CAAGAGGAAGTCTCTTGGCACT
mKI67-R	ACTCTTGTTTCCCTGGAGACTG
mPADI1-F	ATGACCCCCAACACTCAGC
mPADI1-R	CGGCCGTGGATATCTGTC
mPADI2-F	GATCCTCATCGGAAGCAGTT
mPADI2-R	AGTCGCGTACCACCTTGG

mPADI3-F	CCCCTAGCAATGACCTCAAC
mPADI3-R	ATAGGCCAGGGGCAAATG
mPADI4-F	TGACCCTACAGGTGAAAGCA
mPADI4-R	GGGTCCATAGTATGAAACTCGAA
mACTB-F	CTAAGGCCAACCGTGAAAAG
mACTB-R	ACCAGAGGCATACAGGGACA

Table 2.4: Primers for human quantitative RT-PCR (SYBR)

Primer Name	Sequence
hPADI2-F	TCTCAGGCCTGGTCTCCAT
hPADI2-R	AAGATGGGAGTCAGGGGAAT
hECAD-F	TGGAGGAATTCTTGCTTTGC
hECAD-R	CGCTCTCCTCCGAAGAAAC
hVIM-F	GGCTCGTCACCTTCGTGAAT
hVIM-R	GAGAAATCCTGCTCTCCTCGC
hGSK3β-F	GACATTTCACCTCAGGAGTGC
hGSK3β-R	GTTAGTCGGGCAGTTGGTGT
hSNAIL-F	GCTGCAGGACTCTAATCCAGA
hSNAIL-R	ATCTCCGGAGGTGGGATG
hSLUG-F	TGGTTGCTTCAAGGACACAT
hSLUG-R	GCAAATGCTCTGTTGCAGTG
hNFκB-F	CTGGCAGCTCTTCTCAAAGC
hNFκB-R	TCCAGGTCATAGAGAGGCTCA
hRELA-F	ACCGCTGCATCCACAGTT
hRELA-R	GATGCGCTGACTGATAGCC
hCOX2-F	GCTTTATGCTGAAGCCCTATGA
hCOX2-R	TCCAACTCTGCAGACATTTCC
hIL6-F	GCCCTGAGAAAGGAGACATGTAA
hIL6-R	TTGTTTTCTGCCAGTGCCTC

hIL8-F	ACTGAGAGTGATTGAGAGTGGAC
hIL8-R	AACCCTCTGCACCCAGTTTTC
hCCND1-F	GAAGATCGTCGCCACCTG
hCCND1-R	GACCTCCTCCTCGCACTTCT
hKI67-F	TTACAAGACTCGGTCCCTGAA
hKI67-R	TTGCTGTTCTGCCTCAGTCTT
hMYC-F	CACCAGCAGCGACTCTGA
hMYC-R	GATCCAGACTCTGACCTTTTGC
hHRAS-F	GGACGAATACGACCCCACTAT
hHRAS-R	TGTCCAACAGGCACGTCTC
hACTB-F	CCAACCGCGAGAAGATGA
hACTB-R	CCAGAGGCGTACAGGGATAG

2.7 References

1. Vossenaar, E.R., Zendman, A.J., van Venrooij, W.J. & Pruijn, G.J. PAD, a growing family of citrullinating enzymes: genes, features and involvement in disease. *Bioessays* **25**, 1106-18 (2003).

2. Balandraud, N. et al. A rigorous method for multigenic families' functional annotation: the peptidyl arginine deiminase (PADs) proteins family example. *BMC genomics* **6**, 153 (2005).

3. Chumanevich, A.A. et al. Suppression of colitis in mice by Cl-amidine: a novel peptidylarginine deiminase inhibitor. *American journal of physiology. Gastrointestinal and liver physiology* **300**, G929-38 (2011).

4. Lange, S. et al. Protein deiminases: New players in the developmentally regulated loss of neural regenerative ability. *Developmental biology* (2011).

5. Willis, V.C. et al. N-alpha-benzoyl-N5-(2-chloro-1-iminoethyl)-L-ornithine amide, a protein arginine deiminase inhibitor, reduces the severity of murine collagen-induced arthritis. *J Immunol* **186**, 4396-404 (2011).

6. Yao, H. et al. Histone Arg modifications and p53 regulate the expression of OKL38, a mediator of apoptosis. *J Biol Chem* **283**, 20060-8 (2008).

7. Li, P. et al. Coordination of PAD4 and HDAC2 in the regulation of p53-target gene expression. *Oncogene* **29**, 3153-62 (2010).

8. Tanikawa, C. et al. Regulation of protein Citrullination through p53/PADI4 network in DNA damage response. *Cancer Res* **69**, 8761-9 (2009).

9. Cherrington, B.D., Morency, E., Struble, A.M., Coonrod, S.a. & Wakshlag, J.J. Potential role for peptidylarginine deiminase 2 (PAD2) in citrullination of canine mammary epithelial cell histones. *PloS one* **5**, e11768 (2010).

10. Cherrington, B.D. et al. Potential Role for PAD2 in Gene Regulation in Breast Cancer Cells. *PLoS One* **7**, e41242 (2012).

11. Zhang, X. et al. Peptidylarginine deiminase 2-catalyzed histone H3 arginine 26 citrullination facilitates estrogen receptor alpha target gene activation. *Proc Natl Acad Sci U S A* **109**, 13331-6 (2012).

12. Zhang, X. et al. Genome-Wide Analysis Reveals PADI4 Cooperates with Elk-1 to Activate c-Fos Expression in Breast Cancer Cells. *PLoS genetics* **7**, e1002112 (2011).

13. Hennighausen, L., Wall, R.J., Tillmann, U., Li, M. & Furth, P.A. Conditional gene expression in secretory tissues and skin of transgenic mice using the MMTV-LTR and the tetracycline responsive system. *J Cell Biochem* **59**, 463-72 (1995).

14. Wagner, K.U. et al. Spatial and temporal expression of the Cre gene under the control of the MMTV-LTR in different lines of transgenic mice. *Transgenic research* **10**, 545-53 (2001).

15. Méchin, M.-C. et al. Deimination is regulated at multiple levels including auto-deimination of peptidylarginine deiminases. *Cellular and molecular life sciences : CMLS* **67**, 1491-503 (2010).

16. Kanno, T. et al. Human peptidylarginine deiminase type III: molecular cloning and nucleotide sequence of the cDNA, properties of the recombinant enzyme, and immunohistochemical localization in human skin. *J Invest Dermatol* **115**, 813-23 (2000).

17. Nishijyo, T., Kawada, A., Kanno, T., Shiraiwa, M. & Takahara, H. Isolation and molecular cloning of epidermal- and hair follicle-specific peptidylarginine deiminase (type III) from rat. *J Biochem* **121**, 868-75 (1997).

18. Akiyama, K. & Senshu, T. Dynamic aspects of protein deimination in developing mouse epidermis. *Exp Dermatol* **8**, 177-86 (1999).

19. Nakashima, K. et al. Molecular characterization of peptidylarginine deiminase in HL-60 cells induced by retinoic acid and 1alpha,25-dihydroxyvitamin D(3). *J Biol Chem* **274**, 27786-92 (1999).

20. Chavanas, S. et al. Peptidylarginine deiminases and deimination in biology and pathology: relevance to skin homeostasis. *J Dermatol Sci* **44**, 63-72 (2006).

21. Ishigami, A. et al. Human peptidylarginine deiminase type II: molecular cloning, gene organization, and expression in human skin. *Arch Biochem Biophys* **407**, 25-31 (2002).

22. Bhatia, A. et al. Tamoxifen-loaded novel liposomal formulations: evaluation of anticancer activity on DMBA-TPA induced mouse skin carcinogenesis. *J Drug Target* **20**, 544-50 (2012).

23. Ko, J.H., Jung, B.G., Park, Y.S. & Lee, B.J. Inhibitory effects of interferon-gamma plasmid DNA on DMBA-TPA induced mouse skin carcinogenesis. *Cancer Gene Ther* **18**, 646-54 (2011).

24. Pena, J.C., Rudin, C.M. & Thompson, C.B. A Bcl-xL transgene promotes malignant conversion of chemically initiated skin papillomas. *Cancer Res* **58**, 2111-6 (1998).

25. Fujiki, H. et al. Diversity in the chemical nature and mechanism of response to tumor promoters. *Prog Clin Biol Res* **298**, 281-91 (1989).

26. Fujiki, H. et al. Codon 61 mutations in the c-Harvey-ras gene in mouse skin tumors induced by 7,12-dimethylbenz[a]anthracene plus okadaic acid class tumor promoters. *Mol Carcinog* **2**, 184-7 (1989).

27. Kim, M.O. et al. DMBA/TPA-induced tumor formation is aggravated in human papillomavirus type 16 E6/E7 transgenic mouse skin. *Oncol Res* **16**, 325-32 (2007).

28. Burns, F.J., Vanderlaan, M., Sivak, A. & Albert, R.E. Regression kinetics of mouse skin papillomas. *Cancer Res* **36**, 1422-7 (1976).

29. Hennings, H. et al. Malignant conversion of mouse skin tumours is increased by tumour initiators and unaffected by tumour promoters. *Nature* **304**, 67-9 (1983).

30. Mueller, M.M. Inflammation in epithelial skin tumours: old stories and new ideas. *Eur J Cancer* **42**, 735-44 (2006).

31. Ornitz, D.M., Moreadith, R.W. & Leder, P. Binary system for regulating transgene expression in mice: targeting int-2 gene expression with yeast GAL4/UAS control elements. *Proceedings of the National Academy of Sciences of the United States of America* **88**, 698-702 (1991).

32. Campeau, E. et al. A versatile viral system for expression and depletion of proteins in mammalian cells. *PLoS One* **4**, e6529 (2009).

33. Wang, D., Russell, J.L. & Johnson, D.G. E2F4 and E2F1 have similar proliferative properties but different apoptotic and oncogenic properties in vivo. *Mol Cell Biol* **20**, 3417-24 (2000).

34. Livak, K.J. & Schmittgen, T.D. Analysis of relative gene expression data using real-time quantitative PCR and the 2(-Delta Delta C(T)) Method. *Methods* **25**, 402-8 (2001).

35. Boehnke, K., Falkowska-Hansen, B., Stark, H.J. & Boukamp, P. Stem cells of the human epidermis and their niche: composition and function in epidermal regeneration and carcinogenesis. *Carcinogenesis* **33**, 1247-58.

36. Liu, Y.L., Chiang, Y.H., Liu, G.Y. & Hung, H.C. Functional role of dimerization of human peptidylarginine deiminase 4 (PAD4). *PLoS One* **6**, e21314 (2011).

37. McElwee J.L. et al. Human Peptidylarginine Deiminase 2 (PAD2) Transgene Overexpression in Mice Leads to Skin Neoplasia. *Manuscript in Preparation* (2013).

38. Vargo-Gogola, T. & Rosen, J.M. Modelling breast cancer: one size does not fit all. *Nat Rev Cancer* **7**, 659-72 (2007).

39. Blanco-Aparicio, C. et al. Mice expressing myrAKT1 in the mammary gland develop carcinogen-induced ER-positive mammary tumors that mimic human breast cancer. *Carcinogenesis* **28**, 584-94 (2007).

40. Yao, Y. et al. Increased susceptibility to carcinogen-induced mammary tumors in MMTV-Cdc25B transgenic mice. *Oncogene* **18**, 5159-66 (1999).

41. Zhou, H. et al. MMTV promoter hypomethylation is linked to spontaneous and MNU associated c-neu expression and mammary carcinogenesis in MMTV c-neu transgenic mice. *Oncogene* **20**, 6009-17 (2001).

42. Gasparoto, T.H. et al. Inflammatory events during murine squamous cell carcinoma development. *J Inflamm (Lond)* **9**, 46.

43. Mohanan, S., Horibata, S., McElwee, J.L., Dannenberg, A.J. & Coonrod, S.A. Identification of macrophage extracellular trap-like structures in mammary gland adipose tissue: a preliminary study. *Front Immunol* **4**, 67 (2013).

44. Wang, Y. et al. Histone hypercitrullination mediates chromatin

decondensation and neutrophil extracellular trap formation. *J Cell Biol* **184**, 205-13 (2009).

45. Hanahan, D. & Weinberg, Robert A. Hallmarks of Cancer: The Next Generation. *Cell* **144**, 646-674 (2011).

46. Mantovani, A., Allavena, P., Sica, A. & Balkwill, F. Cancer-related inflammation. *Nature* **454**, 436-44 (2008).

47. Karin, M. & Greten, F.R. NF-kappaB: linking inflammation and immunity to cancer development and progression. *Nat Rev Immunol* **5**, 749-59 (2005).

48. Grivennikov, S.I. & Karin, M. Dangerous liaisons: STAT3 and NF-kappaB collaboration and crosstalk in cancer. *Cytokine Growth Factor Rev* **21**, 11-9 (2009).

49. Yu, H., Kortylewski, M. & Pardoll, D. Crosstalk between cancer and immune cells: role of STAT3 in the tumour microenvironment. *Nat Rev Immunol* **7**, 41-51 (2007).

50. Karin, M. Nuclear factor-kappaB in cancer development and progression. *Nature* **441**, 431-6 (2006).

51. Lee, H.J. et al. Peptidylarginine deiminase 2 suppresses inhibitory {kappa}B kinase activity in lipopolysaccharide-stimulated RAW 264.7 macrophages. *J Biol Chem* **285**, 39655-62 (2010).

52. Proost, P. et al. Citrullination of CXCL8 by peptidylarginine deiminase

alters receptor usage, prevents proteolysis, and dampens tissue inflammation. *J Exp Med* **205**, 2085-97 (2008).

53. Ancrile, B., Lim, K.H. & Counter, C.M. Oncogenic Ras-induced secretion of IL6 is required for tumorigenesis. *Genes Dev* **21**, 1714-9 (2007).

54. Sparmann, A. & Bar-Sagi, D. Ras-induced interleukin-8 expression plays a critical role in tumor growth and angiogenesis. *Cancer Cell* **6**, 447-58 (2004).

55. Aceto, N. et al. Co-expression of HER2 and HER3 receptor tyrosine kinases enhances invasion of breast cells via stimulation of interleukin-8 autocrine secretion. *Breast Cancer Res* **14**, R131 (2012).

56. Fernando, R.I., Castillo, M.D., Litzinger, M., Hamilton, D.H. & Palena, C. IL-8 signaling plays a critical role in the epithelial-mesenchymal transition of human carcinoma cells. *Cancer Res* **71**, 5296-306 (2011).

57. Freund, A. et al. IL-8 expression and its possible relationship with estrogen-receptor-negative status of breast cancer cells. *Oncogene* **22**, 256-265 (2003).

58. Freund, A. et al. Mechanisms underlying differential expression of interleukin-8 in breast cancer cells. *Oncogene* **23**, 6105-14 (2004).

59. Hartman, Z.C. et al. Growth of triple-negative breast cancer cells relies upon coordinate autocrine expression of the proinflammatory cytokines IL-6 and IL-8. *Cancer Res* **73**, 3470-80 (2013).

60. Hartman, Z.C. et al. HER2 overexpression elicits a proinflammatory IL-6 autocrine signaling loop that is critical for tumorigenesis. *Cancer Res* **71**, 4380-91 (2011).

61. Korkaya, H. et al. Activation of an IL6 inflammatory loop mediates trastuzumab resistance in HER2+ breast cancer by expanding the cancer stem cell population. *Mol Cell* **47**, 570-84 (2012).

62. Iliopoulos, D., Hirsch, H.A. & Struhl, K. An epigenetic switch involving NF-kappaB, Lin28, Let-7 MicroRNA, and IL6 links inflammation to cell transformation. *Cell* **139**, 693-706 (2009).

63. Larue, L. & Bellacosa, A. Epithelial-mesenchymal transition in development and cancer: role of phosphatidylinositol 3' kinase/AKT pathways. *Oncogene* **24**, 7443-54 (2005).

64. Tse, J.C. & Kalluri, R. Mechanisms of metastasis: epithelial-to-mesenchymal transition and contribution of tumor microenvironment. *J Cell Biochem* **101**, 816-29 (2007).

65. Stadler, S.C. & Allis, C.D. Linking epithelial-to-mesenchymal-transition and epigenetic modifications. *Semin Cancer Biol* **22**, 404-10 (2012).

66. Stadler, S.C. et al. Dysregulation of PAD4-mediated citrullination of nuclear GSK3beta activates TGF-beta signaling and induces epithelial-to-mesenchymal transition in breast cancer cells. *Proc Natl Acad Sci U S A* **110**, 11851-6 (2013).

67. Hajra, K.M., Chen, D.Y. & Fearon, E.R. The SLUG zinc-finger protein

represses E-cadherin in breast cancer. *Cancer Res* **62**, 1613-8 (2002).

68. Bolos, V. et al. The transcription factor Slug represses E-cadherin expression and induces epithelial to mesenchymal transitions: a comparison with Snail and E47 repressors. *J Cell Sci* **116**, 499-511 (2003).

69. Peinado, H., Olmeda, D. & Cano, A. Snail, Zeb and bHLH factors in tumour progression: an alliance against the epithelial phenotype? *Nat Rev Cancer* **7**, 415-28 (2007).

CHAPTER THREE

ROLE OF HISTONE CITRULLINATION BY PEPTIDYLARGININE DEIMINASE 2 (PAD2) IN MACROPHAGE EXTRACELLULAR TRAP (MET) FORMATION AND CHARACTERIZATION OF METS IN HUMAN TONGUE SQUAMOUS CELL CARCINOMA

Printed from the manuscript: Sunish Mohanan, Angela Yan, Lynne Anguish, Dalton McLean, Sachi Horibata, Paul Thompson, Neil Iyengar, Andrew J. Dannenberg, Scott A. Coonrod. Role of PAD enzymes in macrophage extracellular trap formation (METs) and characterization of tumor associated METs. *In preparation*.

Author contributions: conceived the research design and prepared the manuscript –SM and SAC; performed macrophage *in vitro* studies, immunostaining and imaging experiments – SM; conducted IHC experiments – SM and AY; PCR experiments – AY and DM; PAD2KO mice colony management – LA; provided tissue samples and reagents – NI, PRT and AJD.

3.1 Abstract

Histone citrullination mediated by peptidylarginine deiminases (PAD) is known to play a critical role during neutrophil extracellular trap release (“ETosis”). We previously have shown that site specific histone citrullination marks such as Histone H4 Citrulline 3 (H4Cit3) are abundantly present in the extracellular chromatin released during the process of ETosis by neutrophils. Following the observation that macrophages express high levels of the PAD isozyme, PAD2, we wanted to see if hypercitrullination is mediated by PAD2 in macrophage extracellular trap release (METs). In the present study, using RAW264.7 and primary peritoneal macrophages, we show that PAD2 is involved in ET release and that PAD2 deletion and drug-mediated PAD inhibition in macrophages affect the ability of macrophages to release extracellular chromatin traps following chemical stimulation by phorbol myristate acetate (PMA). Additionally, the morphological characteristics of METs were affected in the absence of nuclear PAD2. In order to study the *in vivo* significance of METs in human diseases, we have also characterized the presence of METs in human tongue squamous cell carcinomas (tSCC). Macrophages form a predominant inflammatory component within the tumor associated microenvironment of various carcinomas and sarcomas. The tSCC tissue sections contain tumor associated macrophages (TAMs) that are strongly positive for nuclear and cytoplasmic PAD2 expression. Immunostaining and confocal microscopic

evaluation of the tumor tissue showed scattered clusters of TAM-associated ETs that were stained positively for both DNA and high levels of citrullinated histones. Our study strongly suggests that PAD2 is involved in MET release and that PAD2 mediated MET release is an important process regulating inflammatory microenvironment in human carcinomas such as tSCC.

3.2 Introduction

Neutrophils can undergo a novel cell death mechanism called Neutrophil Extracellular Trap release (NETosis) following stimulation by pathogens or chemical treatments (LPS, PMA, IFN I and II, IL8) even though the exact induction process is not yet well described [1]. NETs are known to be composed of nuclear constituents such as chromatin DNA and histones in which various peptides and enzymes (e.g. elastase and myeloperoxidase) are embedded. A study by Brinkmann, Reichard [2] have characterized the process of NETosis and several initial studies had focused on the role of NETs in infectious diseases such as pneumococcal pneumonia, mastitis, streptococcal fasciitis and appendicitis. Brinkmann et al (2004) also showed, using electron microscopy, that NETs are composed of fibrous DNA strands with a diameter ranging from 15-17 nm and globular protein domains of various size aggregating to the DNA. It is also important to point out that the maturation of neutrophils is an important factor for their ability to release NETs as described by Martinelli et al. Using a microarray approach, Martinelli et al found that fully differentiated neutrophils highly express interferon target genes and that

interferon treatment can prime neutrophils for faster release of NETs. However, no priming steps were needed to induce NETs by stimulation with PMA, LPS or IL8. More recent studies focus on the broader role of ETosis in non-infectious conditions such as systemic lupus erythematosus [3], deep vein thrombosis and vasculitis [4, 5], cystic fibrosis [6], pre-eclampsia [7, 8], obesity associated adipose tissue inflammation [9] and cancer pathogenesis, and how ETs might be regulating the disease inflammatory microenvironment. The fact that stimulation by a combination of factors such as GM-CSF and LPS or C5a, which offers weaker stimulation compared to PMA mediated activation can still result in NET release suggested that priming of immune cells can predispose them to ET release upon secondary activation [10]. It has also been shown that several groups of immune cells other than neutrophils, such as macrophages, eosinophils, and mast cells are capable of releasing ETs in response to the above mentioned stimuli [9, 11-15].

Macrophage extracellular traps in diseases

Even though many studies have documented the role of NETs in a variety of disease conditions, the importance of METs in diseases are not well studied. Macrophage extracellular traps (METs) were recently characterized in infectious diseases such as *Mannheimia haemolytica* infection in Bovines [11] and *in vitro* exposure of Staphylococcus aureus to RAW 264.7 macrophage cell line [16]. Another study reported that human macrophages and monocytes can form METs in response to gold nanoparticles [17]. The molecular pathways

involved in MET release and the role played by METosis in patho-physiology of these diseases are yet to be understood. Our lab has previously observed that PAD2 is highly expressed in RAW 264.7 macrophage cell line and that PAD2 to tend to localize to DAPI poor, euchromatin regions of the macrophage nuclei [9]. This finding led to the hypothesis that PAD2 is a primary driver of histone hypercitrullination, chromatin decondensation, and ET formation in macrophages. Additionally, this hypothesis is further supported by our recent genomic study, which provided evidence that both global and promoter-specific chromatin decondensation is catalyzed by PAD2 in breast cancer cell lines [18]. In the present study, we focused on macrophage extracellular trap release process and if the underlying fundamental mechanism of chromatin decondensation during MET release is affected by peptidylarginine deiminase mediated histone citrullination.

Role of PADs and histone modifications in ETosis

PAD enzymes catalyze the conversion of positively-charged arginine residues to neutrally-charged citrulline in a hydrolytic reaction termed citrullination or deimination. This results in loss of charge at the citrullinated site and can dramatically alter the target protein's tertiary structure as well as protein-protein interaction [19, 20]. One of the major targets for PAD enzymes in the nucleus is the N-terminal tails of histones such as arginine-rich H3 and H4. Numerous reports have shown that PAD4 and, more recently, PAD2, mediate gene expression via citrullination of histone H4R3 and H3R26, respectively [20,

[21]. The mechanisms by which histone citrullination regulates gene transcription are starting to come to light in recent studies. We recently demonstrated that PAD2-catalyzed histone citrullination promoted localized chromatin decondensation at target gene promoters, thus likely facilitating binding of the basal transcriptional machinery [22]. Previous studies from our lab and several others have shown that PAD4 mediated histone hypercitrullination on a more global chromatin level, evidenced by higher levels of Histone H4 Citrulline 3 (H4Cit3) can promote global chromatin decondensation resulting in NETosis during inflammation. In this study, we showed by transmission electron microscopy that activation of PAD4 in HL60 granulocyte cells promoted a nuclear structural change characterized by the conversion of multi-lobular heterochromatic nuclei into a more round euchromatic nuclear pattern [20]. Additionally, we demonstrated that TNF-□ treatment of blood neutrophils resulted in the release of extracellular chromatin that was extensively citrullinated at histone H4R3. The link between the H4Cit3 modification and ETosis has been proven to be very strong and detection of this modification is now routinely utilized to document the presence of ETs in cells and tissues [9, 20, 23, 24]. Recently, the requirement of citrullination in NET formation *in vivo* was recently documented by investigators who showed that PAD4$^{-/-}$ mice have impaired ability to form NETs in response to various stimuli. Additionally, the investigators found that PAD4$^{-/-}$ mice are more susceptible to bacterial infections [25]. Extensive studies have previously shown that PAD activity is also closely associated with non-infectious immune-mediated inflammatory activity

such as that seen in autoimmune arthritis, colitis, and chronic obstructive pulmonary disease.

Role of ETosis in Cancer Pathogenesis

Immune system pose a double edged sword for cancer progression by either helping the body to identify and destroy tumor cells or assisting in promoting the tumor progression. Often these functions of immune system in tumor pathogenesis is termed as cancer immunoediting [26]. Using pediatric Ewing sarcoma tissue sections, [27]it has been shown that several of the patient samples were positive for the presence of NETs released by tumor associated neutrophils (TANs) and that the presence of TAN-ETs was significantly correlated to metastatic disease. NETs were also attributed to play a role in cancer associated thrombosis because different types of cancer can create a favorable microenvironment for NET release and these NETs in turn provide a scaffold and coagulation pathway stimulus for thrombotic disease to occur [28]. This study showed that lung and breast carcinoma in mice resulted in increased number of blood neutrophils that are prone to releasing NETs and that when a minor systemic infection was induced in tumor bearing mice, a large amount of NET chromatin was released and caused a prothrombotic state in the animal. The proof that NET components can actually sequester circulating tumor cells and assist in tumor metastasis came from the study conducted by Cools-Lartigue et al [29], which used *in vitro* models of static and dynamic interaction of NET and tumor cells and *in vivo* model of infection

using cecal ligation and puncture. They further showed that the NET assisted tumor metastasis can be inhibited by abolishing the NETs through treatment with DNAse or a neutrophil elastase inhibitor.

Tumor associated macrophages

Current integrated approach to cancer treatment has made it essential to further understand the unique role played by tumor microenvironment which can favor or block the malignant progression. Cross talk between cancer cells and the immune cells in the tumor microenvironment is considered an important factor for cancer progression. Immune cells release free radicals, such as reactive oxygen species and nitric oxide following activation and these molecules can cause DNA damage and gene mutations in tumor cells, helping tumor progression. Cancer immune response is predominantly macrophage mediated. Macrophages continuously infiltrate into the tumor microenvironment and are transitioned into TAMs when stimulated by paracrine factors, which are released by cancer cells, other groups of immune cells, and fibroblasts. Macrophages are able to efficiently respond to microenvironment signals given their cellular plasticity and exhibit significantly altered cell physiology in both innate and adaptive immune response [30]. TAMs are the key orchestrators of tumor associated inflammation constituting the main type of inflammatory cells in tumors [31]. The Macrophages can cause both anti- and pro-tumor effects through the expression of various signals based on the microenvironment cues and phenotypic differentiation into either

M1 or M2 types. TAM signature offers a potential therapeutic target and a prognostic marker. Clinical studies conducted in breast cancer patients have shown that TAMs are significantly correlated with micro-vessel density, regional lymph node metastasis, hormone receptor status and tumor grades, treatment efficacy, and survival period [32]. Increased $CD68^+$ index is predictive of high tumor vascularity, nodal metastasis, and decreased duration of disease-free survival [33, 34]. Mahmoud et al [35] showed in a large cohort study of 1322 breast cancer patients that TAMs offer significant predictive value for breast cancer prognosis. Currently, there are no studies characterizing the presence of TAM-ETs and specifically addressing the role of tumor-associated macrophage released ETs in tumor microenvironment regulation. Given the critical role played by TAMs in tumor progression, we hypothesized that TAMs within the human tSCCs may release METs which can further modify the tumor microenvironment by recruiting and activating other immune cells and by altering tumor cell properties such as migration.

3.3 Materials and Methods

Cell culture and MET induction

RAW 264.7 mouse macrophage cells were grown in RPMI 1640 medium (Cellgro, Manassas, VA) supplemented with 10% fetal bovine serum containing penicillin-streptomycin. Peritoneal macrophages were isolated from

wild type and PAD2KO mice using a previously described method [36]. Briefly, mice were humanly euthanized and fur dampened with povidone-iodine. Animal was secured on a dissection board and about 6 ml of sterile PBS was injected into the caudal half of the peritoneal cavity. The abdomen was massaged for about 20 seconds and using 20 gauge needles the PBS containing resident peritoneal macrophages was aspirated out. The cells were spun down at 300g for 10 minutes and the cell pellet was washed twice with RPMI medium. The cells were resuspended at $2X10^6$ cells/mL concentration and placed in the 37^oC incubator for 2 hours to allow the macrophages to adhere. Then the plates were gently washed with RPMI medium to remove non-adherent cells. The macrophages were then grown in a sterile, humidified incubator at 37^oC and 5% CO_2.

To perform IF staining, macrophages were grown on 12 mm glass coverslips for 2 days at 37^oC (Fisher Scientific, Hanover Park, IL). The RAW 264.7 macrophages were treated with PMA for four hours, then washed in 1X phosphate buffered saline (PBS), fixed in 4% cold paraformaldehyde for 20 minutes, washed in 1X PBS, and immunofluorescence staining was performed as described below.

MET isolation and Quantitation

METs were isolated from ET rich supernatant using a previously described method. MET DNA was quantitated using a Sytox Green Assay (REF-NET

epithelial paper). Briefly, following PMA stimulation, medium was collected with extensive pipetting. The cells and cellular debris was centrifuged down in 300g for 10 minutes and the ET containing supernatant was collected and the extracellular DNA in the supernatant measured by Sytox Green Assay. In order to isolate METs, macrophages were treated with PMA, medium was removed after 4 hours of treatment, and the cells were gently washed with RPMI twice. 200 µL of fresh RPMI was added to the cells and extensively pipetted to collect the MET smear present over the macrophage monolayer. The cell debris was separated by 300g centrifugation for 10 minutes and the MET DNA in the supernatant was quantitated using the Sytox Green assay. 10 µg of MET DNA containing supernatant was used for treating macrophages and A431 cancer cells to evaluate the effects of METs in immune and cancer cell properties. Equal amount of RPMI supernatant from DMSO treated macrophages was used as a control.

Immunohistochemistry (IHC) and Immunofluorescence (IF)

IHC and IF experiments followed our previously described protocol [37]. Briefly, paraffin embedded tissue sections from human tSCC were deparaffinized and rehydrated in 3X 5 minute washes in xylene followed by single sequential 5 minute washes in 100, 95, and 75% EtOH. An endogenous peroxidases quenching step was done by incubating the slides for 10 minutes in 0.5% hydrogen peroxide in cold methanol. We used a citrate buffer antigen retrieval method which was performed by boiling slides two times for 10 minutes in

0.01M sodium citrate pH 6.8 and, after cooling, slides were washed in 1X PBS. Tissue slides and fixed coverslips containing RAW264.7 cells were then blocked in 10% normal goat serum and 2X casein (Vector Labs, Burlingame, CA) for 20 minutes at room temperature in a humidified microprobe chamber. Slides were blotted to remove excess blocking solution and then primary antibody diluted in 1X PBS was applied to the slides for 2 hours at room temperature. Slides or cover slips were then stained with primary antibodies (anti-PAD2 - ProteinTech #122100-1-AP, anti-histone H4 Citrulline 3 - Millipore-Upstate # 07-596). Following 3X washing with 1X PBS, slides were incubated with a 1:200 dilution of secondary antibody labelled with peroxidase for IHC or appropriate fluorophore (in 1X PBS) for confocal imaging for 1 hour at room temperature and then washed 3X in 1X PBS. For IHC, slides were incubated in DAB chromagen (Vector Labs) solutions according to the manufacturer's protocol, washed and then counterstained with Gill's hematoxylin and coverslipped. For each experiment, duplicate slides were treated with control rabbit IgG antibody at the appropriate concentration as a negative control. For confocal imaging, DAPI and Sytox Green were used as DNA staining reagents. We observed that Sytox Green offered promising visualization of decondensed chromatin ETs compared to the weaker staining by DAPI.

In order to quantitate changes in levels of citrullinated histones during MET induction in WT and PAD2KO macrophages, a time course experiment was

performed, evaluating H4Cit3 immunofluorescence intensity at 0, 2, 6 and 24 hours. Primary peritoneal macrophages were treated with 2 µg/ml of PMA, fixed and H4Cit3 immunofluorescence staining was performed using the method described above. Five different fields from each time point were imaged using confocal microscopy and the mean integrated fluorescence intensity was calculated using ImageJ software analysis as previously described by Gavet and Pines [38]. The results were then analyzed by one-way ANOVA to detect statistical differences and a p-value < 0.01 was considered significant. The results are presented as mean ± Standard deviation or mean ± Standard error.

3.4 Results and Discussion

PAD2 is highly expressed in RAW 264.7 and peritoneal primary macrophages and is a potential candidate for MET release regulation

We previously have shown the strong expression of PAD2 mRNA and PAD2 protein in RAW 264.7 macrophage cells [9]. In the current study, we also found that primary peritoneal macrophages, similar to RAW 264.7 macrophage cell line, are also highly positive for nuclear and cytoplasmic expression of PAD2 (**Figure 3.1A and 3.1B**). We noticed that PAD2 appeared to localize, in part, to DAPI-poor euchromatic regions of the macrophage nuclei while PAD4 was found only weakly expressed these macrophage cells.

Figure 3.1: PAD2 expression in cultured RAW 264.7 macrophage cells and in mouse primary peritoneal macrophages. (**A**) RT-PCR for PAD2 and PAD4 mRNA expression in cultured RAW 264.7 macrophages and primary peritoneal macrophages. Two unique primer sequence sets were used to test for PAD2 and PAD4 mRNA expression levels. RAW 264.7 macrophages were found to strongly express PAD2 mRNA. GAPDH mRNA expression levels were used as the internal control for RT-PCR. (**B**) Anti-PAD2 immunofluorescence labeling shows positive staining in macrophages. Nuclei are stained with DAPI.

PAD2 mRNA and protein expression in RAW 264.7 macrophage cell line and primary peritoneal macrophages (PMφ)

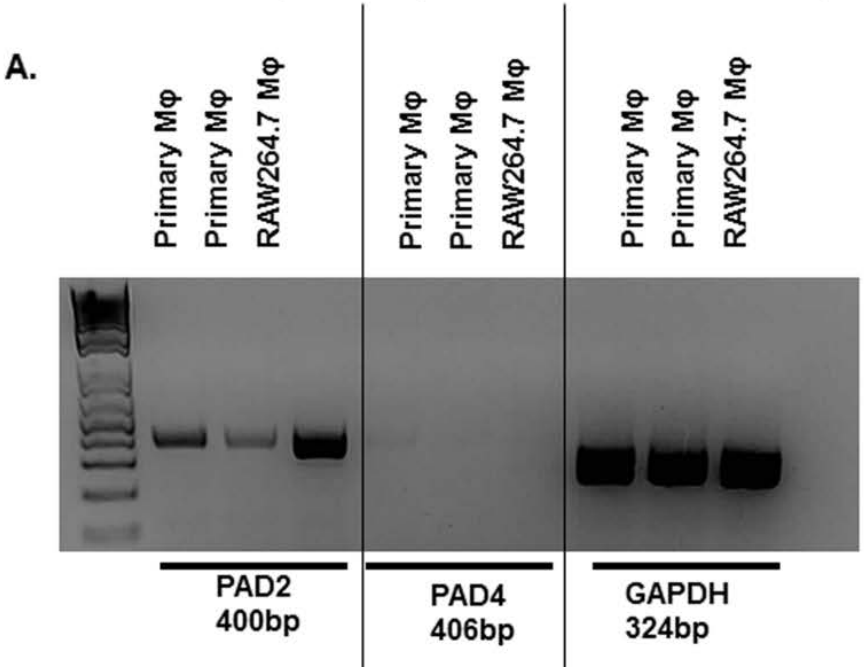

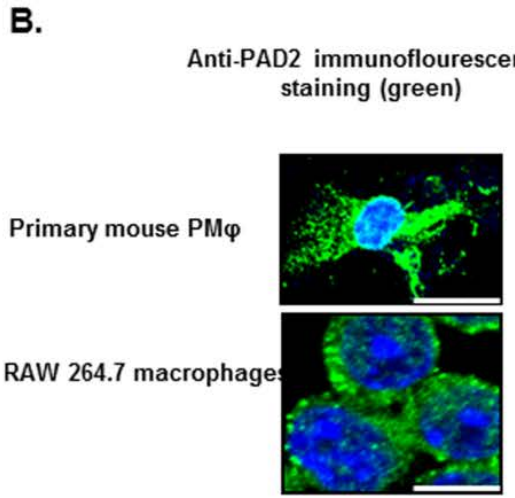

PAD2KO macrophages show an impaired ability to release METs

In order to test the role of PAD2 in MET release, we collected WT and PAD2KO primary peritoneal macrophages from mice and treated them with PMA to induce MET release. The treated macrophages were stained with Diff-Kwik dye to evaluate the number and morphological characteristics of METs. We found that the number of METs was reduced in PAD2KO macrophages and the PAD2KO METs appeared more condensed, less branching, and often failed to form the classically described tangled web-like pattern of ETs (**Figure 3.2**). On the other hand, for WT METs, the released extracellular DNA strands were found to be forming complex webs, or, interestingly clusters of vesicular bodies which are presumed to be DNA-Histone complexes.

METs contain high levels of citrullinated histones which is reduced upon PAD2 deletion

METs released as a result of PMA treatment were stained with anti-H4Cit3 antibody. H4Cit3 is a site specific histone citrullination which has been characterized as a marker of ETs in several previous studies. The METs released by primary PMΦ were highly positive for H4Cit3 staining (**Figure 3.3A**). Using confocal z-stack 3-dimensional microscopy we further evaluated

the METs and showed that citrullinated histone rich METs appears to interact with other macrophages in the vicinity (**Figure 3.3B**). These METs often form long linear or branching web like structures extending far beyond the cell borders which are delineated with Phalloidin staining (**Figure 3.3C**), potentially providing a scaffold for other macrophages to bind and modify the inflammatory microenvironment. In order to evaluate the role of PAD2 in histone citrullination during MET formation, a time course experiment was performed in which the peritoneal macrophages were treated with PMA for 30 minutes, 2 hours or 4 hours and were stained with anti-H4Cit3 antibody. We found by H4Cit3 IF staining that PAD2KO PMΦ nuclei showed reduced levels of histone citrullination at 30 minutes, 2 hours and 4 hours time points as evidenced by weaker H4Cit3 staining intensity (data not shown). These data supported our hypothesis that PAD2 is critical in mediating histone hypercitrullination during MET induction process.

PAD2 deletion and drug-mediated PAD inhibition reduce chromatin decondensation

One of the morphological changes seen after PMA stimulation during MET production is nuclear chromatin decondensation. PADs are known to play a role in chromatin decondensation and our lab has previously shown that PAD4 is involved in chromatin decondensation in neutrophils during NET release. We wanted to see if a PAD inhibitor treatment or PAD2 deletion will cause a reduction in PMΦ chromatin decondensation following PMA stimulation.

Figure 3.2: Peritoneal macrophages release extracellular traps (ETs) in response to PMA stimulation. Diff-Kwik staining shows web of extracellular DNA released by WT macrophages forming an interconnected scaffold of thin chromatin fibers compared to the DMSO control cells (**Figure 3.2a and 3.2b**). Occasionally there are vesicular bodies presumed to be DNA-histone complexes released by PMA treated macrophages (**Figure 3.2c**). The PAD2KO macrophages show reduced number of macrophages releasing METs with more condensed morphological appearance compared to WT METs (**Figure 3.2e**).

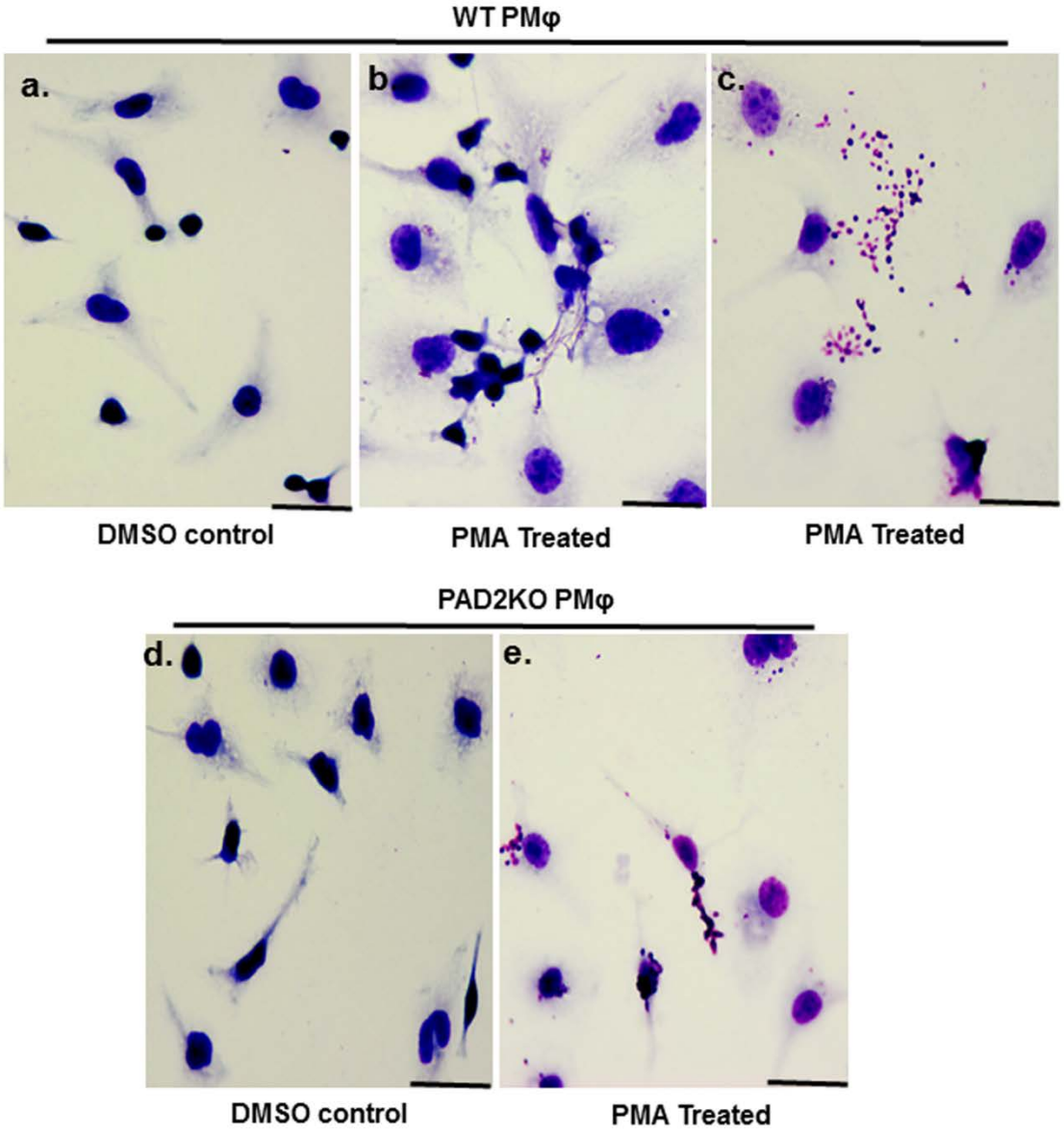
WT PMφ
a.
b
c.
DMSO control
PMA Treated
PMA Treated
PAD2KO PMφ
d.
e.
DMSO control
PMA Treated

Figure 3.3: METs are highly positive for citrullinated histones and MET web interact with other macrophages in their vicinity. Primary PMΦ cells were cultured on coverslips in RPMI medium and stimulated with PMA for four hours. The METs were visualized by DAPI + Anti-H4Cit3 antibody staining. Phalloidin staining for actin is used to visualize the cytoplasmic borders. Intense staining for H4Cit3 is observed in METs. The nuclei of macrophages appear to be distended following PMA treatment and also contain increased H4Cit3 levels. **Figure 3.3B** shows a surface plot of confocal z-scan imaging of H4Cit3 levels in METs. **Figure 3.3C** shows confocal Z-stack imaging of METs released by primary PMΦ extending beyond cell borders.

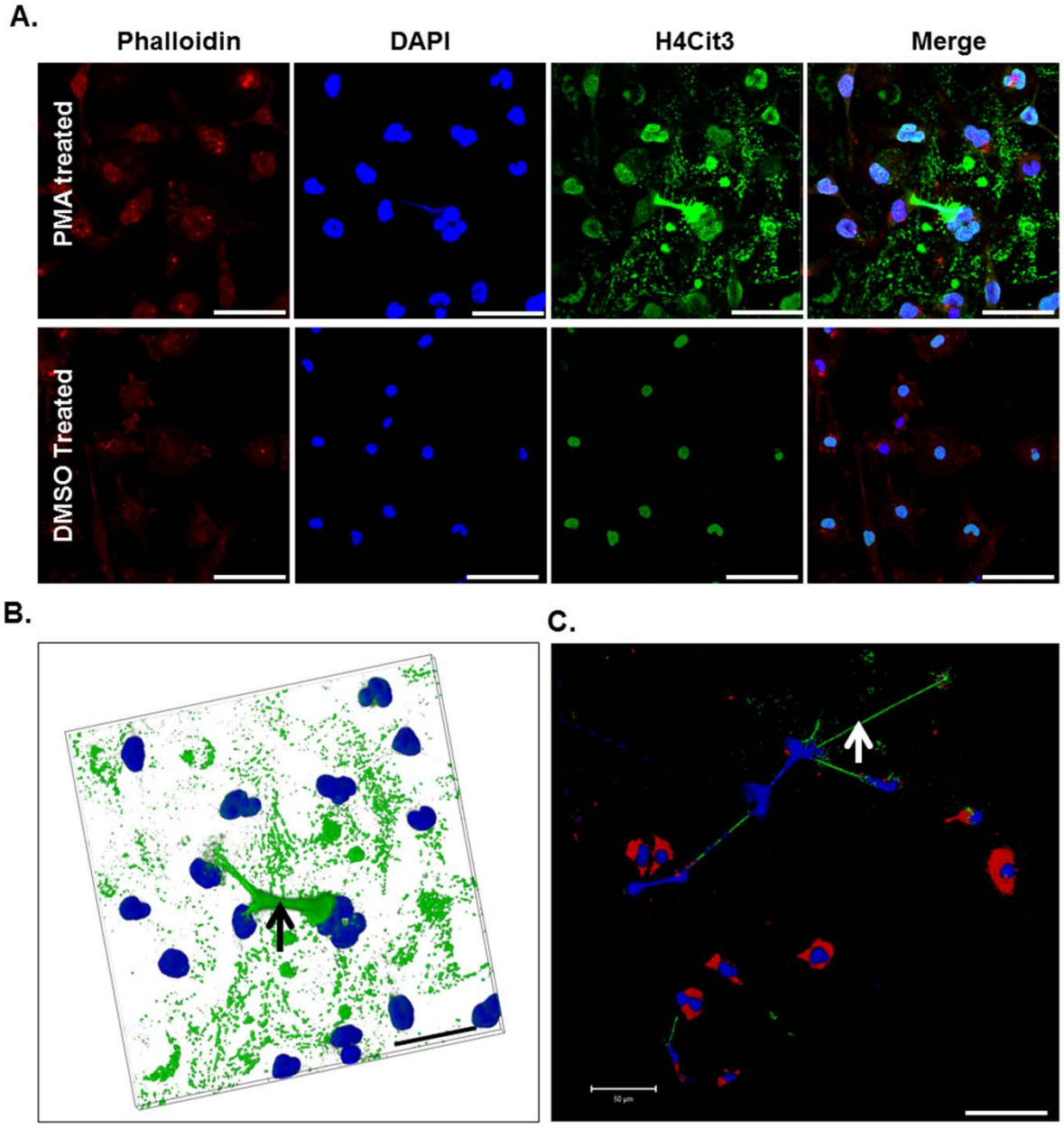
A.
Phalloidin
DAPI
H4Cit3
Merge
PMA treated
DMSO Treated
B.
C.

We treated RAW 264.7 macrophages for 24 hours with a new generation of PAD inhibitor BB-CLA, a PAD inhibitor at a concentration of 2.5 μM/ml and both the control cells and the BB-CLA treated cells were further treated with PMA for 30 minutes. The chromatin structure was visualized by Sytox Green staining and the cells were imaged using confocal microscopy. Both BB-CLA treated cells and PAD2KO PMΦ showed a more condensed chromatin pattern and smaller nuclear size compared to the wild type PMΦ and no-drug treatment group (**Figure 3.4**). In order to quantitate the ability of WT, PAD2 deleted PMΦ and PAD-inhibitor treated macrophages to release METs, a Sytox Green based DNA quantitation assay was performed. PAD2KO PMΦ and BB-CLA treated macrophage cells showed reduced MET release compared to the WT macrophages following PMA stimulation (**Figure 3.5**). This further confirmed the role of PAD2 played specifically in MET release.

PAD2 expression and H4Cit3 levels in TAMs in human tSCC

Though tumor associated NETs were previously described, there are no studies published characterizing tumor associated METs (TAM-ETs) or the role of histone citrullination in TAM-ETs. Head and neck squamous cell carcinomas are known to be associated with a predominant inflammatory component and we decided to evaluate human tongue SCC sections by immunostaining and confocal microscopy for the presence of METs.

Immunohistochemical staining for PAD2 strongly stained cytoplasm and nuclei of the immune cells surrounding the carcinoma cell islands. The cancer cells themselves showed weak cytoplasmic and nuclear staining for PAD2. Scattered tumor associated macrophages showed moderate to intense H4Cit3 nuclear staining and extranuclear streaming pattern (**Figure 3.6**). Using confocal microscopy, we found that MET-like structures exist in tSCC sections which are highly positive for citrullinated histones (**Figure 3.7**). To confirm the identity of the cells that are releasing these traps, we costained the tumor sections with F4/80, a macrophage marker, and DAPI, and found that the trap rich regions, which have streaming DNA and are stained positively for DAPI, were associated with F4/80 positive stained cells, and thus confirming that these ETs are indeed METs (**Figure 3.8**). A more specific marker for tumor associated macrophage that has been well described in the literature is CD68. We then costained the tSCC sections with CD68, anti-H4Cit3 and DAPI and imaged using confocal microscopy. We found that H4Cit3 and DAPI positive extracellular streaming structures consistent with METs are associated with CD68+ macrophages, which are associated with tumor cell clusters (**Figure 3.9A**). It is also interesting to note that we were able to identify MET sparse and MET rich areas within the same tissue section suggesting the inherent variability of the tumor microenvironment in tSCC which may further contribute to tumor heterogeneity (**Figure 3.9B**).

Figure 3.4. PAD2 deletion and drug-mediated inhibition affect nuclear chromatin decondensation in macrophages during MET induction. RAW 264.7 cells were treated with the PAD inhibitor BB-CLA for 24 hours. Untreated RAW 264.7 cells, BB-CLA pre-treated RAW 264.7 cells, PAD2 KO PMΦ and WT PMΦ were then treated with PMA for 30 minutes to observe the early changes during MET induction. The cells were stained with Sytox Green dye to visualize nuclear chromatin structure and nuclear size.

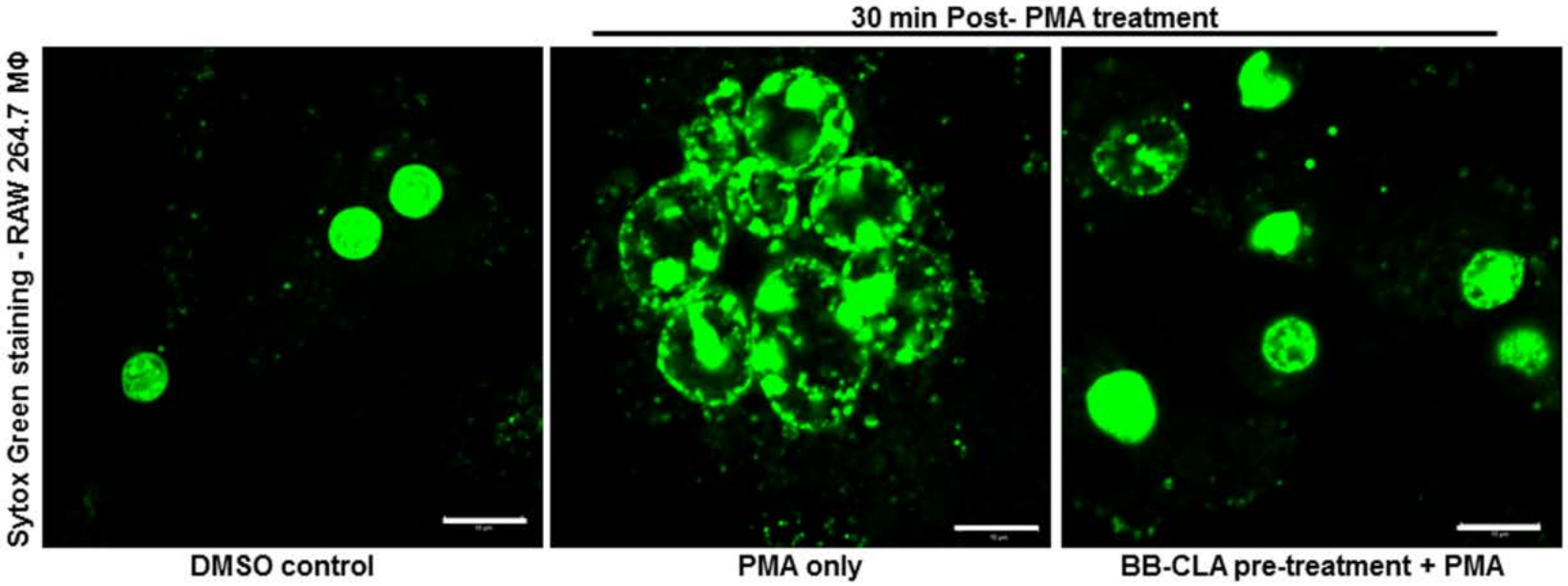
30 min Post- PMA treatment
Sytox Green staining - RAW 264.7 MΦ
DMSO control
PMA only
BB-CLA pre-treatment + PMA

Figure 3.5: Quantitation of MET release by WT, PAD2 KO PMΦ, and PAD inhibitor treated macrophages. The PMΦ cells from WT mice and PAD2KO mice were cultured for 24 hours and treated with PMA to induce MET formation. BB-CLA-PMA group received a 24 hour pretreatment with the PAD inhibitor BB-CLA. After 4 hours of PMA treatment MET containing supernantant was collected and the MET DNA was quantitated using Sytox Green assay. The florescent intensity values were standardized as a ratio to the florescent intensity observed in WT-DMSO control group and plotted as mean ratio ± SE.

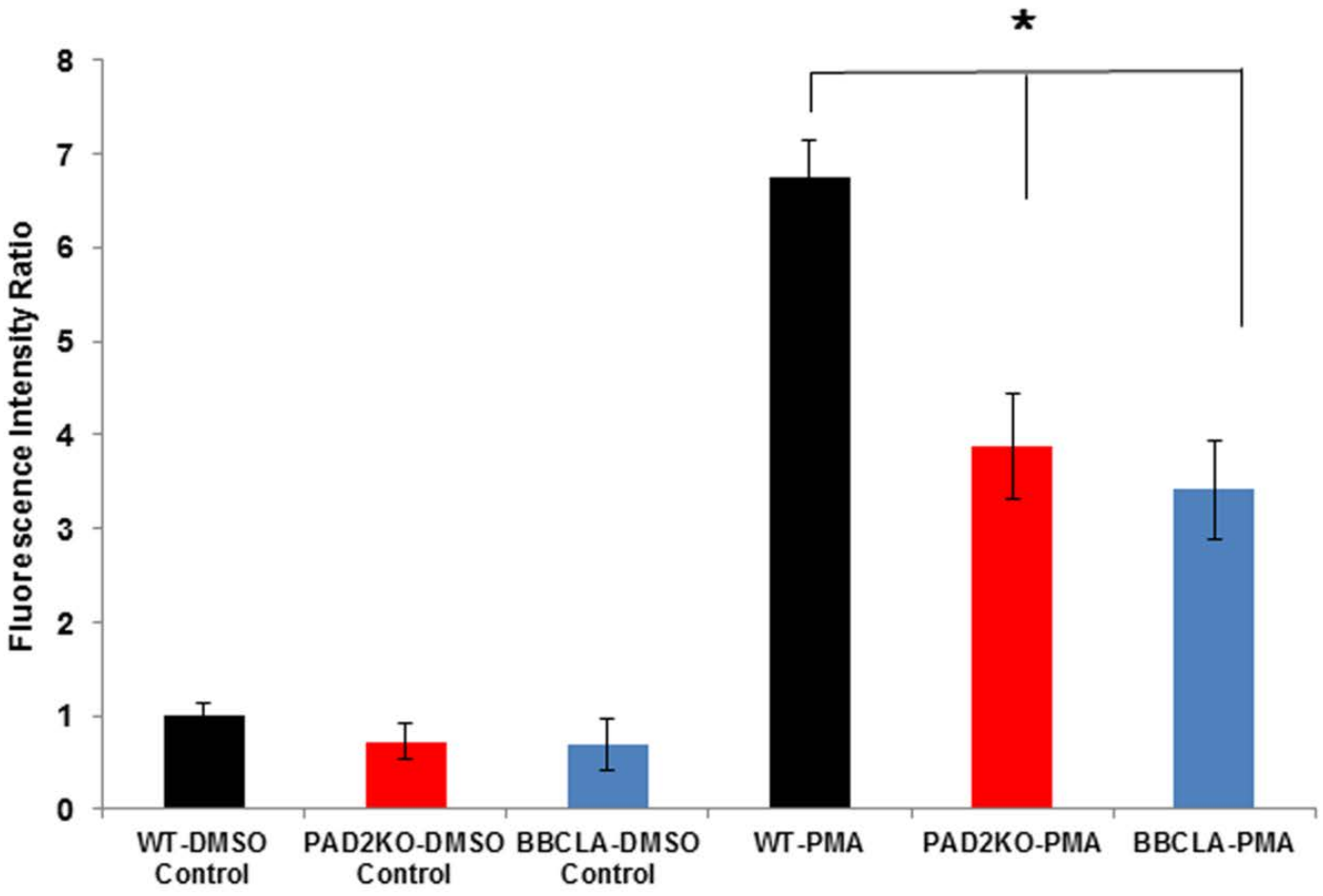
*
Fluorescence Intensity Ratio
0
1
2
3
4
5
6
7
8
WT-DMSO Control
PAD2KO-DMSO Control
BBCLA-DMSO Control
WT-PMA
PAD2KO-PMA
BBCLA-PMA

Figure 3.6: Immunohistochemical staining for H4Cit3 levels in human tongue squamous cell carcinomas. tSCC tissue sections from 12 different human patients were evaluated for PAD2 and H4Cit3 staining by immunohistochemistry. Non-specific IgG was used as the negative control. Immune cells surrounding tumor cell clusters showed strong cytoplasmic and nuclear staining for PAD2. H4Cit3 antibody stained a subset of tumor-associated inflammatory cells which had morphologic features consistent with macrophages. H4Cit3 staining varied in its intensity often showing intense nuclear staining and extranuclear streaming and appeared to extend beyond cell borders.

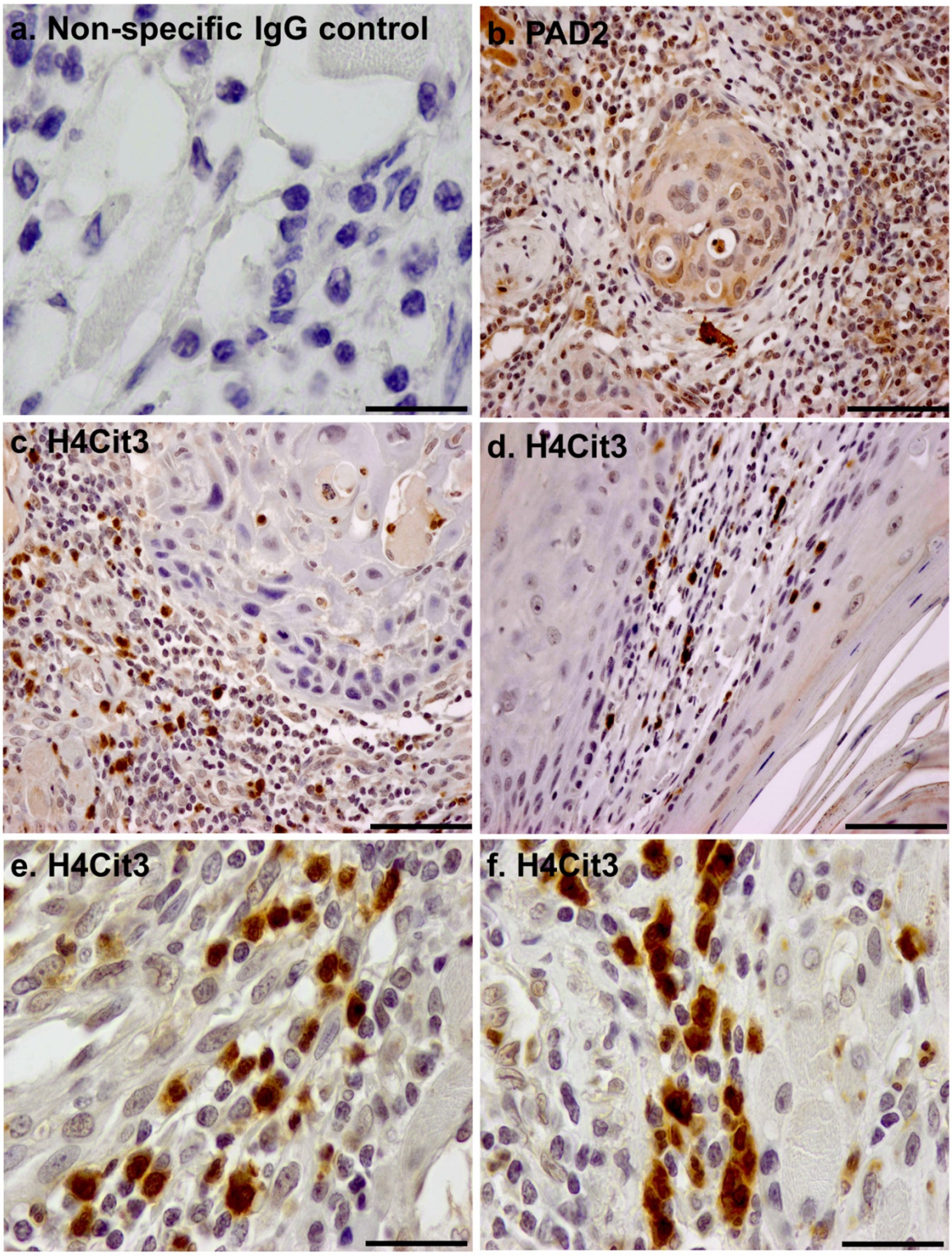
a. Non-specific IgG control
b. PAD2
c. H4Cit3
d. H4Cit3
e. H4Cit3
f. H4Cit3

Figure 3.7: H4Cit3 immunofluorescence staining in extracellular traps associated with tSCC inflammation. tSCC tissue sections from 12 different human patients were evaluated by costaining for the ET marker H4Cit3 and DNA marker DAPI and the immunofluorescence images were acquired by confocal microscopy.

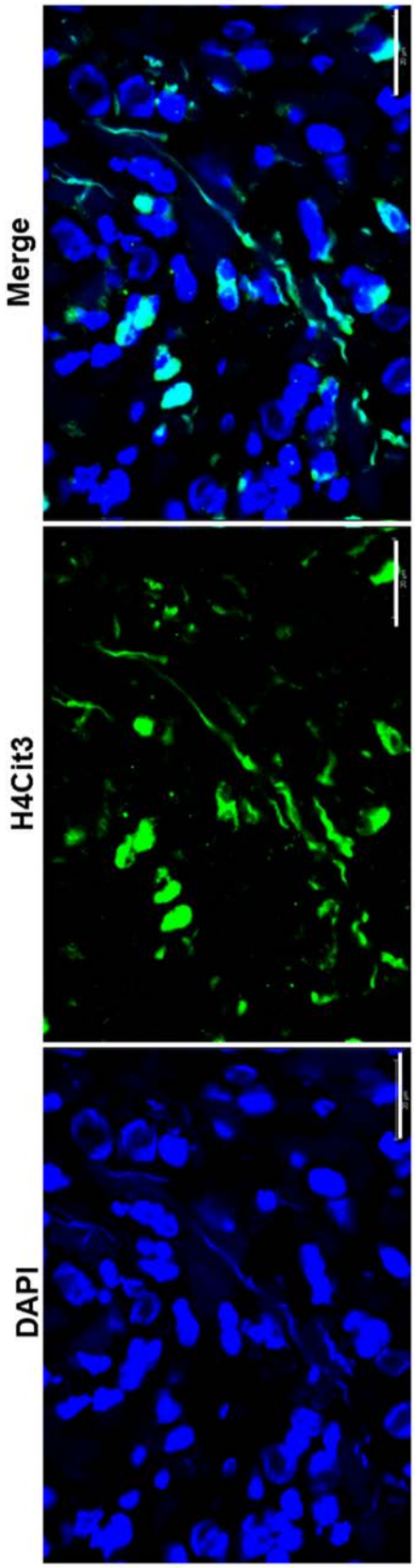
Merge
H4Cit3
DAPI

Figure 3.8: Costaining for macrophage marker F4/80 and DAPI to evaluate METs in tSCC sections. tSCC sections were stained with macrophage marker antibody, anti-F4/80 and nuclear stain DAPI and imaged using a confocal microscope. Scattered areas within the tumor associated inflammatory areas show the presence of extracellular DNA streaming forming an interconnected complex scaffold originating from nuclei of macrophages.

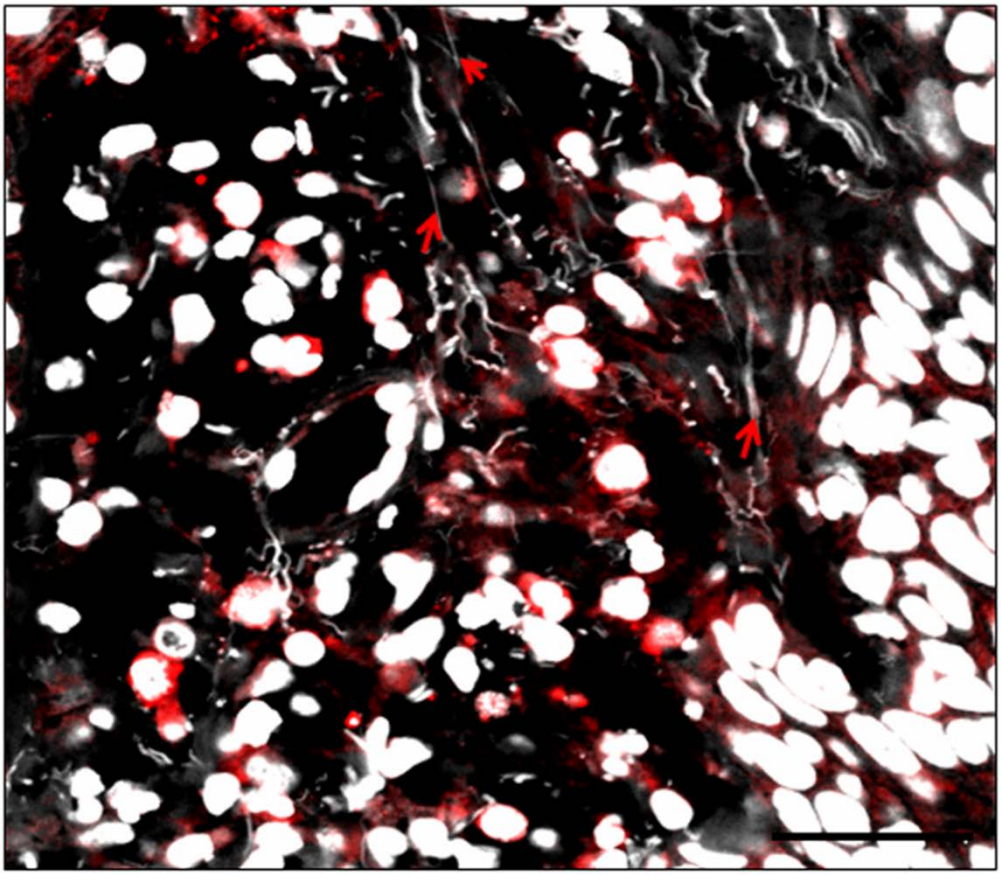

F4/80 - Red

DAPI - white

Figure 3.9: Costaining for TAM marker CD68, H4Cit3 and DAPI in METs associated with tSCC inflammation. (A) tSCC tissue sections were processed and costained with antibodies against CD68, H4Cit3 and the nuclear stain DAPI (B) Overall evaluation of the entire tissue section from each patient tissue sample showed that there are occasional MET rich pockets within the tumor tissue. Costaining for CD68, H4Cit3 and DAPI show that these extracellular traps are associated with CD68+ TAMs.

A.

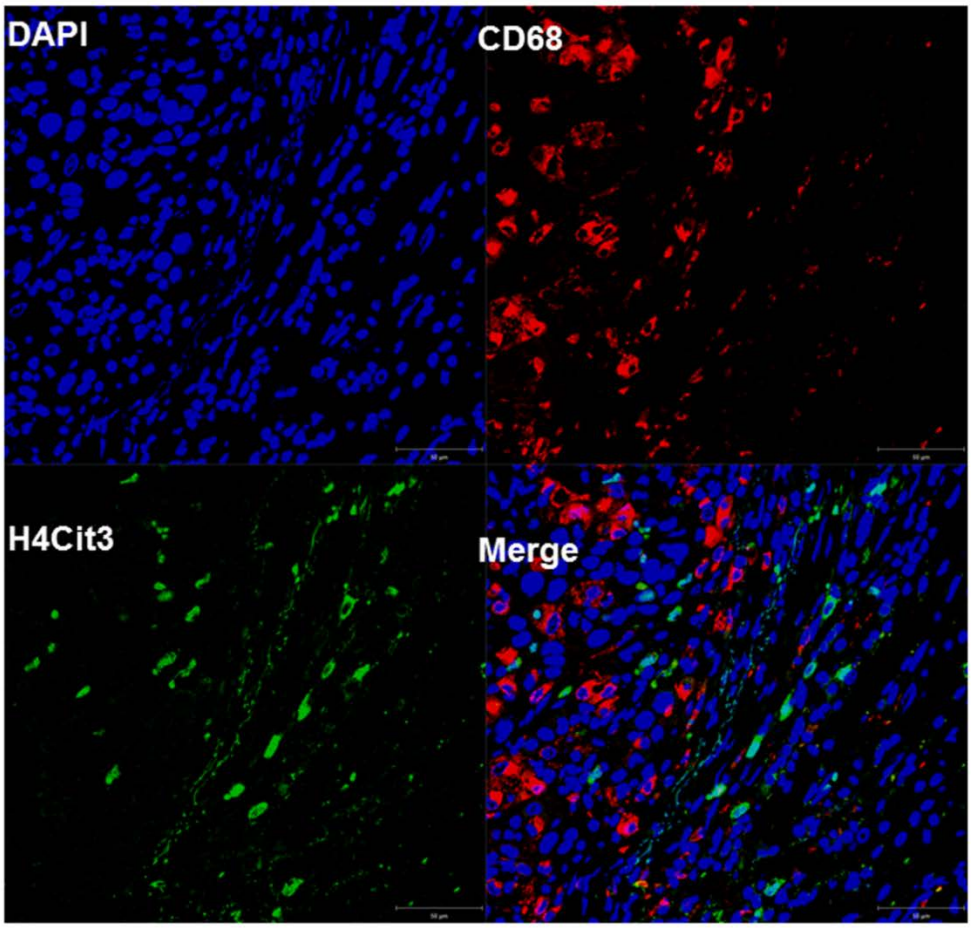
DAPI
CD68
H4Cit3
Merge

B.

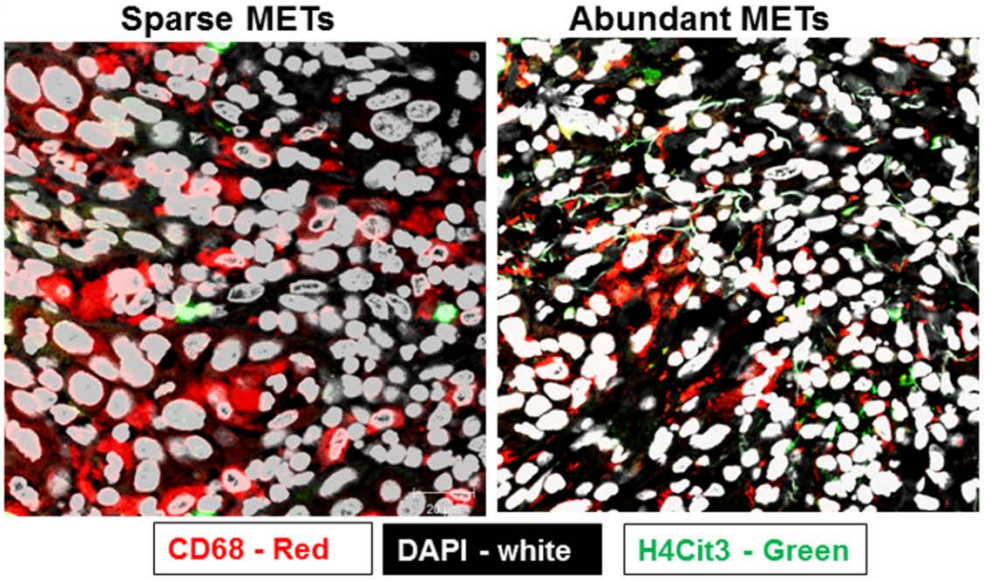
Sparse METs
Abundant METs
CD68 - Red
DAPI - white
H4Cit3 - Green

More recently, a term called “cellular hypercitrullination” is used in the context of rheumatoid arthritis. A study by Romero et al suggested that two main pore-forming pathways are involved in cellular hypercitrullination, namely, perforin and the membrane attack complex (MAC) [39]. Our study is the first to show that TAMs in human carcinomas as such tSCC can be activated to release METs and these METs are highly positive for citrullinated histones. A previous study suggested the possibility that Ewing Sarcoma associated TAN-ETs may be playing an anti-tumorigenic role by NET-mediated immune cell capture and prevention of metastasis or alternatively NET associated components acting as facilitators for metastasis [27]. Several components of NETs can be cytotoxic to cancer cells, for example, the tumoricidal effect on melanoma by MPO was shown by Odajima *et al.* [40]. Further studies are needed to clearly delineate the pro or anti-tumorigenic effects of MET components.

3.5 Conclusions

We identified PAD2 as a critical mediator during MET release using both macrophage cell lines and primary resident macrophages. Hypercitrullination of histones as evidenced by high H4Cit3 levels were observed in METs. The PAD2KO PM cells showed decreased efficiency in producing METs and a similar effect was also observed in macrophages treated with a PAD enzyme inhibitor. We further show that MET rich areas are present within human tSCC tissue sections and these tumor METs also contain high levels of citrullinated

histones. METs may play a critical role in regulating tumor associated inflammatory microenvironment and MET components may act as DAMPs, thus regulating tumor cell migration and immune cell recruitment. A summary of the potential functional roles for METs released into the tumor microenvironment is given in **Figure 3.10**. Previous studies have shown that histones can act as DAMPs and activate TLR4 signaling in immune cells thus further regulating immune cell – tumor cell paracrine signaling network. A MET rich environment may also regulate tumor cell properties such as migration and metastasis. PAD inhibitors may be used in vivo to dampen the MET release activity of TAMs and thus assist in immune modulation of tumor inflammatory microenvironment.

Figure 3.10: Proposed functional roles of METs in regulation of tumor microenvironment. METs may be critical mediators of tumor associated inflammation thus regulating tumor microenvironment. Our study shows that nuclear PAD2 is involved in chromatin decondensation during MET induction. The resulting extracellular traps are rich source of histones and nuclear proteins including citrullinated histones. Previous studies have shown that histones can act as DAMPs and activate TLR4 signaling activating adjacent macrophages and further regulating immune cell – tumor cell paracrine signaling. A MET rich environment may also regulate tumor cell properties such as migration and metastasis. PAD inhibitors may be used in vivo to dampen the MET release activity of TAMs and thus assist in immune modulation of tumor inflammatory microenvironment.

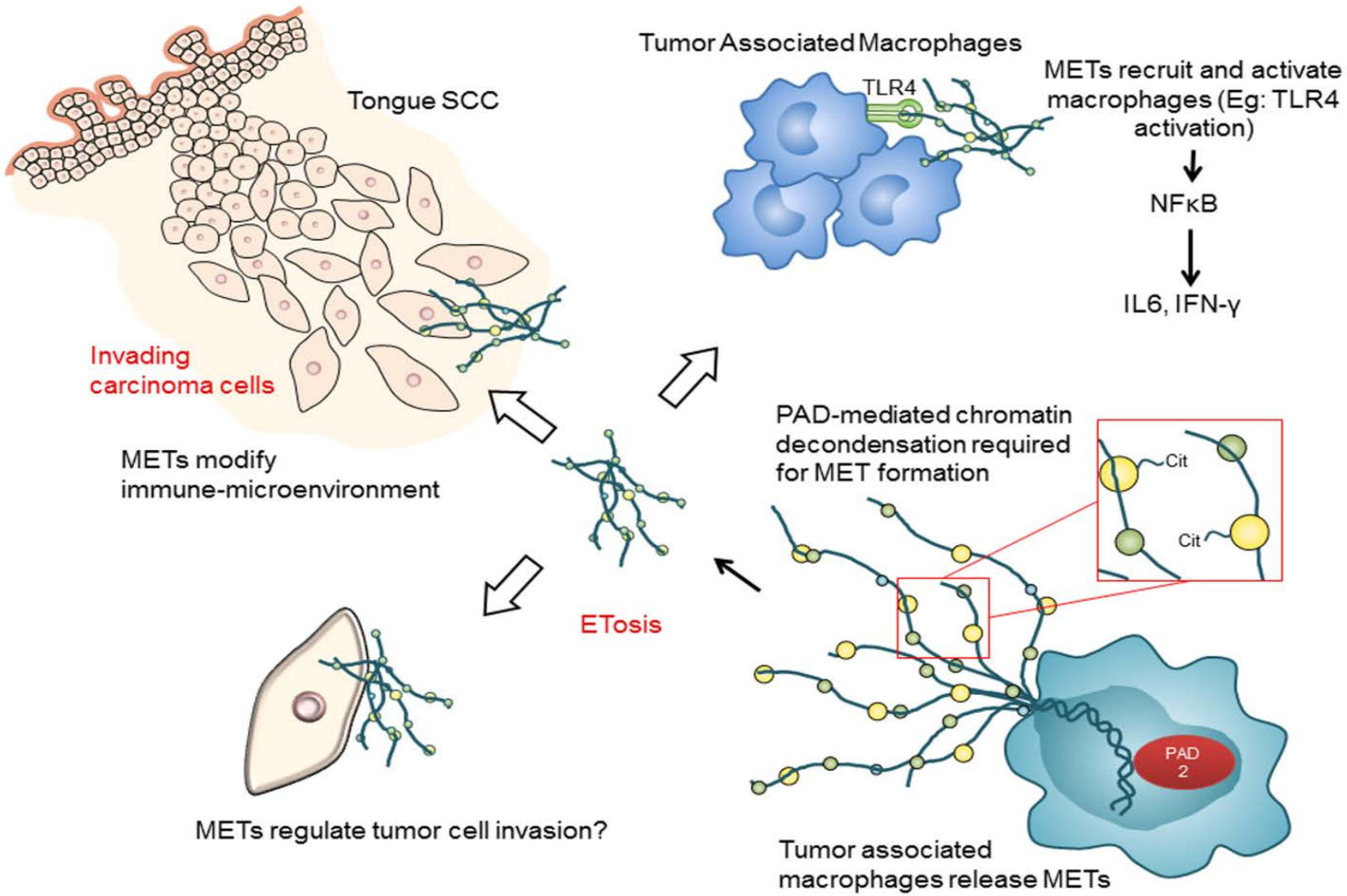
Tongue SCC
Invading carcinoma cells
METs modify immune-microenvironment
Tumor Associated Macrophages
TLR4
METs recruit and activate macrophages (Eg: TLR4 activation)
NFκB
IL6, IFN-γ
PAD-mediated chromatin decondensation required for MET formation
Cit
Cit
PAD 2
ETosis
METs regulate tumor cell invasion?
Tumor associated macrophages release METs

3.6 References

1. Wartha, F., Beiter, K., Normark, S. & Henriques-Normark, B. Neutrophil extracellular traps: casting the NET over pathogenesis. *Curr Opin Microbiol* **10**, 52-6 (2007).

2. Brinkmann, V. et al. Neutrophil extracellular traps kill bacteria. *Science* **303**, 1532-5 (2004).

3. Hakkim, A. et al. Impairment of neutrophil extracellular trap degradation is associated with lupus nephritis. *Proc Natl Acad Sci U S A* **107**, 9813-8 (2010).

4. Kessenbrock, K. et al. Netting neutrophils in autoimmune small-vessel vasculitis. *Nat Med* **15**, 623-5 (2009).

5. Brill, A. et al. Neutrophil extracellular traps promote deep vein thrombosis in mice. *J Thromb Haemost* **10**, 136-44 (2012).

6. Marcos, V. et al. CXCR2 mediates NADPH oxidase-independent neutrophil extracellular trap formation in cystic fibrosis airway inflammation. *Nat Med* **16**, 1018-23 (2010).

7. Gupta, A.K., Hasler, P., Holzgreve, W. & Hahn, S. Neutrophil NETs: a novel contributor to preeclampsia-associated placental hypoxia? *Semin Immunopathol* **29**, 163-7 (2007).

8. Gupta, A., Hasler, P., Gebhardt, S., Holzgreve, W. & Hahn, S.

Occurrence of neutrophil extracellular DNA traps (NETs) in pre-eclampsia: a link with elevated levels of cell-free DNA? *Ann N Y Acad Sci* **1075**, 118-22 (2006).

9. Mohanan, S., Horibata, S., McElwee, J.L., Dannenberg, A.J. & Coonrod, S.A. Identification of macrophage extracellular trap-like structures in mammary gland adipose tissue: a preliminary study. *Front Immunol* **4**, 67 (2013).

10. Yousefi, S., Mihalache, C., Kozlowski, E., Schmid, I. & Simon, H.U. Viable neutrophils release mitochondrial DNA to form neutrophil extracellular traps. *Cell Death Differ* **16**, 1438-44 (2009).

11. Aulik, N.A., Hellenbrand, K.M. & Czuprynski, C.J. Mannheimia haemolytica and its leukotoxin cause macrophage extracellular trap formation by bovine macrophages. *Infect Immun* **80**, 1923-33 (2012).

12. Yousefi, S., Simon, D. & Simon, H.U. Eosinophil extracellular DNA traps: molecular mechanisms and potential roles in disease. *Curr Opin Immunol* **24**, 736-9 (2012).

13. Kerstan, A., Simon, H.U., Yousefi, S. & Leverkus, M. Extensive accumulation of eosinophil extracellular traps in bullous delayed-pressure urticaria: a pathophysiological link? *Br J Dermatol* **166**, 1151-2 (2012).

14. Dworski, R., Simon, H.U., Hoskins, A. & Yousefi, S. Eosinophil and neutrophil extracellular DNA traps in human allergic asthmatic airways. *J Allergy Clin Immunol* **127**, 1260-6 (2011).

15. Simon, D. et al. Eosinophil extracellular DNA traps in skin diseases. *J Allergy Clin Immunol* **127**, 194-9 (2011).

16. Chow, O.A. et al. Statins enhance formation of phagocyte extracellular traps. *Cell Host Microbe* **8**, 445-54 (2010).

17. Bartneck, M., Keul, H.A., Zwadlo-Klarwasser, G. & Groll, J. Phagocytosis independent extracellular nanoparticle clearance by human immune cells. *Nano Lett* **10**, 59-63 (2010).

18. Zhang, X. et al. Peptidylarginine deiminase 2-catalyzed histone H3 arginine 26 citrullination facilitates estrogen receptor alpha target gene activation. *Proc Natl Acad Sci U S A* **(In Press)** (2012).

19. Mohanan, S. et al. Potential Role of Peptidylarginine Deiminase Enzymes and Protein Citrullination in Cancer Pathogenesis. *Biochemistry Research International* **2012** (2012).

20. Wang, Y. et al. Histone hypercitrullination mediates chromatin decondensation and neutrophil extracellular trap formation. *J Cell Biol* **184**, 205-13 (2009).

21. Cherrington, B.D. et al. Potential role for PAD2 in gene regulation in breast cancer cells. *PLoS One* **7**, e41242 (2012).

22. Zhang, X. et al. Peptidylarginine deiminase 2-catalyzed histone H3 arginine 26 citrullination facilitates estrogen receptor alpha target gene activation. *Proc Natl Acad Sci U S A* **109**, 13331-6 (2012).

23. Neeli, I., Khan, S.N. & Radic, M. Histone deimination as a response to inflammatory stimuli in neutrophils. *J Immunol* **180**, 1895-902 (2008).

24. Wong, K.W. & Jacobs, W.R., Jr. Mycobacterium tuberculosis exploits human interferon gamma to stimulate macrophage extracellular trap formation and necrosis. *J Infect Dis* **208**, 109-19 (2013).

25. Li, P. et al. PAD4 is essential for antibacterial innate immunity mediated by neutrophil extracellular traps. *J Exp Med* **207**, 1853-62 (2010).

26. Kim, R., Emi, M. & Tanabe, K. Cancer immunoediting from immune surveillance to immune escape. *Immunology* **121**, 1-14 (2007).

27. Berger-Achituv, S. et al. A proposed role for neutrophil extracellular traps in cancer immunoediting. *Front Immunol* **4**, 48 (2013).

28. Demers, M. et al. Cancers predispose neutrophils to release extracellular DNA traps that contribute to cancer-associated thrombosis. *Proc Natl Acad Sci U S A* **109**, 13076-81 (2012).

29. Cools-Lartigue, J. et al. Neutrophil extracellular traps sequester circulating tumor cells and promote metastasis. *J Clin Invest* (2013).

30. Mosser, D.M. & Edwards, J.P. Exploring the full spectrum of macrophage activation. *Nat Rev Immunol* **8**, 958-69 (2008).

31. Solinas, G., Germano, G., Mantovani, A. & Allavena, P. Tumor-associated macrophages (TAM) as major players of the cancer-related inflammation. *J Leukoc Biol* **86**, 1065-73 (2009).

32. Jezequel, P. et al. Validation of tumor-associated macrophage ferritin light chain as a prognostic biomarker in node-negative breast cancer tumors: A multicentric 2004 national PHRC study. *Int J Cancer* **131**, 426-37 (2012).

33. Leek, R.D. et al. Association of macrophage infiltration with angiogenesis and prognosis in invasive breast carcinoma. *Cancer Res* **56**, 4625-9 (1996).

34. Jubb, A.M. et al. Expression of vascular notch ligand delta-like 4 and inflammatory markers in breast cancer. *Am J Pathol* **176**, 2019-28 (2010).

35. Mahmoud, S.M. et al. Tumour-infiltrating macrophages and clinical outcome in breast cancer. *J Clin Pathol* **65**, 159-63 (2012).

36. Davies, J.Q. & Gordon, S. in Basic cell culture protocols 91-103 (Springer, 2005).

37. Cherrington, B.D., Morency, E., Struble, A.M., Coonrod, S.A. & Wakshlag, J.J. Potential role for peptidylarginine deiminase 2 (PAD2) in citrullination of canine mammary epithelial cell histones. *PLoS One* **5**, e11768 (2010).

38. Gavet, O. & Pines, J. Progressive activation of CyclinB1-Cdk1 coordinates entry to mitosis. *Dev Cell* **18**, 533-43 (2010).

39. Romero, V. et al. Immune-mediated pore-forming pathways induce cellular hypercitrullination and generate citrullinated autoantigens in

rheumatoid arthritis. *Sci Transl Med* **5**, 209ra150 (2013).

40. Odajima, T. et al. Cytolysis of B-16 melanoma tumor cells mediated by the myeloperoxidase and lactoperoxidase systems. *Biol Chem* **377**, 689-93 (1996).

CHAPTER FOUR

IDENTIFICATION OF MACROPHAGE EXTRACELLULAR TRAP-LIKE STRUCTURES IN MAMMARY GLAND ADIPOSE TISSUE

Chapter reprinted from: Sunish Mohanan, Sachi Horibata, John L. McElwee, Andrew J. Dannenberg, Scott A. Coonrod. Identification of macrophage extracellular trap-like structures in mammary gland adipose tissue: a preliminary study. Frontiers in Immunology. 2013 Mar 18;4:67. doi: 10.3389/fimmu.2013.00067. eCollection 2013. PMID: 23508122; PMCID: PMC3600535.

Author contributions: Conducted immunofluorescence, IHC and confocal micrcoscopy and RAW264.7 macrophage *in vitro* experiments – SM; conceived the research design and prepared the manuscript –SM and SAC; PCR experiments – SH, JLM; provided tissue samples and manuscript editing – AJD.

4.1 Abstract

PAD4-mediated hypercitrullination of histone H4 arginine 3 (H4R3) has been previously found to promote the formation of Neutrophil Extracellular Traps (NET) in inflamed tissues and the resulting histone H4 citrulline 3 (H4Cit3) modification is thought to play a key role in extracellular trap (ET) formation by promoting chromatin decondensation. In addition to neutrophils, macrophages have also recently been found to generate functional extracellular traps (METs). However, a role for PADs in ET formation in macrophages has not been previously described. Transcripts for PAD2 and PAD4 are found in mature macrophages and these cells can be induced to citrullinate proteins, thus raising the possibility that PADs may play a direct role in ET formation in macrophages via histone hypercitrullination. In breast and visceral white adipose tissue from obese patients, infiltrating macrophages are often seen to surround dead adipocytes forming characteristic “crown-like structures” (CLS) and the presence of these lesions is associated with increased levels of inflammatory mediators. In light of these observations, we have initiated studies to test whether PADs are expressed in CLS macrophages and whether these macrophages might form METs. Our preliminary findings show that PAD2 (and to a lesser extent, PAD4) is expressed in both in the macrophage cell line (RAW 264.7) and in CLS lesions. Additionally, we provide evidence that macrophage-derived extracellular histones are seen around presumptive macrophages within CLS lesions and that these histones contain the H4Cit3 modification. These initial findings support our hypothesis

that obesity-induced adipose tissue inflammation promotes the formation of METs within CLS lesions via PAD-mediated histone hypercitrullination. Subsequent studies are underway to further validate these findings and to investigate the role in PAD-mediated MET formation in CLS function in the mammary gland.

4.2 Introduction

ETosis is a recently described cell death-associated phenomenon that results in the release of a complex lattice of chromatin that contains DNA, histones, and other associated proteins [1-3]. These extracellular chromatin webs can be used to entrap and kill microbial organisms. Initially, this phenomenon was described in neutrophils, termed NETosis (Neutrophil Extracellular Traps), but subsequent studies have found that this mechanism also exists in other cell types such as macrophages, eosinophils, and mast cells. Given the ever-expanding array of cell types that can form extracellular traps, this activity is now more generally referred to as ETosis. Various infectious agents such as bacteria, fungi, and protozoa, have been found to induce ETosis, as have cytokines, such as IL-8, and chemicals, such as phorbol myristate acetate (PMA) [4].

At the molecular level, ETs were first shown to be comprised of decondensed DNA scaffolds and various neutrophil granular proteins [4]. Later proteomic studies further concluded that ETs contain histones (the most abundant

fraction), elastase, glycolytic enzymes, and several other cytosolic proteins [5]. Immunofluorescence studies have also shown additional components in ETs such as NADPH oxidase subunits, pentraxin-3, and cathelicidin. Interestingly, the localization of these proteins to NETs was not supported by subsequent biochemical studies, suggesting that some of these components may be loosely associated with ETs [6]. While the precise mechanisms underlying ET induction and formation are not completely understood, several morphological features of ETosis have been observed across various studies. These features include loss of distinct segregation of euchromatin and heterochromatin, disappearance of the lobular nuclear architecture in neutrophil nuclei, granular membrane disruption, and nuclear membrane swelling. ET induction is thought to occur when proteolytic enzymes are released from cytosolic granules where these enzymes then cause a collapse of the nuclear envelope, leading to disruption of plasma membrane integrity and, eventually, release of ETs into the extracellular space [7, 8].

While many studies have now documented a role for NETs in an array of activities, much less is known about ETosis in other cell lines such as macrophages. Two recent studies found that the bacterial organisms *Histophilus somni* and *Mannheimia haemolytica* can induce ETs in bovine macrophages (METs) [9, 10]. Additionally, another study showed that human THP-1-derived macrophages and the RAW 264.7 macrophage cell line formed METs in response to *E. coli* toxins. Interestingly, while MET formation has been documented in tissue macrophages, it has yet to be reported in

peripheral blood monocytes [10].

PAD enzymes catalyze the conversion of positively-charged arginine residues to neutrally-charged citrulline in a hydrolytic reaction termed citrullination or deimination. The resulting loss of charge at this site can dramatically alter the target protein's tertiary structure as well as its ability to interact with other proteins [11, 12]. The N-terminal tails of histones such as H3 and H4 are arginine-rich and appear to represent major target for PAD enzymes. For example, numerous reports have shown that PAD4 and, more recently, PAD2, regulate gene expression via citrullination of histone H4R3 and H3R26, respectively [12, 13]. While the mechanisms by which histone citrullination regulates gene transcription are not fully understood, we recently demonstrated that PAD2-catalyzed histone citrullination promoted localized chromatin decondensation at target gene promoters, thus likely facilitating binding of the basal transcriptional machinery [14]. On a more global level, we have also recently shown that activation of PAD4 in neutrophils promotes histone hypercitrullination, global chromatin decondensation, and NET formation [12]. In this previous study, we showed by transmission electron microscopy that activation of PAD4 in HL60 granulocytes promoted the conversion of multi-lobular heterochromatic nuclei into a more round euchromatic nuclear pattern [12]. Additionally, we demonstrated that TNF-α treatment of blood neutrophils resulted in the release of extracellular chromatin that was extensively citrullinated at histone H4R3. The link between the H4Cit3 modification and

NET formation is very strong and this modification is now routinely utilized to document the presence of ETs in cells and tissues [12, 15]. In addition to TNF- α, LPS and H_2O_2 have also been shown to induce PAD-mediated histone deimination [15]. Importantly, the requirement of citrullination in NET formation *in vivo* was recently documented by investigators who showed that $PAD4^{-/-}$ mice have reduced ability to form NETs in response to various stimuli. Additionally, the investigators found that these mice are more susceptible to bacterial infections [16]. More generally, PAD activity is also closely associated with non-microbial induced immune-mediated inflammatory activity such as that seen in autoimmune arthritis, colitis, and chronic obstructive pulmonary disease. Along these lines, excessive PAD-mediated ETosis has also recently been found to play a role in deep vein thrombosis and cystic fibrosis. [17]

Obesity is a major public health concern and, among other things, is a risk factor for hormone receptor-positive breast cancer in postmenopausal women [18, 19]. Numerous studies in obese humans and animals have shown that macrophages infiltrate visceral adipose tissue and surround dead adipocytes forming a characteristic “crown like structure” (CLS) morphology. These macrophages are believed to primarily function at these sites by “cleaning up” the remnants of dead/dying adipocytes via phagocytosis of lipids, cytoplasmic debris, and karyorrhectic remnants [20]. Additionally, these immune cells produce proinflammatory mediators that are found in the circulation of obese women and have been linked to breast cancer progression.

Recent studies have shown that CLS lesions occur in white adipose tissue of the breast in obese women and in the mammary gland of experimental models of obesity [21, 22]. Importantly, in mouse models of obesity, CLS occur in association with activation of NF-κB and elevated levels of inflammatory mediators including TNF-α, IL-1β, and COX-2 [23]. Increased levels of TNF-α at these sites is thought to enhance inflammatory activity due to a paracrine signaling loop between TNF-α, saturated fatty acids, and adipocytes [24]. Given that TNF-α can induce extracellular trap formation in neutrophils, that PADs are intimately associated with inflammation, and that macrophages can form ETs, we predicted that macrophages may undergo ETosis in CLS lesions. As outlined below, we performed a preliminary study to test this hypothesis. Our findings suggest that METs do form in CLS structures, thus laying the groundwork for future studies to investigate the functional role for METs in the resolution of inflamed white adipose tissue in the mammary gland.

4.3 Materials and methods

RAW 264.7 cell culture and MET induction

RAW 264.7 mouse macrophage cells were grown in RPMI 1640 (Cellgro, Manassas, VA) supplemented with 10% fetal bovine serum containing penicillin-streptomycin. The cells were grown in a sterile, humidified incubator

and maintained in these conditions at 37^{o}C and 5% CO_2. To perform IF staining, macrophages were grown on 12 mm glass coverslips for 2 days at 37^{o}C (Fisher Scientific, Hanover Park, IL). The RAW 264.7 macrophages were treated with recombinant TNF- α (20 ng/ml, R&D systems, Minneapolis, MN, USA) for two hours, then washed in 1X phosphate buffered saline (PBS), fixed in 4% cold paraformaldehyde for 20 minutes, washed in 1X PBS, and immunofluorescence staining was performed as described below.

Mammary gland adipose tissue from obese mice

Mammary gland adipose tissue sections were prepared from a dietary model of obesity as described previously [22, 25]. Ovariectomized C57BL/6J mice (Jackson Laboratories) at 5 weeks of age were given high fat diet (60 kcal% fat, D12492i, Research Diets) to generate obese mice. Mice were fed *ad libitum* for 10 weeks and sacrificed to collect mammary gland tissue. Tissue samples were formalin fixed for histological and immunohistochemical analyses. The animal protocol was approved by the Institutional Animal Care and Use Committee at Weill Cornell Medical College.

mRNA isolation and RT-PCR

RNA was isolated from the RAW 264.7 macrophage cells using the Qiagen RNeasy mini kit, including on-column DNAse treatment to remove genomic DNA (Qiagen # 74104). The purified RNA was reverse-transcribed using the Applied Biosystems High Capacity RNA-to-cDNA kit according to

manufacturer's protocol (Applied Biosystems # 4387406, Foster City, CA). The cDNA (100 ng) was mixed with Go-Taq DNA polymerase (Promega # M3005, Madison, WI) and primer set. The following primer pairs were used (size of the amplicons are in parentheses): PAD2 primer set #1 (400 bp): Fwd - 5'-AGAAGGGAGGCTCTGAGGTC-3'and Rev - 5'-CTGGCCAGAGAATTGAGGAC-3'; PAD2 primer set #2 (188 bp): Fwd - 5'-CAAGATCCTGTCCAATGAGAG-3' and Rev - 5'-ATCATGTTCACCATGTTAGGGA-3'; PAD4 primer set #1 (406 bp): Fwd - 5'-TCTCCCTGCTGGACAAGTCT-3' and Rev - 5'-AGCCCAGTGAGCTCTGACAT-3'; PAD4 primer set #2 (193 bp): Fwd - 5'-CTACTCTGACCAAGAAAGCC-3' and Rev - 5'-ATTTGGACCCATAACTCGCT-3'; GAPDH primer set #1 (324 bp): Fwd - 5'-CCCACTAACATCAAATGGGG-3' and Rev - 5'-ATCCACAGTCTTCTGGGTGG-3'; and GAPDH primer set #2 (209 bp): Fwd - 5'-GGGCATCTTGGGCTACAC-3' and Rev - 5'-GGTCCAGGGTTTCTTACTCC-3'. PCR was performed using the following set up: 5 minutes at 95°C, 30 cycles of (30 s, 94°C; 30 s, 58°C; 30 s, 72°C), 5 minutes at 72°C. The PCR products were analyzed on a 1% agarose gel using Geldoc (Biorad) software.

Immunohistochemistry (IHC) and Immunofluorescence (IF)

IHC and IF experiments followed our previously described protocol [26]. Briefly, paraffin embedded tissue sections were deparaffinized and rehydrated in 3X 5

minute washes in xylene followed by single sequential 5 minute washes in 100, 95, and 75% EtOH. Slides were then incubated for 10 minutes in 0.5% hydrogen peroxide in methanol to quench endogenous peroxidases. Antigen retrieval was performed by boiling slides 2X for 10 minutes in 0.01M sodium citrate pH 6.8 and, after cooling, slides were washed in 1X PBS. Tissue slides and fixed coverslips containing RAW264.7 cells were then blocked in 10% normal goat serum and 2X casein (Vector Labs, Burlingame, CA) for 20 minutes at room temperature in a humidified microprobe chamber. Slides were blotted to remove excess blocking solution and then primary antibody diluted in 1X PBS was applied to the slides for 2 hours at room temperature. Slides or cover slips were then stained with either anti-PAD2 (ProteinTech #122100-1-AP, Chicago, IL) at a 1:100 dilution, anti-PAD4 (Sigma-Aldrich # P4749) at a 1:100 dilution or with anti-histone H4 Citrulline 3 (Millipore-Upstate # 07-596) at a 1:100 dilution. Following 3X washing with 1X PBS, slides were incubated with a 1:200 dilution of biotinylated secondary antibody (in 1X PBS) for 1 hour at room temperature and then washed 3X in 1X PBS. For IHC, slides were incubated in DAB chromagen (Vector Labs) solutions according to the manufacturer's protocol, washed and then counterstained with Gill's hematoxylin and coverslipped. For each experiment, duplicate slides were treated with control rabbit IgG antibody at the appropriate concentration as a negative control. For immunofluorescence, slides were incubated in streptavidin conjugated-488 or 555 (Invitrogen), washed and then mounted using Vectashield containing DAPI (Vector Labs). As a negative control,

duplicate slides were treated with control rabbit IgG at the appropriate concentrations.

In order to quantitate changes in levels of citrullinated histones following TNF-α treatment, a time course experiment was performed evaluating H4Cit3 immunofluorescence intensity at 0, 2, 6 and 24 hours. RAW 264.7 macrophages were treated with 20 ng/ml of TNF-α, fixed and H4Cit3 immunofluorescence staining was performed using the method described above. Five different fields from each time point were imaged using confocal microscopy and the mean integrated fluorescence intensity was calculated using ImageJ software analysis as previously described by Gavet and Pines [27]. The results were then analyzed by one-way ANOVA to detect statistical differences and a p-value < 0.01 was considered significant. All values are presented as mean ± Standard deviation.

4.4 Results and Discussion

TNF-α appears to induce MET formation in RAW 264.7 macrophages

Given that TNF-α induces ET formation in neutrophils, we first tested whether TNF-α could promote ET formation in the RAW 264.7 macrophage cell line. As shown in **Figure 4.1A**, we found that TNF-α treatment led to DAPI-stained chromatin in characteristic strands outside of ~5-10% of the phalloidin-bound RAW264.7 cells. Two different microscopic fields from 2 hour treatment groups are shown in **Figure 4.1** as representative images. By contrast, these

characteristic strands were not seen in untreated control cells. This observation supports the hypothesis that TNF- α induced the release of chromatin from the cell nucleus into the extracellular space. As a further test of this hypothesis, we then stained the TNF- α -treated RAW264.7 cells with the anti-H4Cit3 antibody. Results show that the extracellular chromatin appeared to be extensively citrullinated at H4R3, thus suggesting that PAD-mediated histone hypercitrullination promotes ETosis in macrophages. In an effort to quantitate the extent to which TNF-α promoted the formation of extracellular chromatin in RAW264.7 cells, we quantitated the staining intensity for the anti-H4Cit3 antibody at different time points following treatment. Results show that the mean integrated fluorescence intensity at 2, 6, and 24 hours was significantly increased (as determined by ANOVA) when compared to the 0 hour time point ($p<0.01$). We also note that the H4Cit3 intensity gradually increased until the 6 hour time point, while levels were lower at the 24 hour time point. This result supports the hypothesis that, as with neutrophils, TNF-α stimulates histone hypercitrullination and ETosis in macrophages.

Figure 4.1: (A) H4Cit3 immunofluorescence staining in RAW 264.7 macrophages following 0 and 2 hour TNF-α treatment. Cultured RAW 264.7 macrophage cells appear to form METs following TNF- α stimulation and these METs contain citrullinated histones. DAPI staining (blue) shows that DNA extends beyond the Phalloidin-stained cell borders. Anti-Histone H4Cit3 staining shows presence of citrullinated histones within METs (Arrows). Two separate fields from the 2 hour treatment group (Fields 1 and 2) are included for reference.

(**B**) Integrated anti-H4Cit3 fluorescence intensity quantitation at 0, 2, 6, and 24 hours of TNF-α treatment. The RAW 264.7 macrophages were treated with 20 ng/ml of TNF-α, fixed, stained with the anti-H4Cit3 antibody, and imaged by indirect immunofluorescence at the indicated time points. Five unique fields were imaged by confocal microscopy at each time point and the mean integrated fluorescence intensity was calculated using ImageJ software analysis. Results were analyzed by ANOVA and the graphs represent mean ± standard deviation (*p-value < 0.01).

A.

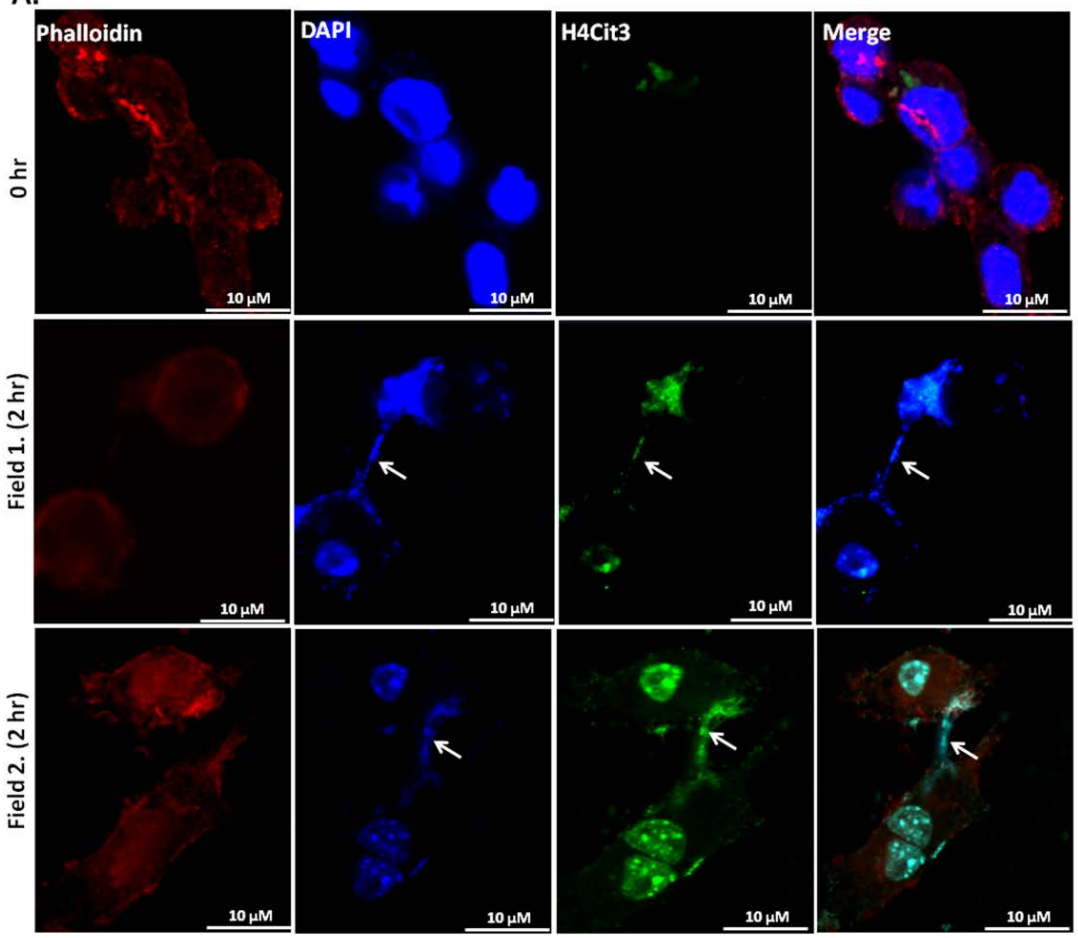
Phalloidin
DAPI
H4Cit3
Merge
0 hr
Field 1. (2 hr)
Field 2. (2 hr)
10 µM

B.

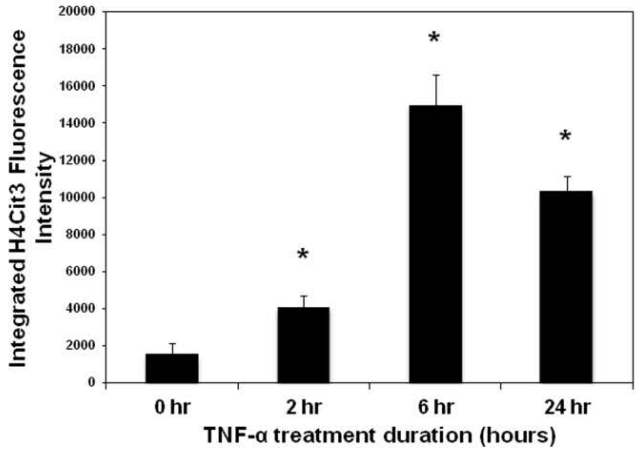
Integrated H4Cit3 Fluorescence Intensity
20000
18000
16000
14000
12000
10000
8000
6000
4000
2000
0
*
*
*
0 hr
2 hr
6 hr
24 hr
TNF-α treatment duration (hours)

PAD2 is a likely candidate for catalyzing histone hypercitrullination during ETosis in macrophages

While PAD4 is the only PAD family member to have been shown to be required for ETosis, both PAD2 and PAD4 have been previously shown to be expressed in macrophages. Therefore, as an initial investigation into which PAD family member may catalyze ET production in RAW264.7 cells, we first investigated mRNA expression levels of PAD2 and PAD4 in this cell line. Surprisingly, RT-PCR analysis found that PAD4 expression was very low in RAW264.7 cells (**Figure 4.2A**), suggesting that this family member may not play a critical role in macrophage function. We note, however, that we have yet to test for PAD4 levels in *in vivo*-derived macrophages. Given the high level of PAD2 mRNA observed in these cells, we then carried out indirect immunofluorescence to test whether RAW264.7 macrophages also expressed PAD2 protein. Results showed PAD2 staining was strong in these cells **(Figure 4.2B)** and appeared to localize, in part, to DAPI-poor euchromatic regions of the RAW 264.7 cell nucleus **(Figure 5.2B, bottom right panel)**. While not conclusive, this finding supports the hypothesis that PAD2 is a primary driver of histone hypercitrullination, chromatin decondensation, and ET formation in macrophages. We note that the localization of PAD2 to the cell nucleus fits well with this hypothesis. Additionally, this hypothesis is further supported by our recent finding that both global and promoter-specific chromatin decondensation is catalyzed by PAD2 in breast cancer cell lines [14].

Figure 4.2: PAD2 expression in cultured RAW 264.7 macrophage cells.

(**A**) RT-PCR for PAD2 and PAD4 mRNA expression in cultured RAW 264.7 macrophages. Two unique primer sequence sets were used to test for PAD2 and PAD4 mRNA expression levels. RAW 264.7 macrophages were found to strongly express PAD2 mRNA. GAPDH mRNA expression levels were used as the internal control for RT-PCR.

(**B**) Anti-PAD2 immunofluorescence labeling shows positive staining in the nucleus and cytoplasm of RAW 264.7 macrophages. Nuclei are stained with DAPI.

A.

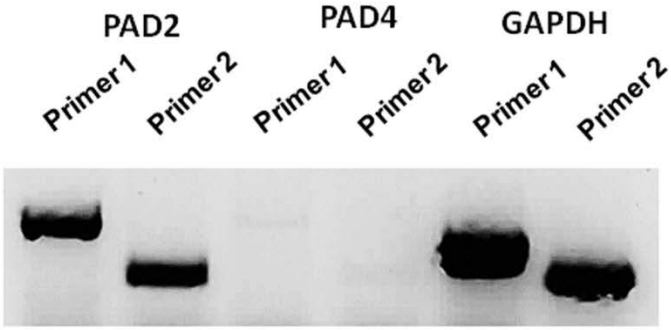
PAD2
PAD4
GAPDH
Primer 1
Primer 2
Primer 1
Primer 2
Primer 1
Primer 2

B.

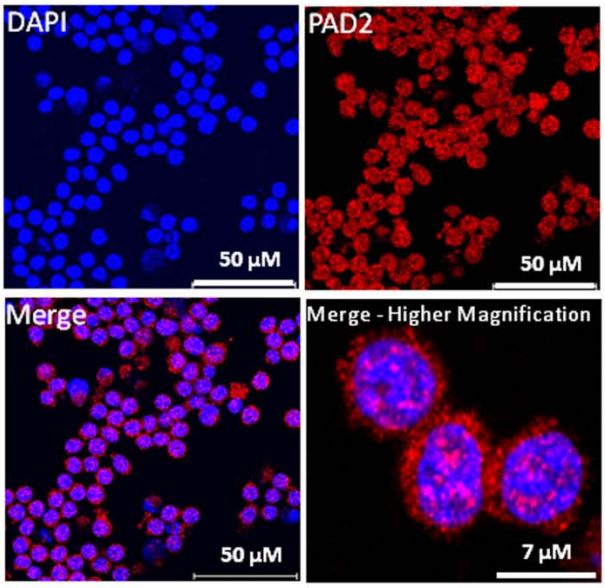
DAPI
PAD2
50 µM
50 µM
Merge
Merge - Higher Magnification
50 µM
7 µM

Evidence supporting the hypothesis that METs exist in mouse mammary gland CLS lesions

Our findings in the RAW264.7 cell line suggested that PAD2-catalyzed histone hypercitrullination may promote ETosis in CLS-localized macrophages. In order to begin testing this hypothesis, we next investigated whether PAD2 was expressed in the nucleus of macrophages in CLS lesions. Results show that PAD2 expression appeared to be robust in these cells (**Figure 5.3**). Importantly, similar to the RAW264.7 cells, PAD2 was found to concentrate in the DAPI-poor regions of the presumptive macrophage cell nucleus, again suggesting that PAD2 localizes to euchromatic regions of the nucleus. We then stained these samples with the anti-H4Cit3 antibody and found positive staining for the histone H4Cit3 modification extending from numerous CLS cell nuclei (**Figure 4.4**). This staining is highlighted by arrows in the two representative images (**Figure 4.4, Field 1 and Field 2**) and appears to extend into the extracellular space between CLS cells. In order to more precisely refine the localization of H4Cit3-stained chromatin, we next carried out immunohistochemical staining of the CLS-containing sections using the anti-histone H4Cit3 antibody. Results showed that CLS cell nuclei were frequently stained with this antibody (**Figure 4.5**). Importantly, the anti-H4Cit3 staining is particularly intense in fragmented nuclear particles and, in such cases, the staining appeared to extend well into the cell cytoplasm and extracellular space.

Figure 4.3: PAD2 expression in cells within CLS lesions of the murine mammary gland. Immunofluorescence staining of mammary gland adipose tissue sections with anti-PAD2 antibodies shows that cells within the CLS lesions appear to express PAD2. Nuclei are stained with DAPI. Nonspecific rabbit IgG was used as a negative control.

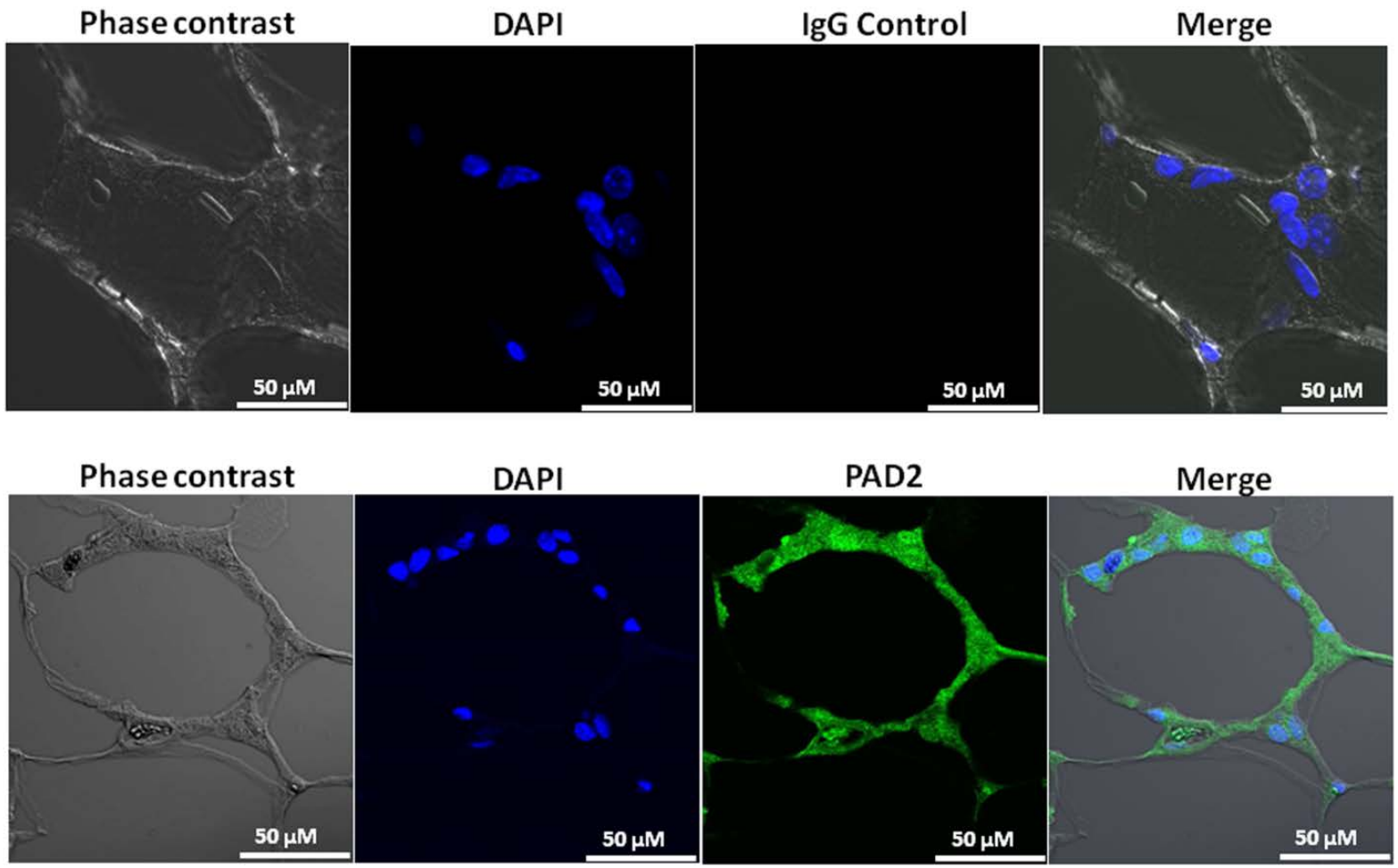
Phase contrast
DAPI
IgG Control
Merge
50 µM
50 µM
50 µM
50 µM
Phase contrast
DAPI
PAD2
Merge
50 µM
50 µM
50 µM
50 µM

<u>Figure 4.4</u>: Extracellular trap-like structures within CLS lesions of the murine mammary gland stain positive for the histone H4Cit3 modification. Immunostaining of mouse mammary gland adipose tissue with the anti-H4Cit3 antibody shows that extranuclear citrullinated histones appear to extend into the extracellular space between cells within CLS lesions. Arrow highlights nuclei from which the extracellular histones appear to originate.

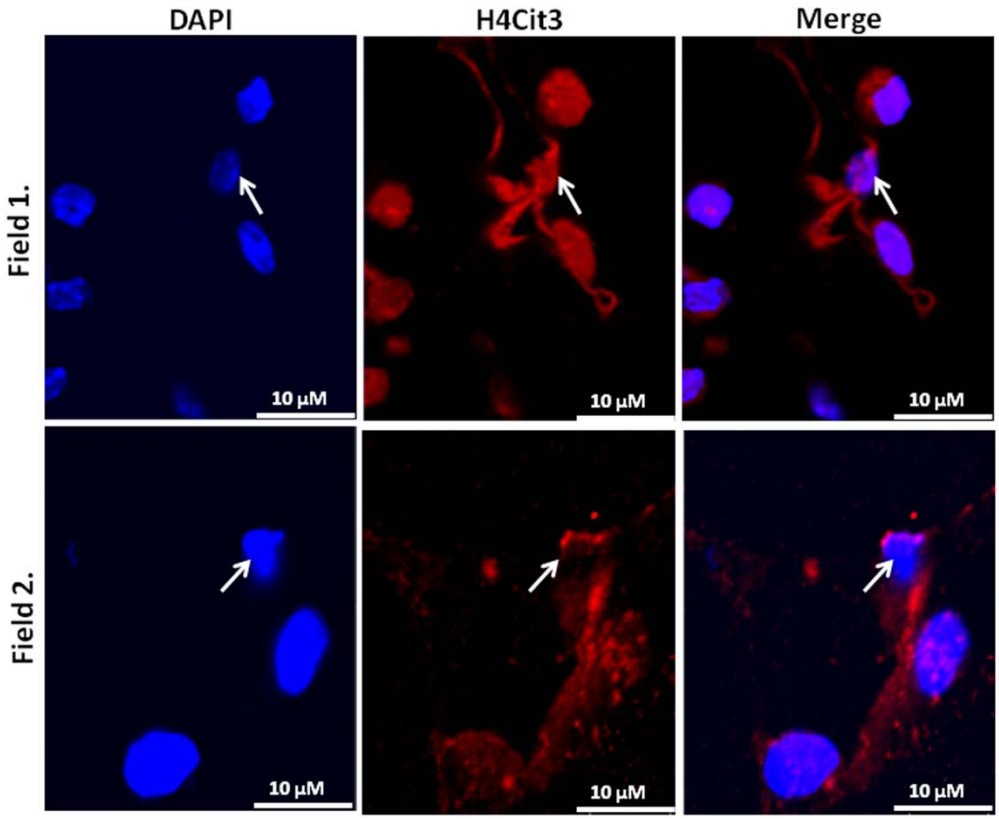

<u>Figure 4.5:</u> Immunohistochemical localization of the histone H4Cit3 modification within CLS lesions of the mammary gland. (**A**) Negative control showing adipose tissue sections stained with nonspecific rabbit IgG and hematoxylin counterstain. (**B**) - (**D**) Arrows indicate CLS lesions with positive immunostaining for the H4Cit3 modification. A higher magnification of the CLS lesion from B is given in C.

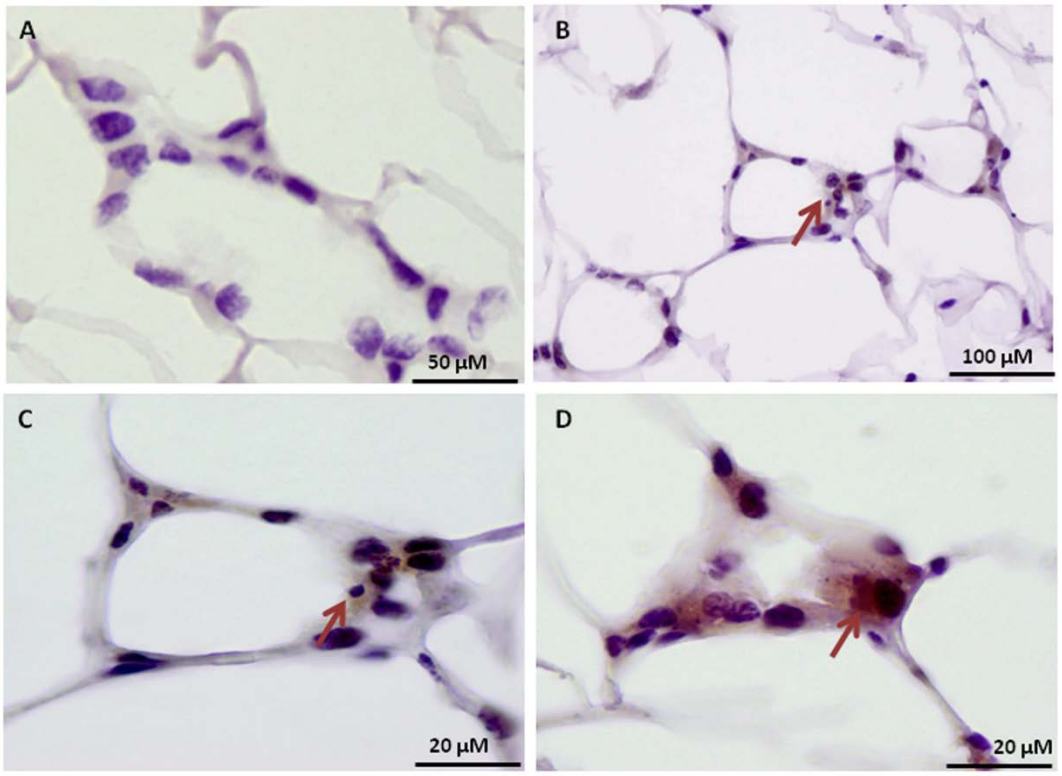

Outcomes from this study suggest that macrophages undergo ETosis following TNF- α stimulation *in vitro* and within mammary gland CLS lesions in obese mice. Our IF and IHC experiments using the anti-H4Cit3 antibody (a well validated marker for ET chromatin) finds that histone hypercitrullination is seen in extracellular chromatin in both RAW264.7 cells and in CLS macrophages, thus supporting the hypothesis that the observed ETosis is likely PAD-mediated. Additionally, we show that PAD2, but not PAD4, expression is robust within the nucleus of RAW264.7 cells and CLS-localized macrophages, thus identifying PAD2 as a strong candidate for catalyzing ETosis formation in macrophages. These preliminary findings provide support for the hypothesis that METs occur in CLS lesions of mammary gland adipose tissue from obese mice and lay the groundwork for future studies aimed at identifying a role for METs in CLS function. Given the close ties between PAD activity and inflammation, we favor the hypothesis that the release of hypercitrullinated histones from the macrophage nucleus into the extracellular space during MET formation plays a critical role in promoting inflammatory signaling pathways within microenvironment of mammary gland adipose tissue (**Figure 4.6.**). Experiments are currently underway to test this hypothesis.

Figure 4.6: Schematic illustration of the role of PAD2 mediated histone citrullination during MET formation in CLS lesions. (**A**) Macrophages infiltrate obese adipose tissue and surround dead adipocytes forming the CLS lesions. (**B**) TNF-α and other cytokines released from adipocytes may stimulate ETosis in these surrounding CLS macrophages thus promoting PAD2-mediated histone citrullination, chromatin decondensation and extracellular chromatin scaffold formation. (**C**) We hypothesize that the citrullinated histones released during MET formation may regulate the inflammatory microenvironment of mammary adipose tissue by influencing the macrophage infiltration and/or macrophage activation.

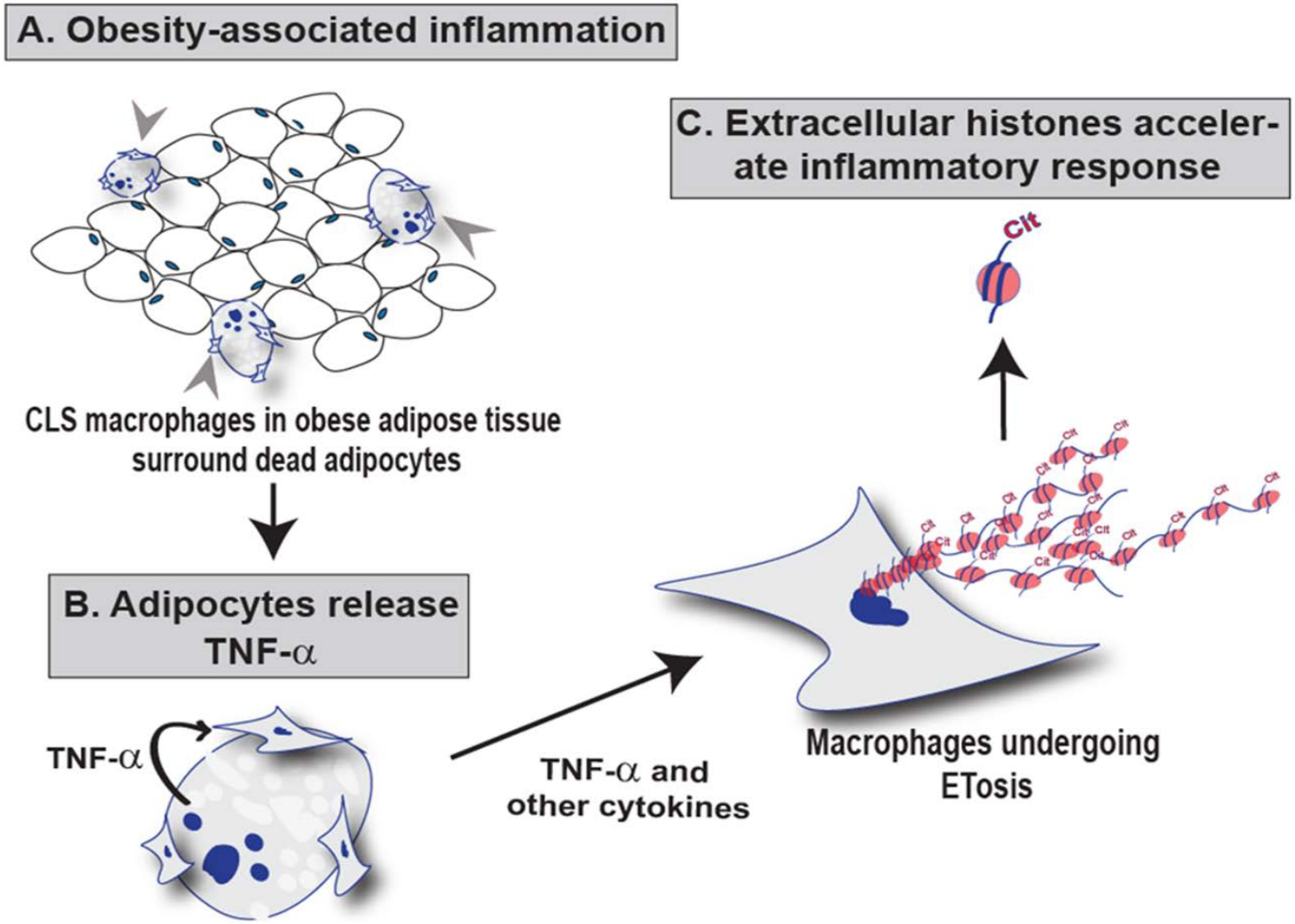
A. Obesity-associated inflammation
CLS macrophages in obese adipose tissue surround dead adipocytes
B. Adipocytes release TNF-α
TNF-α
TNF-α and other cytokines
C. Extracellular histones acceler-ate inflammatory response
Cit
Macrophages undergoing ETosis

4.5 References

1. Saffarzadeh, M. et al. Neutrophil extracellular traps directly induce epithelial and endothelial cell death: a predominant role of histones. *PLoS One* **7**, e32366 (2012).

2. Liu, C.L. et al. Specific post-translational histone modifications of neutrophil extracellular traps as immunogens and potential targets of lupus autoantibodies. *Arthritis Res Ther* **14**, R25 (2012).

3. Amulic, B. & Hayes, G. Neutrophil extracellular traps. *Curr Biol* **21**, R297-8 (2011).

4. Brinkmann, V. et al. Neutrophil extracellular traps kill bacteria. *Science* **303**, 1532-5 (2004).

5. Urban, C.F. et al. Neutrophil extracellular traps contain calprotectin, a cytosolic protein complex involved in host defense against Candida albicans. *PLoS Pathog* **5**, e1000639 (2009).

6. Guimaraes-Costa, A.B., Nascimento, M.T., Wardini, A.B., Pinto-da-Silva, L.H. & Saraiva, E.M. ETosis: A Microbicidal Mechanism beyond Cell Death. *J Parasitol Res* **2012**, 929743 (2012).

7. Fuchs, T.A. et al. Novel cell death program leads to neutrophil extracellular traps. *J Cell Biol* **176**, 231-41 (2007).

8. Remijsen, Q. et al. Neutrophil extracellular trap cell death requires both

autophagy and superoxide generation. *Cell Res* **21**, 290-304 (2011).

9. Hellenbrand, K.M., Forsythe, K.M., Rivera-Rivas, J.J., Czuprynski, C.J. & Aulik, N.A. Histophilus somni causes extracellular trap formation by bovine neutrophils and macrophages. *Microb Pathog* **54**, 67-75 (2013).

10. Aulik, N.A., Hellenbrand, K.M. & Czuprynski, C.J. Mannheimia haemolytica and its leukotoxin cause macrophage extracellular trap formation by bovine macrophages. *Infect Immun* **80**, 1923-33 (2012).

11. Mohanan, S. et al. Potential Role of Peptidylarginine Deiminase Enzymes and Protein Citrullination in Cancer Pathogenesis. *Biochemistry Research International* **2012** (2012).

12. Wang, Y. et al. Histone hypercitrullination mediates chromatin decondensation and neutrophil extracellular trap formation. *J Cell Biol* **184**, 205-13 (2009).

13. Cherrington, B.D. et al. Potential role for PAD2 in gene regulation in breast cancer cells. *PLoS One* **7**, e41242 (2012).

14. Zhang, X. et al. Peptidylarginine deiminase 2-catalyzed histone H3 arginine 26 citrullination facilitates estrogen receptor alpha target gene activation. *Proc Natl Acad Sci U S A* **109**, 13331-6 (2012).

15. Neeli, I., Khan, S.N. & Radic, M. Histone deimination as a response to inflammatory stimuli in neutrophils. *J Immunol* **180**, 1895-902 (2008).

16. Li, P. et al. PAD4 is essential for antibacterial innate immunity mediated

by neutrophil extracellular traps. *J Exp Med* **207**, 1853-62 (2010).

17. Marcos, V. et al. CXCR2 mediates NADPH oxidase-independent neutrophil extracellular trap formation in cystic fibrosis airway inflammation. *Nat Med* **16**, 1018-23 (2010).

18. Cleary, M.P. & Grossmann, M.E. Minireview: Obesity and breast cancer: the estrogen connection. *Endocrinology* **150**, 2537-42 (2009).

19. van Kruijsdijk, R.C., van der Wall, E. & Visseren, F.L. Obesity and cancer: the role of dysfunctional adipose tissue. *Cancer Epidemiol Biomarkers Prev* **18**, 2569-78 (2009).

20. Cinti, S. et al. Adipocyte death defines macrophage localization and function in adipose tissue of obese mice and humans. *J Lipid Res* **46**, 2347-55 (2005).

21. Morris, P.G. et al. Inflammation and increased aromatase expression occur in the breast tissue of obese women with breast cancer. *Cancer Prev Res (Phila)* **4**, 1021-9 (2011).

22. Subbaramaiah, K. et al. Obesity is associated with inflammation and elevated aromatase expression in the mouse mammary gland. *Cancer Prev Res (Phila)* **4**, 329-46 (2011).

23. Subbaramaiah, K. et al. Increased levels of COX-2 and prostaglandin E2 contribute to elevated aromatase expression in inflamed breast tissue of obese women. *Cancer Discov* **2**, 356-65 (2012).

24. Suganami, T. & Ogawa, Y. Adipose tissue macrophages: their role in adipose tissue remodeling. *J Leukoc Biol* **88**, 33-9 (2010).

25. Hong, J., Stubbins, R.E., Smith, R.R., Harvey, A.E. & Nunez, N.P. Differential susceptibility to obesity between male, female and ovariectomized female mice. *Nutr J* **8**, 11 (2009).

26. Cherrington, B.D., Morency, E., Struble, A.M., Coonrod, S.A. & Wakshlag, J.J. Potential role for peptidylarginine deiminase 2 (PAD2) in citrullination of canine mammary epithelial cell histones. *PLoS One* **5**, e11768 (2010).

27. Gavet, O. & Pines, J. Progressive activation of CyclinB1-Cdk1 coordinates entry to mitosis. *Dev Cell* **18**, 533-43 (2010).

CHAPTER FIVE

DISCUSSION – SUMMARY AND FUTURE ROLE FOR PAD2 IN CARCINOGENESIS AND REGULATION OF TUMOR INFLAMMATORY MICROENVIRONMENT

5.1 Summary of findings

Previous research studies in our lab using MCF10AT breast cancer progression series cell lines, MCF10DCIS tumor spheroids, tumor xenografts and human breast cancer tissue samples found that PAD2 has a critical role in breast cancer progression. Prior to these studies even though PAD2 mediated protein citrullination has been associated with various autoimmune disease conditions, PAD4 was the only PAD family isozyme with an established role in carcinogenesis. The goal of this thesis research was to further elucidate the role of PAD2 in epithelial carcinogenesis using PAD2 overexpression tumor cell lines and a MMTV-FLAG-hPAD2 transgenic mouse model and evaluate how PAD2 may be playing a role in regulating inflammation associated with tumors and other chronic conditions such as obesity especially via a process termed extracellular chromatin trap release ("ETosis"). The results from this thesis research would help in advancing the significance of PAD2 as a novel therapeutic target and as a clinically relevant biomarker.

To achieve the goal to study the role of PAD2 in epithelial carcinogenesis, we used an in vitro model of PAD2 overexpressing human SCC cell line , A431 and an in vivo model of human PAD2 overexpression in mice under the regulation of MMTV promoter (**Chapter 2**). To achieve the goal to study the role of PAD2 in regulation of inflammatory microenvironment, we focused on

histone citrullination, chromatin decondensation and extracellular chromatin trap release (ETosis) mediated by PAD2 in immune cells, especially in macrophages using *in vitro* models such as RAW 264.7 macrophages and peritoneal macrophages and in vivo using human tongue SCC tissue sections and obese mammary adipose tissue sections (**Chapter 3 and 4**). Additional studies were also conducted to characterize comparative PAD2 expression in feline and canine mammary tumors which further validated the significance of PAD2 as a potential cancer biomarker and therapeutic target in these species[1].

In order to test whether PAD2 was sufficient for tumorigenesis *in vivo,* we generated a transgenic mouse model overexpressing human PAD2 under the control of the hormone-responsive MMTV-LTR promoter in FVB mice (**Chapter 1**). The immunohistochemical staining and western blotting showed that hPAD2 transgene is expressed in the mammary glands, but the MMTV-FLAG-PAD2 mice failed to develop any mammary tumors. Given the knowledge that MMTV-LTR promoter while predominantly expressed in mammary and salivary gland, expression has also been reported in other tissues such as skin and ovaries [2, 3]. An unexpected phenotype was observed in these mice and approximately 40% of the mice developed proliferative skin lesions after five months of age. The tumors expressed the transgenic form of FLAG-hPAD2 and showed increased expression for inflammatory cytokines such as IL6, IL8 homologues (MIP2 and LIX) and CCL17. Histopathological

analysis showed that the proliferative skin lesions in these mice ranged from hyperplasia, dysplasia, and benign papillomas to invasive SCC.

Intrigued by the skin pathology phenotype in PAD2 overexpressing mice, we conducted a two stage chemical carcinogenesis study using the DMBA-TPA model to further evaluate the predilection of MMTV-FLAG-hPAD2 mice to develop more invasive skin tumors and compare the histopathology of these tumors with the WT tumors which do not express the hPAD2 transgene (**chapter 2**). We found that a higher percentage of MMTV-FLAG-hPAD2 developed skin papillomas at an earlier time point following the DMBA-TPA treatment compared to the WT mice. Also, the transgenic mice tumors were larger and showed more invasive macroscopic features. The histopathological features of these tumors were characterized and were blindly scored for inflammation, invasiveness, EMT morphology and mitotic index. The transgenic tumors received significantly higher scores for invasion and inflammation suggesting the potential of PAD2 transgene to assist malignant conversion and also had higher mitotic index compared to WT tumors suggesting the increased tumor cell proliferation in the presence of PAD2 transgene. We studied the expression of inflammatory cytokines in these transgenic tumors in order to find an explanation of the highly inflamed tumor microenvironment present in these tumors. Interestingly we find that MMTV-FLAG-hPAD2 tumors express significantly higher levels of IL8 homologues (MIP2 and LIX), IL6, CCL17 all of which may act as potential chemoattractants

for immune cells to the tumor microenvironment. hPAD2 levels highly positively correlated with these chemokine levels and negatively correlated with the cell adhesion marker, E-cadherin, expression. This study provided a direct comparison of PAD2 overexpressing tumors with WT tumors to evaluate the differences in tumor invasiveness and tumor associated inflammation using a transgenic mouse model.

Our lab had previously published the critical role played by PAD4 isozyme in neutrophil extracellular trap release [4] via a phenomenon commonly called NETosis and is being currently widely studied [5-7]. During the tumor tissue evaluations (**chapter 2 and 3**), we observed following immunohistochemical examination that tumor associated inflammatory cells especially macrophages are highly positive for PAD2 protein expression. There are only a few publications reporting the phenomenon of extracellular trap release by macrophages (METs) [8]. In two related projects (**chapter 3 and 4**) we studied how PAD2 involved in MET release and characterized the presence of the METs in tumor associated inflammation and obesity associated inflammation. In chapter 4, using *in vitro* models of RAW 264.7 macrophage cell line and PAD2 knockout peritoneal macrophages we found that PAD2 is critical in functional MET release. These METs contained high levels of histone H4 citrulline 3 (H4Cit3) modification in WT macrophages while the H4Cit3 levels were reduced in PAD2KO METs. In order to test the significance of METs in chronic inflammatory conditions such as tumor associated inflammation, we

co-immunostained human tongue SCC sections with MET markers such as anti-H4Cit3 antibody, Sytox Green DNA marker and macrophage markers (F4/80, CD68). Our findings confirm the presence of METs released by TAMs and we also observed that these METs are predominantly found surrounding invasive carcinoma cell islands. This novel study sheds light into the role of histone citrullination mediated by PAD2 in regulating the tumor inflammatory milieu. In order to test if this phenomenon of PAD2 regulated METs are present in other chronic inflammatory conditions, we chose obesity associated macrophage rich inflammation as a model. We characterized the macrophages present within the “CLS” (crown-like structure) lesions which are infiltrating macrophages surrounded a single dying adipocyte. Using co-immunostaining for MET markers we showed that citrullinated histone rich MET structures exist in CLS lesions suggesting that PAD2 may also be playing a role in obesity-associated inflammation.

Collectively, these studies provide strong experimental evidence establishing PAD2 as a potential novel oncogene, therapeutic target for cancer therapy and a regulator of obesity and tumor associated inflammation. However, there are some unanswered questions regarding the molecular mechanism by which PAD2 regulate tumor inflammation and invasion. Specifically, is there a transcriptional role for PAD2 in regulating E-cadherin / Vimentin and IL6/IL8/CCL17 expression? Also, is there a microenvironment effect which may be regulating PAD2 expression (e.g.: IFN-γ priming) in macrophages

which makes a subset of macrophages susceptible to MET release? Lastly, more experiments need to be done to further elucidate the role of PAD2 in tumorigenesis. The following sections will focus on several future directions and hypotheses to further explore the remaining questions.

5.2 PAD2 may function differently in tumor cell regulation Vs immune cell ETosis

The finding that PAD2 is involved in MET release raises the question – How PAD2 may mediate chromatin wide hypercitrullination in macrophages during ETosis while in mammary and skin carcinoma cells PAD2 seems to citrullinate specific gene promoters regulating EMT and cell proliferation? One of the possible explanations lies in the drastic cell physiological changes involved in the ETosis process which ultimately results in the immune cell death especially the sharp upregulation of calcium influx. PADs are calcium dependent enzymes and the loss of calcium homeostasis and a sudden increase in intracellular calcium levels during ETosis may assist in rapid increase of PAD activity resulting in both nuclear and cytoplasmic protein hypercitrullination. There is a possibility that chromatin hypercitrullination during ETosis also requires priming of immune cells by other cytokines (e.g. IFN-γ) which will result in significant increase in PAD2 expression even before the cells enter ETosis and cause increased genome-wide binding of PAD2 to chromatin. These primed, PAD2 rich immune cells which are in a ready-to-citrullinate stage may be highly responsive to ETosis stimuli and may form the

subset of immune cells initially releasing chromatin traps.

In tumor and immune cell biology, PAD2 may play two distinct roles. 1. Transcriptional regulation of specific oncogenes and cytokines by citrullinating histones and transcriptional cofactors; 2. Direct citrullination of cytokines and ECM proteins leading to alteration in their structure and function. Studies have previously shown that citrullination of cytokines (eg. IL8) can lead to altered immune function [9]. So the results observed in this thesis research should be further evaluated to differentiate the effect of direct cytokine and ECM protein citrullination (e.g. basement membrane proteins such as Collagen IV and fibronectin citrullination by PADs) and transcriptional regulation of these proteins by PAD2.

5.3 Role of PAD2 in breast cancer progression and basement membrane integrity

In a foundational study conducted in our lab to evaluate role of PAD2 in cancer progression, MCF10DCIS tumor xenograft bearing mice were treated with PAD inhibitor Cl-amidine and PAS stained tissue sections were evaluated for basement membrane integrity surrounding the ductal structures within this model of comedo-DCIS. Interestingly we found that basement membrane integrity was significantly reduced in PAD-inhibitor treated tumors compared to the PBS control treated group (**Figure 5.1**). This is a clinically significant finding and if explored further may prove to be yielding further insight into how PAD2 regulate cross talk between myoepithelial and luminal epithelial cells in

regulating basement membrane deposition [10-12]. Also PAD2 mediated citrullination is known to play a role in cytoskeletal and intermediate filament fiber structures [13, 14]. No literature is available on the role of PAD2 in regulating structure and 3-dimensional compactness of Collagen IV, laminin, or fibronectin which are important extracellular matrix components in carcinomas. Further *in vitro* studies are needed to specifically study the structural regulation of basement membrane components by citrullination mediated by PAD2 and how this may change the integrity of basement membrane during tumor progression to invasiveness.

<u>Figure 5.1</u>: Cl-amidine (PAD inhibitor) decreases the growth of MCF10DCIS tumors in a xenograft model of comedo-DCIS and enhances the basement membrane integrity

MCF10DCIS cells (1 x 106) were injected subcutaneously into female nude (nu/nu) mice (Charles River). After 2 weeks of tumor growth (tumor volumes ~100-200 mm^3), mice were randomly treated with intraperitoneal injections of Cl-amidine at 50 mg/kg/day (n = 7) or PBS as a vehicle control (n = 7). PAS stained sections (10X, scale bar = 200 μm) from representative treated (I) and control tumors (II), arrows in (I) show an intact basement membrane (BM), while the arrow in (II) shows breaching of the BM with infiltrating leukocytes. BM integrity was also scored on a scale from 1-3 and scores were analyzed using Mann-Whitney-U test. The treated tumors have a lower score, indicating a higher level of BM integrity (* $p < 0.05$ MWU) (Figure obtained from McElwee JL et al, BMC cancer, 2012) [15]

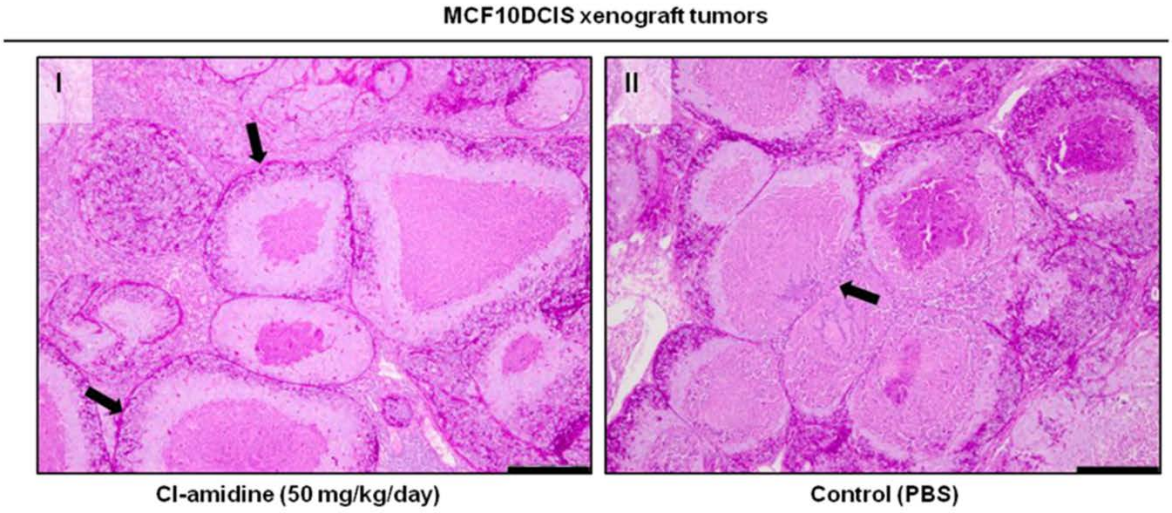

5.4 PAD2 mediated regulation of tumor associated inflammation and EMT

PAD2 inhibitor Cl-amidine has been shown to alleviate the inflammatory symptoms in mouse models of colitis [16]. PADs also regulate citrullination of vimentin which is shown to be important in autoimmune diseases such as rheumatoid arthritis [17]. Increasing evidence supports the key role played by immune cells and inflammatory processes and recently tumor-promoting inflammation is also being defined as an emerging hallmark of cancer [18, 19]. Many inflammatory mediators (e.g. cytokines/chemokines) are important for the growth and proliferation of pre-malignant cells [20]. These mediators often activate oncogenic transcription factors, such as NFκB and STAT3 [21-23].Our lab has found that PAD2 is critical in regulating HER2 expression in breast cancer cells and interestingly others have shown that HER2 in turn regulates IL6-STAT3 pathway activation [24]. Activation of such an inflammatory loop sets the stage for further recruitment of inflammatory cells, endothelial cells, and growth factors involved in cancer cell survival, proliferation and invasion and eventual local and distant organ metastasis (**Figure 5.2**). PAD family members have previously been shown to promote the inflammatory microenvironment by regulating cytokine signaling in macrophages via citrullination of IKKγ, which controls NFκB expression activity [25].

In this thesis research I have shown that MMTV-FLAG-hPAD2 tumors show increased expression of *IL6* and *IL8* in both spontaneous skin tumors and in DMBA-TPA induced tumors. This pattern of cytokine upregulation was confirmed using an in vitro experiment in which hPAD2 was stably transfected in human SCC cell line, A431 cell line. Both IL6 and IL8 have been shown in previous studies to be important in tumor progression and play a critical role in tumor growth, angiogenesis, and EMT [26-30]. Additional experiments are needed to identify the mechanism by which PAD2 regulates the expression of these inflammatory mediators. Future experiments may use ChIP to examine whether PAD2 binds to either IL6 or IL8 promoter. Also co-immunoprecipitation (Co-IP) will be useful to examine whether there are any protein-protein interactions.

Figure 5.2: Tumor promoting inflammation as an emerging hallmark of cancer. Tumor associated inflammation assist in tumor progression by the release of paracrine signaling molecules such as EGF, VEGF and other proangiogenic factors. These cytokines further accelerates inflammation and matrix breakdown by a positive feedback look to recruit more immune cells, especially tumor associated macrophages and further supporting the tumor cell growth, neovascularization of the tumor and increased invasiveness of the tumor cells.

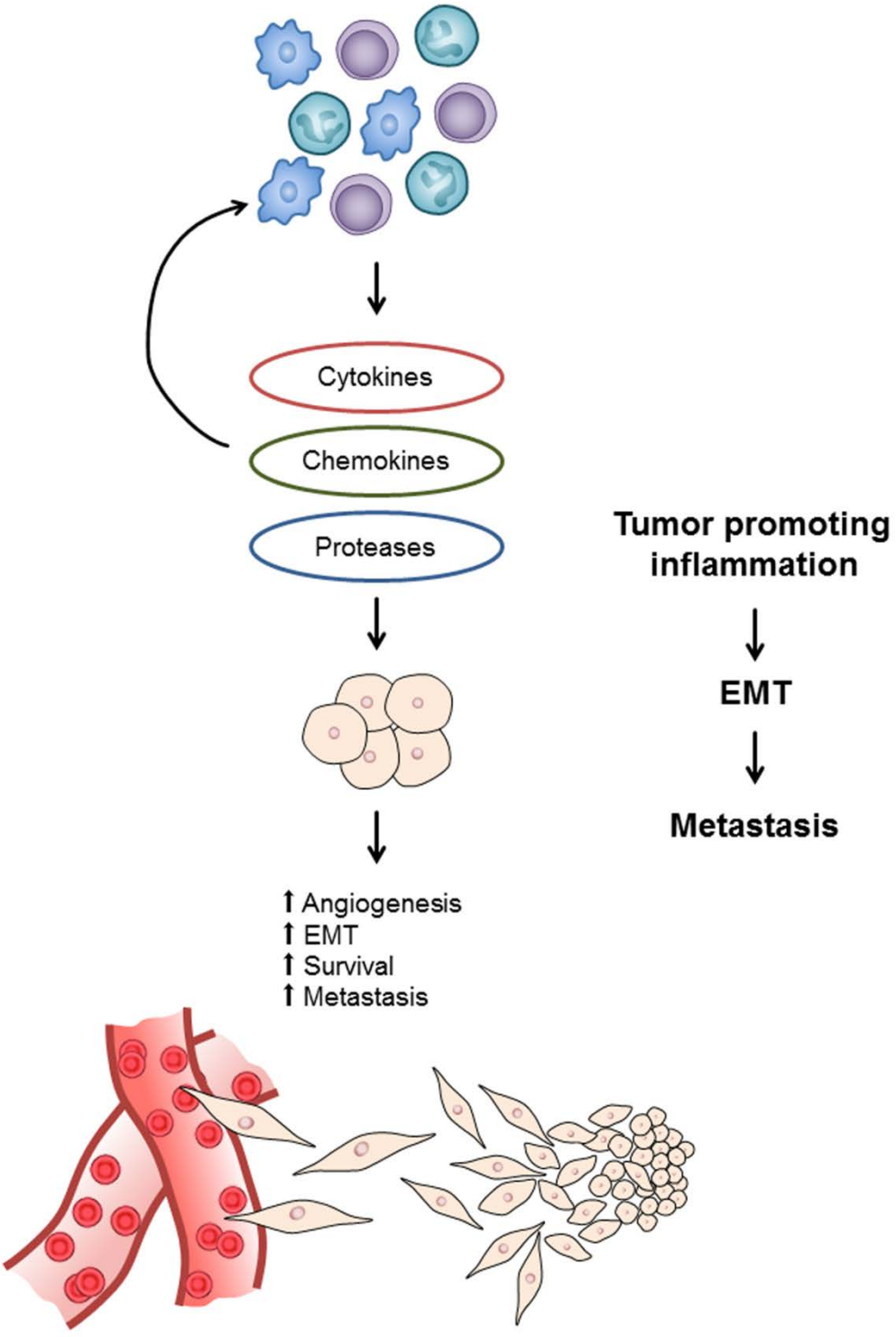
Cytokines
Chemokines
Proteases
Tumor promoting inflammation
EMT
Metastasis
↑ Angiogenesis
↑ EMT
↑ Survival
↑ Metastasis

PAD2 overexpressing SCC cells also showed an increased migratory potential in transwell migration assay (**Chapter 2**). Cells undergoing the EMT phenomenon are often at the leading edge of invasive tumors. EMT is an important process during normal development and tumor invasion of epithelial tumors by which epithelial cells acquire mesenchymal, fibroblast-like properties, and show reduced intercellular adhesion and increased motility (**Figure 5.3**). Several oncogenic pathways have been implicated in regulation of EMT, including Src, Ras, Wnt/β-catenin, as well as downstream signaling from the PI3K-AKT-axis resulting from IGF1, as well as TGFβ, EGFR, and HER2 activation[31-33]. Further experiments will be needed to understand the mechanism by which PAD2 regulates EMT process. First, we need to look at whether PAD2 directly binds the E-cadherin promoter to regulate transcription. The stable A431-FLAG-PADI2 (A431-FP2) cell line used in experiments described in **chapter 2** could be effectively used to analyze chromatin binding of PAD2. On a global level, it would be interesting to evaluate the transcriptomic differences between these two cell lines, to gain a deeper understanding of what genes are involved in PAD2-mediated oncogenesis and EMT regulation.

Figure 5.3: Overview of epithelial to mesenchymal transition (EMT). EMT describes a series of molecular and morphologic events that occur in epithelial cells during normal development or tumor progression. During EMT, normal polarized epithelial cells undergo morphologic and functional transition into more spindle shaped, migratory/invasive mesenchymal cells. The common markers for each transition stage are listed. E-cadherin expression is shown to be downregulated during this transition, while Vimentin levels are upregulated. E-cadherin suppressors (Snail and Slug), which bind to E-boxes in the promoter of E-cadherin leading to direct repression, are also upregulated. This process is usually accompanied by the degradation of the basement membrane which allows the local invasion and distant site metastasis of tumor cells.

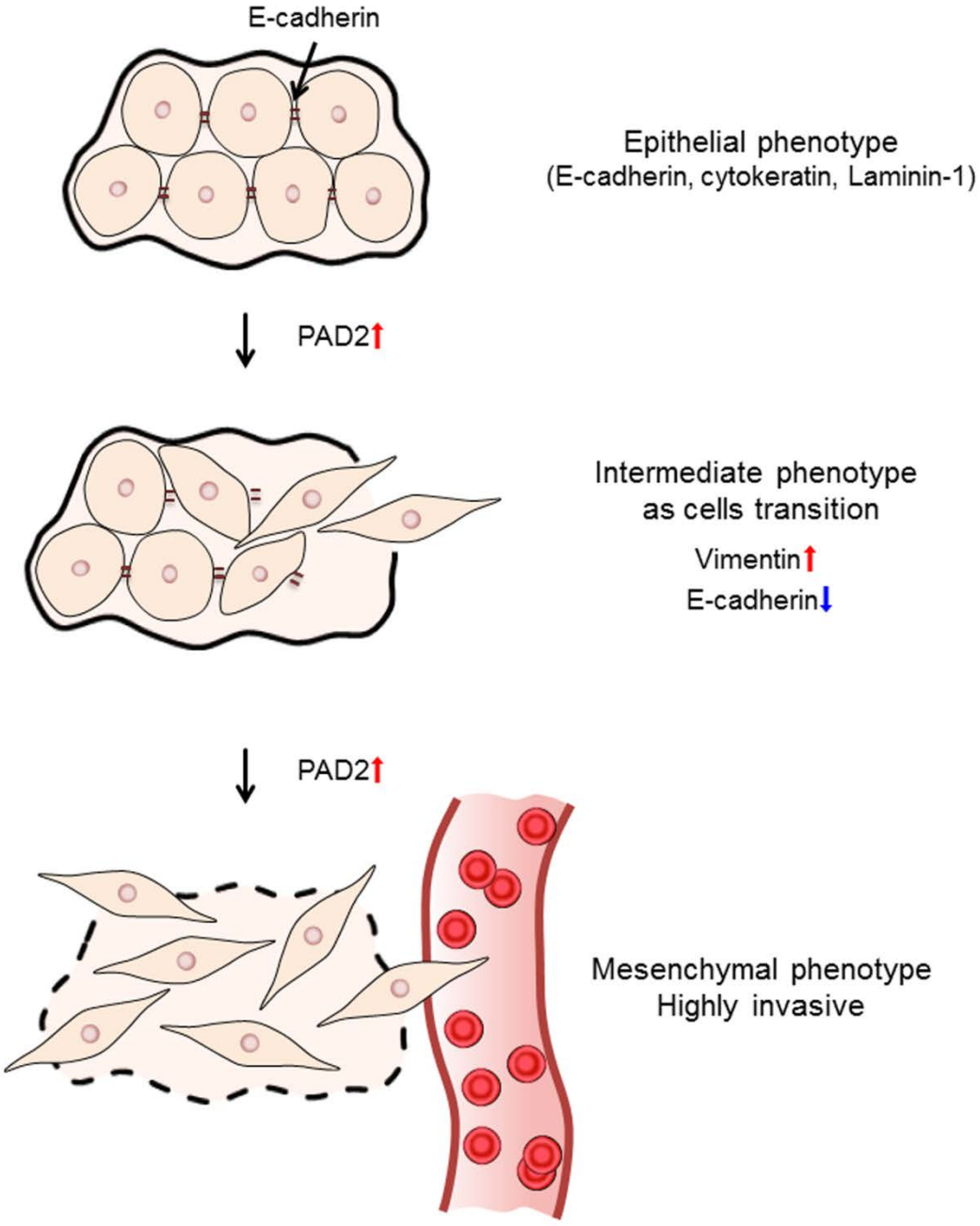
E-cadherin
Epithelial phenotype
(E-cadherin, cytokeratin, Laminin-1)
PAD2↑
Intermediate phenotype
as cells transition
Vimentin↑
E-cadherin↓
PAD2↑
Mesenchymal phenotype
Highly invasive

(**Figure 5.3**). Several oncogenic pathways have been implicated in regulation of EMT, including Src, Ras, Wnt/β-catenin, as well as downstream signaling from the PI3K-AKT-axis resulting from IGF1, as well as TGFβ, EGFR, and HER2 activation[31-33]. Further experiments will be needed to understand the mechanism by which PAD2 regulates EMT process. First, we need to look at whether PAD2 directly binds the E-cadherin promoter to regulate transcription. The stable A431-FLAG-PADI2 (A431-FP2) cell line used in experiments described in chapter 2 could be effectively used to analyze chromatin binding of PAD2. On a global level, it would be interesting to evaluate the transcriptomic differences between these two cell lines, to gain a deeper understanding of what genes are involved in PAD2-mediated oncogenesis and EMT regulation.

Stadler et al. have shown that PAD4 knockdown in xenografted MCF7 breast cancer cells leads to an increase in tumor invasiveness and associated EMT markers via the citrullination of GSK3β, which subsequently activates TGFβ signaling [34]. We are in the process of using MCF10DCIS cells which are known to recapitulate invasive comedo-DCIS cancers when xenografted into nude mice to further study the role of PAD2 in EMT. Preliminary evidence shows that when PAD2 knockdown DCIS cells, E-cadherin is upregulated and cellular migration is decreased in MCF10DCIS cells. This suggests a direct relationship between PAD2 and E-cadherin expression. The xenografted MCF10DCIS tumors were used to further investigate this relationship.

Preliminary immunostaining experiments shown that Cl-amidine treated DCIS xenografts express higher levels of E-cadherin consistent with the PAD2 knockdown DCIS cells.

5.5 Role of PAD2 mediated extracellular chromatin trap release in DAMP pathway activation in tumors

The process of cancer immune surveillance function to destroy the newly formed neoplastic cells such that most lesions capable of forming tumors are eliminated early during tumorigenesis by a process called “elimination” phase [35-39]. In some cases, a subpopulation of cancer cells “evolves” by acquiring capabilities of surviving the elimination phase. During this phase cancer cells gain immunomodulatory functions that help to decrease their immunogenicity and gain in immunoevasive abilities. An “equilibrium” phase follows during which the immune system encounters immunosusceptible cancer cells, and the immunoevasive subpopulation of tumor cells which are of low immunogenic properties. Immune selection actively eliminates the remaining highly immunogenic cancer cells while leading to escape and the clonal expansion of the low immunogenic cancer cells [36, 38]. Dying cancer cells and immune cells can release or emit DAMPs (Damage Associated Molecular Patterns) which may act as danger signals.

Figure 5.4: The potential role of ETosis inflammatory microenvironment regulation and DAMP pathway activation. The extracellular traps released may play a critical role in cell signaling in adjacent tumor cells and immune cells. The MET scaffold when released into the circulation can act as a meshwork to assist in tumor thrombi formation. Histones and other nuclear proteins can lead to DAMP pathway activation and downstream signaling of RAGE (Receptor for advanced glycation end products), TLR4, TLR2 signaling axis thus releasing further inflammatory mediators.

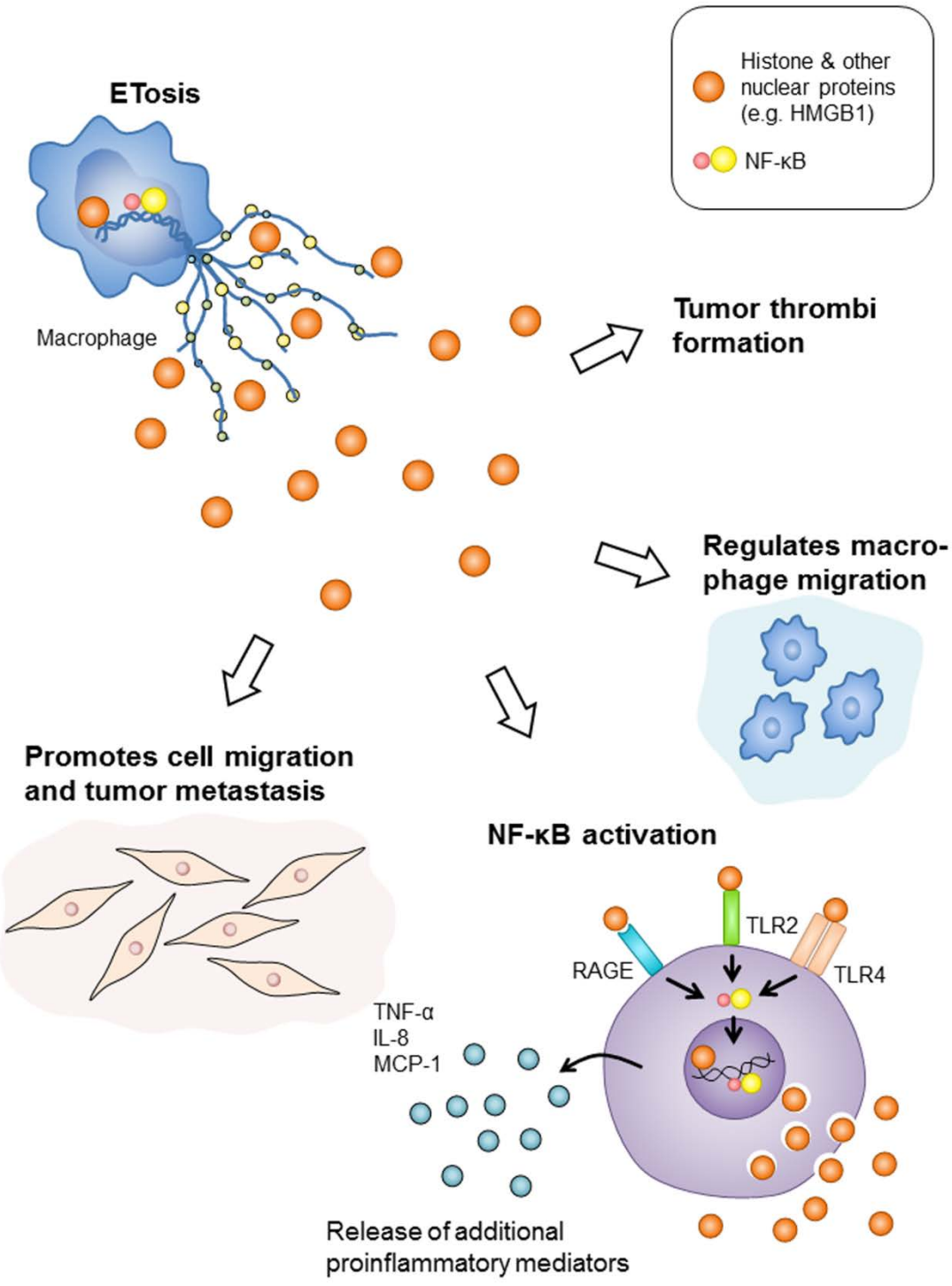
Histone & other nuclear proteins (e.g. HMGB1)
NF-κB
ETosis
Macrophage
Tumor thrombi formation
Regulates macro-phage migration
Promotes cell migration and tumor metastasis
NF-κB activation
TLR2
RAGE
TLR4
TNF-α
IL-8
MCP-1
Release of additional proinflammatory mediators

Recent reports suggest that tumor cells undergoing accidental or primary necrosis do not generate a strong CD8+ T cell-dependent immune responses [40]. Even though a close association with cell death pathways and DAMP release exist, given our finding that ETosis and citrullinated histone rich METs exist in tumor microenvironment suggest the value of further experiments to specifically study the effect of METs in activating DAMP pathways in adjacent tumor cells and stromal cells (**Figure 5.4**). It has been shown that histones release from dying cells can activate TLR4 signaling and downstream NF-kB activation. Additional experiments in which METs are isolated from *in vitro* experiments, and exposing cancer cells and cultured macrophages to these MET containing medium will be useful in identifying the specific pathways activated by MET proteins.

We also have initiated experiments to explore the role of ETosis in tumor associated inflammation in other type of human tumors such as breast cancer and Ewing's sarcoma. Our preliminary results from IHC experiments using Ewing's sarcoma tissue array indicate that PAD2 is highly expressed in a these tumors with a subset of tumors showing strong nuclear staining (**Figure 5.5**). Morphologic features of several of the strongly stained cells within these tumor tissue cores suggest high PAD2 expression in immune cells associated with tumor inflammation. It is also interesting to note that there is a recent study showing the abundance of extracellular chromatin traps in Ewing's sarcoma even though that study did not address the potential role of PAD2 in

<u>Figure 5.5</u>: Ewing's sarcoma as a model to study the role of PAD2 mediated ETosis in regulating tumor associated inflammation. Ewing's sarcoma tumor tissue array obtained from human patients (collaborator – Dr. Jeffrey Toretsky, Georgetown University) and immunostained to test for PAD2 expression. There is moderate to strong cytoplasmic expression of PAD2 in these cases (Fig 5.5A and 5.5C) while some cases show low expression (Fig 6.5D). Interestingly a subset of cases showed predominantly nuclear localization of PAD2 (Fig 5.5B).

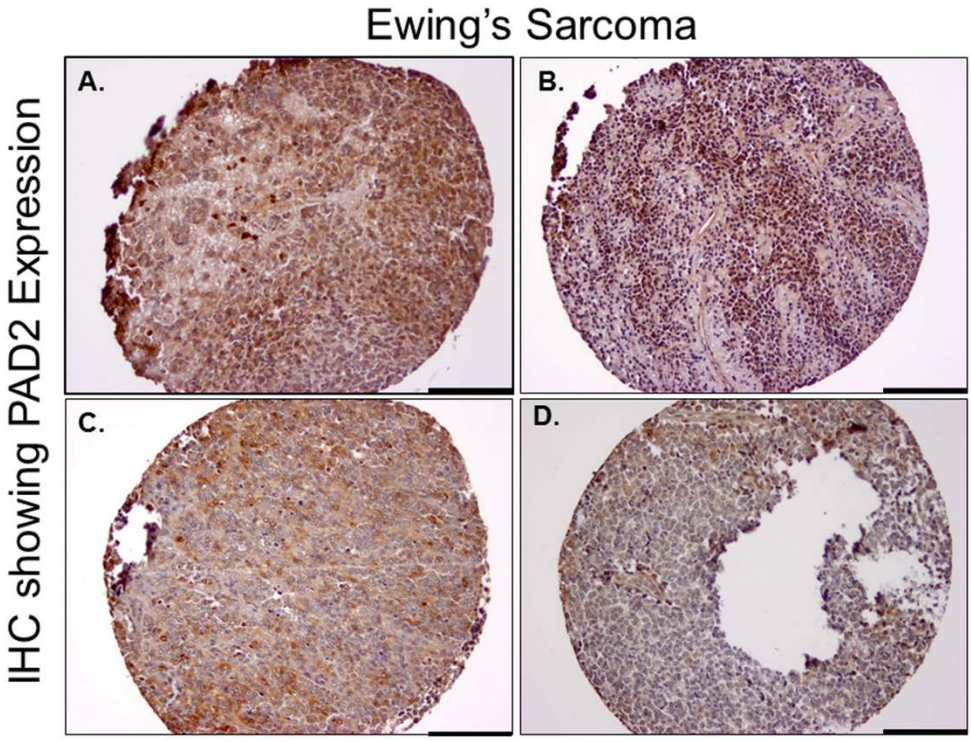

Figure 5.6: 4-NQO chemical carcinogenesis model to study oral tumor progression and inflammation. WT, PAD2KO and MMTV-FLAG-hPAD2 mice will be treated with 4-NQO administration for 12 weeks followed by ethanol treatment. Another set of mice will receive vehicle treatment. Preliminary characterization of this model in our lab suggests that this is a useful model to study oral tumor progression and tumor associated inflammation. The tissue sections for the preliminary IHC staining experiments to detect PAD2 and H4Cit3 levels were obtained from our collaborator Dr. Lorraine Gudas, Weill School of Medicine.

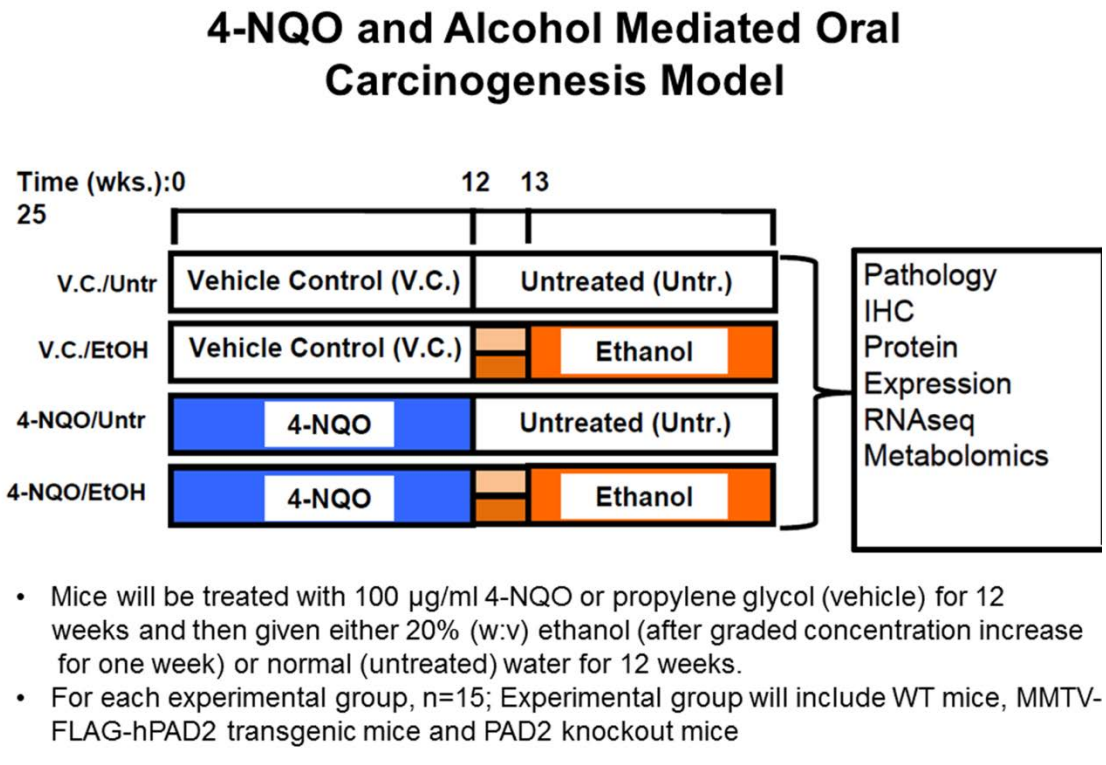

mediating this phenomenon [41]. Future experiments in our lab will focus on immunostaining and confocal imaging of breast cancer sections from human patients using ET markers and macrophage markers.

5.6 4-NQ-O oral carcinogenesis model to study the role of PAD2 in head and neck tumor-associated inflammation

In this thesis research we provide strong evidence for the role of METs in tumor associated inflammation in tongue SCC. Additional experiments using a mouse model of oral carcinogenesis will be very informative to specifically show the role of PAD2 in regulation of oral carcinoma progression and associated inflammation. We plan to use a well characterized chemical carcinogenesis model to induce tongue tumors in mice called the 4-NQO – alcohol mediated carcinogenesis [42]. Preliminary IHC studies conducted in our lab show that PAD2 is strongly expressed in immune cells associated with tongue papillomas in induced by 4-NQO and that the MET associated histone citrullination (H4Cit3) is present in a subset of immune cells associated with tongue tumors. In this model, the mice will be treated with 100 µg/ml 4-NQO or the vehicle control for 12 weeks and then with 20% ethanol or water for 12 more weeks (**Figure 5.6**). The experimental groups will include WT, MMTV-FLAG-hPAD2 mice and PAD2 knockout mice. This *in vivo* experiment will be

valuable in further understanding the role of inflammatory cells expressing PAD2 in oral carcinoma progression.

5.7 Reflections on the role of PAD2 and CLS METs in obesity-associated inflammation and its clinical relevance

Outcomes from our study (**Chapter 5**) in obesity associated subclinical inflammation suggested that macrophages undergo ETosis following TNF-α and other paracrine signal stimulation *in vitro* and within mammary gland CLS lesions in obese mice. Histone hypercitrullination marks were evident in extracellular chromatin in both RAW264.7 cells and in CLS macrophages using IF-confocal imaging and IHC methods which supported the hypothesis that the observed ETosis is likely PAD-mediated. We also showed that PAD2, but not PAD4, expression is robust within the nucleus of RAW264.7 cells and CLS-localized macrophages, thus identifying PAD2 as a strong candidate for mediator of ETosis process in macrophages. In order to further test the hypothesis of METs are modifying adipose tissue microenvironment future experiments will be needed using *in vitro* coculture systems using macrophages and cultured adipocytes. Peritoneal macrophages from PAD2 knockout mice can be used for this purpose to specifically show the role of PAD2 in macrophage function in CLS lesions.

Figure 5.7: The potential role of ETosis obesity-associated inflammatory microenvironment regulation. CLS lesions represent subclinical "smoldering" foci of inflammation consisting of macrophages which surround dying adipocytes. We found that these macrophages release METs which contain high levels of citrullinated histones. Histones are known to upregulate TLR4 signaling in immune cells. Future experiments will focus on identifying the potential of using citrullinated histones and other citrullinated proteins in patient serum samples as a clinical biomarker in order to detect obesity associated inflammation.

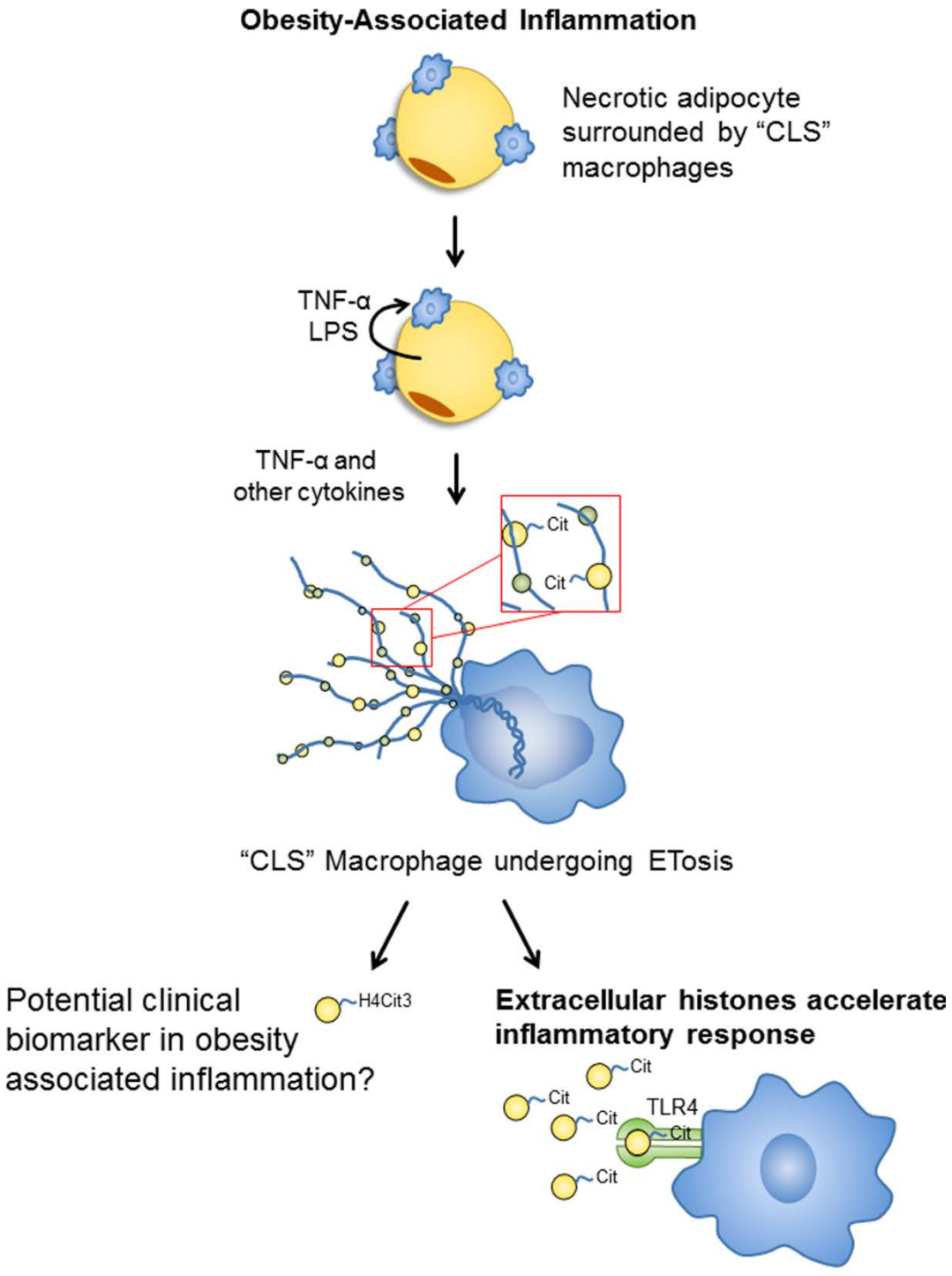
Obesity-Associated Inflammation
Necrotic adipocyte surrounded by "CLS" macrophages
TNF-α
LPS
TNF-α and other cytokines
Cit
Cit
"CLS" Macrophage undergoing ETosis
Potential clinical biomarker in obesity associated inflammation?
H4Cit3
Extracellular histones accelerate inflammatory response
Cit
Cit
Cit
TLR4
Cit
Cit

The hypercitrullinated histones and other nuclear proteins from the macrophage nucleus released into the extracellular space during MET formation may play a critical role in promoting inflammatory signaling pathways within microenvironment of mammary gland adipose tissue (**Figure 5.7**). Given the lack of strong biomarkers to differentiate the amount of inflammation within obese adipose tissue in clinical cases [43], the idea of using a method of detection to quantitate citrullinated histones and other nuclear protein in the patient serum samples is very promising. With this translational goal in mind, we are in the process of testing a newly developed fluorescence based system to detect citrullinated proteins in the serum samples.

One of our collaborators, Dr. Paul Thompson at Scripps Institute, has recently developed a citrulline specific chemical probe rhodamine-phenylglyoxal (Rh-PG), which can be used to investigate the array of protein citrullination in cells and tissue extracts. A nonbiased evaluation of protein citrullination levels in obese mice and human patients' serum samples using this novel, high throughput phenylglycoxal-based fluorescent probe system can be promising. Previously described methods for studying citrullination include the Color Development Reagent (COLDER) assay and a commercially available Anti-Citrulline (Modified) Detection Kit (ACM kit, Millipore, Billerica, MA). But this high throughput Rh-PG method provides superior sensitivity over these existing methods. The Rh-PG method is based on the chemoselective reaction that occurs between glyoxals and either citrulline or arginine under acidic or

basic conditions, respectively. This system may offer a sensitive method to detect citrullinated proteins in obese patient samples and evaluate if this can be used as a clinical biomarker for obesity associated inflammation.

5.8 Connecting the dots – Current understanding of PAD2's role in epithelial carcinogenesis and tumor-associated inflammation

The objective of this thesis research was to gain insight into the potential function of PAD2 in cancer progression and inflammation. This study has helped in advancing our understanding of PAD2 biology and helped to strongly establish a role for PAD2 as a novel oncogene, a therapeutic target for cancer therapy and a regulator of tumor and obesity associated inflammation. An overview of the potential functions of PAD2 in cancer and inflammation based on the experimental evidence presented in this thesis is reviewed in **figure 5.8**. We show here for the first time that PAD2 is capable of inducing spontaneous tumors in a PAD2 overexpressing transgenic mouse model. We also show that PAD2 overexpressing mice develop more invasive tumors with features of increased tumor associated inflammation. Two critical processes associated with tumor progression, EMT and onco-inflammation are enhanced in these transgenic tumors. This research study also lead the way in further understanding the role of PAD2 in the process of ETosis and how chromatin traps can modify chronic inflammatory conditions such as tumor-associated and obesity associated inflammation. These critical insights extend the role of PAD2 into clinically significant disease areas involving cancer and

metabolic disease and provide a strong basis for future clinically oriented research studies.

Figure 5.8: Overview of the potential role of PAD2 in cancer progression and regulation of inflammatory microenvironment. This thesis research and other studies in our lab have shown that PAD2 plays a critical role in breast cancer and skin cancer pathogenesis. One of the mechanisms by which PAD2 regulate ER-target gene recruitment is via Histone H3 arginine 26 (H3R26) citrullination. This also leads to upregulation of *HER2*. Using the MMTV-FLAG-hPAD2 mouse model, we show that PAD2 overexpression can lead to skin carcinogenesis and increased amount of tumor associated inflammation. PAD2 overexpression resulted in upregulation of cytokine/chemokine expression such as IL8, IL6 and CCL17. PAD2 upregulation also favor the EMT phenomenon and lead to downregulation of E-Cadherin. Furthermore, PAD2 is critical in macrophage extracellular trap formation and these traps are enriched with citrullinated histones. We characterize the features of macrophage released chromatin traps within tumor associated inflammation and obesity associated inflammatory microenvironment. Our study emphasizes the significance of PAD2 as a biomarker and therapeutic target in epithelial tumor progression and tumor- and obesity-associated inflammation.

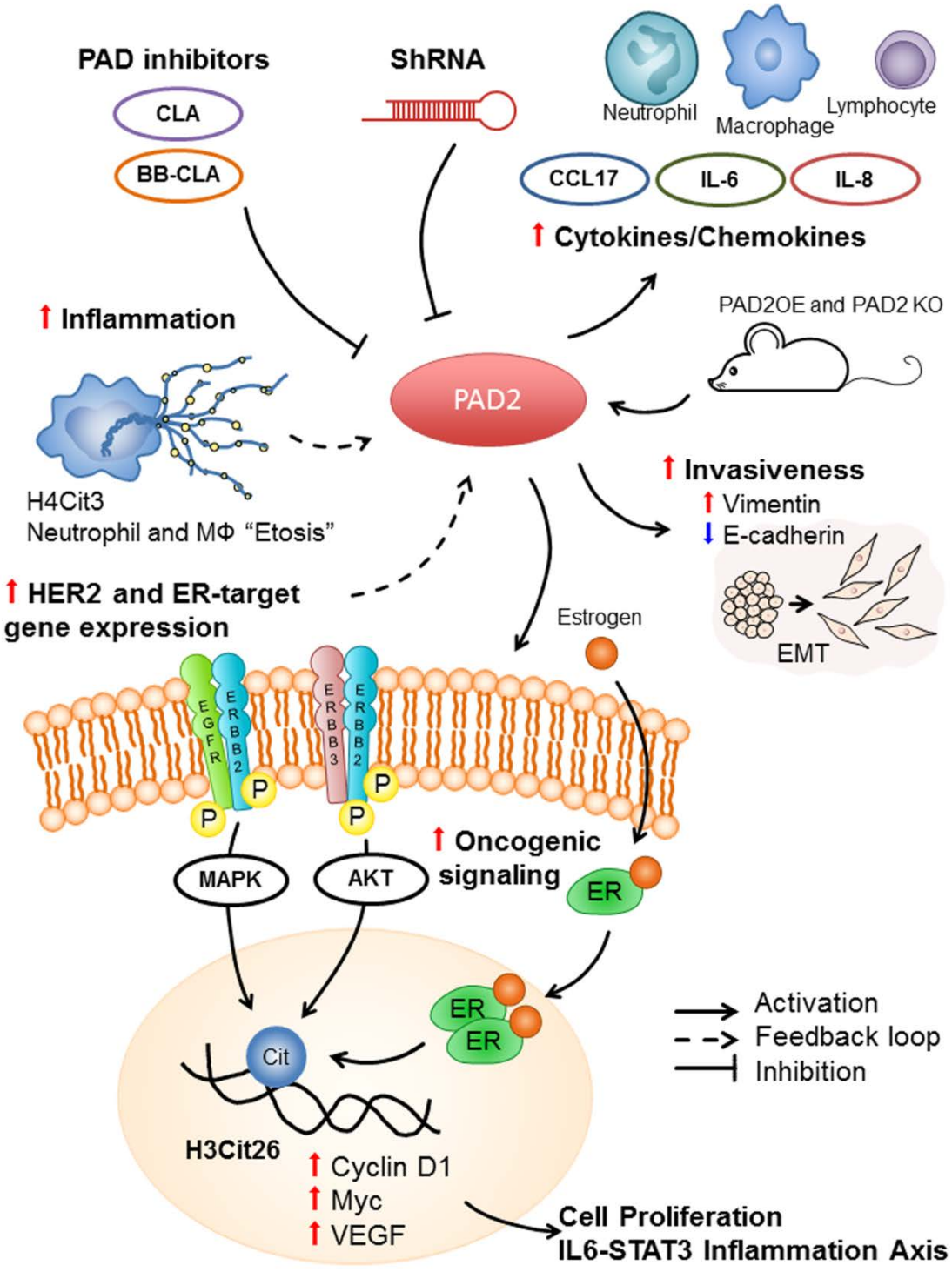
PAD inhibitors
CLA
BB-CLA
ShRNA
Neutrophil
Macrophage
Lymphocyte
CCL17
IL-6
IL-8
↑ Cytokines/Chemokines
↑ Inflammation
PAD2OE and PAD2 KO
PAD2
H4Cit3
Neutrophil and MΦ "Etosis"
↑ Invasiveness
↑ Vimentin
↓ E-cadherin
EMT
↑ HER2 and ER-target gene expression
Estrogen
EGFR
ERBB2
ERBB3
ERBB2
P
MAPK
AKT
↑ Oncogenic signaling
ER
ER
ER
Cit
H3Cit26
↑ Cyclin D1
↑ Myc
↑ VEGF
Cell Proliferation
IL6-STAT3 Inflammation Axis
Activation
Feedback loop
Inhibition

5.8 References

1. Cherrington, B.D. et al. Comparative analysis of peptidylarginine deiminase-2 expression in canine, feline and human mammary tumours. *J Comp Pathol* **147**, 139-46 (2012).

2. Hennighausen, L., Wall, R.J., Tillmann, U., Li, M. & Furth, P.A. Conditional gene expression in secretory tissues and skin of transgenic mice using the MMTV-LTR and the tetracycline responsive system. *J Cell Biochem* **59**, 463-72 (1995).

3. Wagner, K.U. et al. Spatial and temporal expression of the Cre gene under the control of the MMTV-LTR in different lines of transgenic mice. *Transgenic Res* **10**, 545-53 (2001).

4. Wang, Y. et al. Histone hypercitrullination mediates chromatin decondensation and neutrophil extracellular trap formation. *J Cell Biol* **184**, 205-13 (2009).

5. Arazna, M., Pruchniak, M.P., Zycinska, K. & Demkow, U. Neutrophil extracellular trap in human diseases. *Adv Exp Med Biol* **756**, 1-8 (2013).

6. Brinkmann, V., Laube, B., Abu Abed, U., Goosmann, C. & Zychlinsky, A. Neutrophil extracellular traps: how to generate and visualize them. *J*

Vis Exp (2010).

7. Neeli, I. & Radic, M. Knotting the NETs: Analyzing histone modifications in neutrophil extracellular traps. *Arthritis Res Ther* **14**, 115 (2012).

8. Aulik, N.A., Hellenbrand, K.M. & Czuprynski, C.J. Mannheimia haemolytica and its leukotoxin cause macrophage extracellular trap formation by bovine macrophages. *Infect Immun* **80**, 1923-33 (2012).

9. Proost, P. et al. Citrullination of CXCL8 by peptidylarginine deiminase alters receptor usage, prevents proteolysis, and dampens tissue inflammation. *J Exp Med* **205**, 2085-97 (2008).

10. Gudjonsson, T. et al. Normal and tumor-derived myoepithelial cells differ in their ability to interact with luminal breast epithelial cells for polarity and basement membrane deposition. *J Cell Sci* **115**, 39-50 (2002).

11. Rudland, P.S., Hallowes, R.C., Cox, S.A., Ormerod, E.J. & Warburton, M.J. Loss of production of myoepithelial cells and basement membrane proteins but retention of response to certain growth factors and hormones by a new malignant human breast cancer cell strain. *Cancer Res* **45**, 3864-77 (1985).

12. Warburton, M.J., Ferns, S.A. & Rudland, P.S. Enhanced synthesis of basement membrane proteins during the differentiation of rat mammary tumour epithelial cells into myoepithelial-like cells in vitro. *Exp Cell Res* **137**, 373-80 (1982).

13. Bang, H. et al. Mutation and citrullination modifies vimentin to a novel autoantigen for rheumatoid arthritis. *Arthritis Rheum* **56**, 2503-11 (2007).

14. Chang, X., Jian, X. & Yan, X. Expression and citrullination of keratin in synovial tissue of rheumatoid arthritis. *Rheumatol Int* **29**, 1337-42 (2009).

15. McElwee, J.L. et al. Identification of PADI2 as a potential breast cancer biomarker and therapeutic target. *BMC Cancer* **12**, 500 (2012).

16. Chumanevich, A.A. et al. Suppression of colitis in mice by Cl-amidine: a novel peptidylarginine deiminase inhibitor. *Am J Physiol Gastrointest Liver Physiol* **300**, G929-38 (2011).

17. Fan, L. et al. Citrullinated vimentin stimulates proliferation, pro-inflammatory cytokine secretion, and PADI4 and RANKL expression of fibroblast-like synoviocytes in rheumatoid arthritis. *Scand J Rheumatol*, [Epub ahead of print] (2012).

18. Hanahan, D. & Weinberg, R.A. Hallmarks of cancer: the next generation. *Cell* **144**, 646-74 (2011).

19. Mantovani, A., Allavena, P., Sica, A. & Balkwill, F. Cancer-related inflammation. *Nature* **454**, 436-44 (2008).

20. Grivennikov, S.I., Greten, F.R. & Karin, M. Immunity, inflammation, and cancer. *Cell* **140**, 883-99 (2010).

21. Grivennikov, S.I. & Karin, M. Dangerous liaisons: STAT3 and NF-kappaB collaboration and crosstalk in cancer. *Cytokine Growth Factor Rev* **21**, 11-9 (2010).

22. Yu, H., Kortylewski, M. & Pardoll, D. Crosstalk between cancer and immune cells: role of STAT3 in the tumour microenvironment. *Nat Rev Immunol* **7**, 41-51 (2007).

23. Karin, M. & Greten, F.R. NF-kappaB: linking inflammation and immunity to cancer development and progression. *Nat Rev Immunol* **5**, 749-59 (2005).

24. Hartman, Z.C. et al. HER2 overexpression elicits a proinflammatory IL-6 autocrine signaling loop that is critical for tumorigenesis. *Cancer Res* **71**, 4380-91 (2011).

25. Lee, H.J. et al. Peptidylarginine deiminase 2 suppresses inhibitory {kappa}B kinase activity in lipopolysaccharide-stimulated RAW 264.7 macrophages. *J Biol Chem* **285**, 39655-62 (2010).

26. Anglesio, M.S. et al. IL6-STAT3-HIF signaling and therapeutic response to the angiogenesis inhibitor sunitinib in ovarian clear cell cancer. *Clin Cancer Res* **17**, 2538-48 (2011).

27. Yoon, S. et al. NF-kappaB and STAT3 cooperatively induce IL6 in starved cancer cells. *Oncogene* **31**, 3467-81 (2012).

28. Aceto, N. et al. Co-expression of HER2 and HER3 receptor tyrosine kinases enhances invasion of breast cells via stimulation of interleukin-

8 autocrine secretion. *Breast Cancer Res* **14**, R131 (2012).

29. Sparmann, A. & Bar-Sagi, D. Ras-induced interleukin-8 expression plays a critical role in tumor growth and angiogenesis. *Cancer Cell* **6**, 447-58 (2004).

30. Fernando, R.I., Castillo, M.D., Litzinger, M., Hamilton, D.H. & Palena, C. IL-8 signaling plays a critical role in the epithelial-mesenchymal transition of human carcinoma cells. *Cancer Res* **71**, 5296-306 (2011).

31. Iwatsuki, M. et al. Epithelial-mesenchymal transition in cancer development and its clinical significance. *Cancer Sci* **101**, 293-9 (2010).

32. Larue, L. & Bellacosa, A. Epithelial-mesenchymal transition in development and cancer: role of phosphatidylinositol 3' kinase/AKT pathways. *Oncogene* **24**, 7443-54 (2005).

33. Vincent-Salomon, A. & Thiery, J.P. Host microenvironment in breast cancer development: epithelial-mesenchymal transition in breast cancer development. *Breast Cancer Res* **5**, 101-6 (2003).

34. Stadler, S.C. et al. Dysregulation of PAD4-mediated citrullination of nuclear GSK3beta activates TGF-beta signaling and induces epithelial-to-mesenchymal transition in breast cancer cells. *Proc Natl Acad Sci U S A* **110**, 11851-6 (2013).

35. Zitvogel, L., Tesniere, A. & Kroemer, G. Cancer despite immunosurveillance: immunoselection and immunosubversion. *Nat Rev Immunol* **6**, 715-27 (2006).

36. Garg, A.D., Dudek, A.M. & Agostinis, P. Cancer immunogenicity, danger signals, and DAMPs: what, when, and how? *Biofactors* **39**, 355-67 (2013).

37. Krysko, D.V. et al. Immunogenic cell death and DAMPs in cancer therapy. *Nat Rev Cancer* **12**, 860-75 (2012).

38. Garg, A.D. et al. Immunogenic cell death, DAMPs and anticancer therapeutics: an emerging amalgamation. *Biochim Biophys Acta* **1805**, 53-71 (2010).

39. Dunn, G.P., Bruce, A.T., Ikeda, H., Old, L.J. & Schreiber, R.D. Cancer immunoediting: from immunosurveillance to tumor escape. *Nat Immunol* **3**, 991-8 (2002).

40. Gamrekelashvili, J. et al. Primary sterile necrotic cells fail to cross-prime CD8(+) T cells. *Oncoimmunology* **1**, 1017-1026 (2012).

41. Berger-Achituv, S. et al. A proposed role for neutrophil extracellular traps in cancer immunoediting. *Front Immunol* **4**, 48 (2013).

42. Hawkins, B.L. et al. 4NQO carcinogenesis: a mouse model of oral cavity squamous cell carcinoma. *Head Neck* **16**, 424-32 (1994).

43. Lu, J.Y. et al. Adiponectin: a biomarker of obesity-induced insulin resistance in adipose tissue and beyond. *J Biomed Sci* **15**, 565-76 (2008).